Author Manuscript

Author Manuscript

Author Manuscript

Author Manuscript

HHS Public Access

Author manuscript

Prog Retin Eye Res. Author manuscript; available in PMC 2024 July 24.

Published in final edited form as:

Prog Retin Eye Res. 2022 July ; 89: 101033. doi:10.1016/j.preteyeres.2021.101033.

Diabetic macular ischaemia- a new therapeutic target?

Chui Ming Gemmy Cheung[a,b], **Amani Fawzi**[c], **Kelvin YC. Teo**[a], **Hisashi Fukuyama**[d], **Sagnik Sen**[e], **Wei-Shan Tsai**[f], **Sobha Sivaprasad**[f,*]

[a]Singapore Eye Research Institution, Singapore National Eye Centre, Singapore

[b]Duke-NUS Medical School, National University of Singapore, Singapore

[c]Northwestern University, Illinois, USA

[d]Hyogo College of Medicine, Nishinomiya, Japan

[e]Aravind Eye Hospital, Madurai, India

[f]NIHR Moorfields Biomedical Research Centre, Moorfields Eye Hospital, London, United Kingdom

Abstract

Diabetic macular ischaemia (DMI) is traditionally defined and graded based on the angiographic evidence of an enlarged and irregular foveal avascular zone. However, these anatomical changes are not surrogate markers for visual impairment. We postulate that there are vascular phenotypes of DMI based on the relative perfusion deficits of various retinal capillary plexuses and choriocapillaris. This review highlights several mechanistic pathways, including the role of hypoxia and the complex relation between neurons, glia, and microvasculature. The current animal models are reviewed, with shortcomings noted. Therefore, utilising the advancing technology of optical coherence tomography angiography (OCTA) to identify the reversible DMI phenotypes may be the key to successful therapeutic interventions for DMI. However, there is a need to standardise the nomenclature of OCTA perfusion status. Visual acuity is not an ideal endpoint for DMI clinical trials. New trial endpoints that represent disease progression need to be

*Corresponding author. NIHR Moorfields Biomedical Research Centre, Moorfields Eye Hospital, 162, City Road, London, EC1V 2PD, United Kingdom. senswathi@aol.com (S. Sivaprasad).

Author statement

Chui Ming Gemmy Cheung: Conceptualisation, Investigation, Methodology, Project administration, Supervision, Writing- Original draft, Writing- Review and editing.
Amani Fawzi: Resources, Supervision, Writing- Original draft, Writing- Review and editing.
Kelvin YC Teo: Visualisation, Writing- Original draft, Writing- Review and editing.
Hisashi Fukuyama: Writing- Review and editing.
Sagnik Sen: Writing- Review and editing.
Wei-Shan Tsai: Visualisation, Writing- Review and editing.
Sobha Sivaprasad: Conceptualisation, Investigation, Methodology, Project administration, Supervision, Writing- Original draft, Writing- Review and editing.

Declarations of interest

Chui Ming Gemmy Cheung: Bayer, Novartis, Roche, Allergan, Boehringer-Ingelheim, Topcon, Zeiss.
Amani Fawzi: Roche, Regeneron, Genentech, Boehringer-Ingelheim.
Kelvin YC Teo: Bayer, Novartis, Roche.
Sagnik Sen: None.
Hisashi Fukuyama: None.
Wei-Shan Tsai: None.
Sobha Sivaprasad has received funding/fees from Bayer, Novartis, Allergan, Roche, Boehringer Ingelheim, Optos, Oxurion, Oculis, Biogen, Apellis and Heidelberg Engineering.

Author Manuscript Author Manuscript Author Manuscript Author Manuscript

developed before irreversible vision loss in patients with DMI. Natural history studies are required to determine the course of each vascular and neuronal parameter to define the DMI phenotypes. These DMI phenotypes may also partly explain the development and recurrence of diabetic macular oedema. It is also currently unclear where and how DMI fits into the diabetic retinopathy severity scales, further highlighting the need to better define the progression of diabetic retinopathy and DMI based on both multimodal imaging and visual function. Finally, we discuss a complete set of proposed therapeutic pathways for DMI, including cell-based therapies that may provide restorative potential.

Keywords

Diabetic macular ischaemia; Optical coherence tomography; Optical coherence tomography angiography; Diabetic macular oedema; Diabetic retinopathy; Foveal avascular zone

1. Introduction

Diabetes mellitus (DM) is one of the fastest-growing chronic diseases worldwide (Bhanushali et al., 2016). According to the International Diabetes Federation, the total number of people with diabetes in the world is 537 million in 2021 and is projected to increase to 700 million in 2045 (www.idf.org). Therefore, there is an unmet need to reduce the public health burden caused by the morbidities associated with the microvascular and macrovascular complications of diabetes. In particular, research into the currently untreatable sequelae of diabetes needs to be prioritised.

Diabetic retinopathy (DR) is one of the microvascular complications of DM and a leading cause of acquired vision loss in working-age adults worldwide (Bhanushali et al., 2016; de Carlo et al., 2015; Di et al., 2016). The most common vision-threatening complications of DR (VTDR) are proliferative diabetic retinopathy (PDR) and diabetic macular oedema (DMO). While preventing and treating these two complications remain a priority, diabetic macular ischaemia (DMI) is another cause of visual loss. Research on DMI is still in its infancy. The prevalence and characterisation of DMI with and without visual loss are ill-defined. Currently, visual loss due to DMI is irreversible, and there are no known preventive options for this condition. Systemic risk factors of DR also apply to DMI, but there may be other risk factors that have not been investigated fully (Aiello et al., 2001).

Although the pathophysiology of DR is characteristically described as diabetes-related loss or dysfunction of the retinal capillary bed in both the peripheral and central retina, increased vascular permeability, inflammation, and neurodegeneration are also significant retinal sequelae of diabetes. The initiation sequence of these changes, their interdependence, relation and the course they pursue are key areas of ongoing investigations. Together, these changes lead to clinically visible changes such as microaneurysms, dot and blot haemorrhages, venous beading, and eventually retinal and optic disc neovascularisation. The severity of DR is graded based on these clinically visible features. However, laboratory research into the molecular pathology of diabetic retinae have shown that neurodegeneration and vasoregression precede visible DR changes (Hammes et al., 2011; Antonetti et al., 2012), and these findings have now been substantiated clinically with the

Author Manuscript Author Manuscript Author Manuscript Author Manuscript

availability of optical coherence tomography (OCT) and OCT-Angiography (OCT-A). These clinicopathological correlations may provide insights into the better characterisation of DMI to explore preventive and therapeutic options. In addition, newer imaging tools such as adaptive optics scanning laser ophthalmoscope (AOSLO) provide us with opportunities to study real-time changes in retinal blood flow and photoreceptors, allowing novel structure-function correlations. These recent opportunities in humans are a breakthrough given the lack of ideal animal models to study the pathobiology of DR that mirror all changes (Robinson et al., 2012).

Clinically, there is also an unmet need to re-classify DR based on the advances in our understanding of the disease. For this, there are several aspects of DMI that need to be considered. Firstly, the current DR severity grades do not include DMI. Although the prevalence of DMI increases with the severity of DR, not all eyes with PDR have an enlarged and irregular foveal avascular zone (FAZ), the current parameter used to define DMI (Bhanushali et al., 2016; Durbin et al., 2017). Secondly, both the DR and DMI severity grades do not correlate with visual acuity loss. An enlarged moth-eaten appearance of FAZ or non-FAZ related macular perfusion deficits only correlates modestly with functional losses due to DMI. With further clarification of the definition of DMI, vision-threatening DMI needs to be considered within VTDR definitions. Thirdly, there is a need to understand the relationship between DMO and DMI because vasoregression precedes visible DR changes, and vascular hyperpermeability may precede, co-exist or occur subsequently. Although DMO can occur at any DR severity level and progress independently of DR severity, the question of whether DMO can occur in the absence of any other DR changes remain unanswered. It is also yet to be determined whether DMO triggers DMI or whether DMI is partly responsible for recurrent DMO. Fourth, neuronal changes that co-exist with DMO and DMI need to be considered in phenotyping these entities. These changes may represent neuronal degeneration that does not affect visual function, or they may be reversible, especially if consequent to mechanical compression caused by DMO, while other changes may be irreversible. Lastly, unlike retinal neovascularisation elsewhere that typically occurs at the margins of areas of retinal capillary nonperfusion, neovascularisation at the margin of en enlarged FAZ is a rarity. These observations raise the possibility of specific cellular or molecular changes in the central macula in DMI that differ from the rest of the retina. Currently, DMO is classified morphologically on OCT, but these DMO phenotypes do not aid treatment decisions or serve as visual prognostic factors, highlighting the need to incorporate neuronal changes into DMO phenotyping. Although these neuronal changes may result from mechanical compression caused by macular fluid, they may also represent neuronal degeneration that may precede, co-exist with DMO, or develop as a sequela of DMI. DMI may affect either or both the outer and inner retina, substantiating that DMI is not one entity (Vujosevic et al., 2020).

The prevalence of DMI is also likely underestimated as fundus fluorescein angiography (FA) is not routinely performed as part of baseline clinical assessment unless there is significant visual impairment. With the recent advances in OCT-A, it is now possible to diagnose and monitor the progression of DMI non-invasively, even in asymptomatic patients and in those with no visible DR. A key improvement in clinical interpretation is the ability to evaluate DMI across the retina by analysing the superficial, intermediate and deep retinal plexus

Author Manuscript Author Manuscript Author Manuscript Author Manuscript

independently. This advantage allows us to recognise different phenotypes of DMI and quantify the severity to reach a precise assessment of progression longitudinally. Different phenotypes of DMI, in turn, may explain the variability in functional deficit in different individuals. It is also interesting to note that with OCTA, changes in the FAZ area and circularity are seen prior to the development of DR, suggesting that these alterations are potential early biomarkers for DR (de Carlo et al., 2015; Di et al., 2016; Durbin et al., 2017). Cross-sectional OCTA studies have found that the FAZ area and vessel density in the deep plexus correlate more closely with visual acuity than similar changes in the superficial vascular plexus (Dupas et al., 2018; Samara et al., 2017). In addition to evaluating the FAZ, many additional parameters have been proposed to be valuable endpoints for assessing DMI, such as vessel density. Collectively, OCTA research has paved the way for a better understanding of macular perfusion deficits (Vujosevic et al., 2019b, 2021). The ability to visualise the superficial and deep retinal vascular plexus and the choriocapillaris has provided us with new knowledge of macular vascular deficits in DMI. Together with the structural changes on OCT representing neuronal changes, it is an ideal opportunity to re-visit the structure-function correlation of DMI to better define and phenotype it.

In this review, we aim to summarise the pathophysiology and functional correlates of DMI and the diagnostic considerations based on OCTA features. We will focus on opportunities to utilise these features to address critical gaps in our current clinical knowledge. In particular, we will align the progress made in basic science in understanding retinal ischaemia with advances made in retinal imaging to aid the translation of potential DMI prevention and treatment options. To achieve this, we will review reported OCT and OCT-A parameters, highlight further work to aid standardisation of the definition of DMI, address technical considerations related to the OCTA artefacts and highlight potential clinical trial endpoints. We will also identify areas of clinical research, especially on the normative values of macular perfusion and the progression rates of various markers of perfusion deficits; therefore, accurate, repeatable and comparable clinical endpoints can be established across different settings as well as longitudinally (Hormel et al., 2021).

2. Retinal capillary network in health

The retinal vascular system, neurons and glia form a neurovascular unit and communicate with each other (Hammes et al., 2011; Antonetti et al., 2012). Neuronal cells, including photoreceptors, bipolar cells, ganglion cells, horizontal cells, and amacrine cells, convert visual stimuli to electrical activity transmitted to the brain. Both glia and microglia wrap around the retinal microvasculature. The Müller cells are the main retinal glial cell, and they span the whole retina, including the floor of the fovea. In addition to contributing to the neurovascular coupling by initiating vascular responses to neuronal activity, these cells also recycle neurotransmitters, provide structural support and supply lactate to retinal neurons. The astrocytes in the nerve fibre layer are another group of glial cells that contribute to neurovascular coupling, autoregulation, maintain the blood-retinal barrier and provide structural support. Microglia are phagocytic cells that remove dead cells; however, they also contribute to local synapses and immune regulation (Moran et al., 2016).

Author Manuscript Author Manuscript Author Manuscript Author Manuscript

The human retina is supplied by two independent vascular systems, the retinal and choroidal vessels. The outer retinal layers that consist of the photoreceptors and the larger portion of the outer plexiform layer are mainly nourished by choroidal vessels, whereas the inner retina is supplied solely by the retinal vessels. The retinal circulation is an end-artery circulation of the central retinal artery. The retinal capillary network is arranged in four layers: (1) radial peripapillary capillaries (RPCs) around the optic nerve within the retinal nerve fibre layer (RNFL), (2) superficial capillary plexuses (SCP) located within the retinal ganglion cell layer (RGCL) and the superficial portion of the inner plexiform layer (IPL), (3) intermediate capillary plexuses (ICP) at the inner border of IPL and the superficial portion of the inner nuclear layer (INL), and (4) deep capillary plexuses (DCP) lying at the outer border of INL (Hayreh, 1963) (Fig. 1).

When we interpret the retinal layers and the microvasculature on OCT and OCTA, the ganglion cell layer on OCT, corresponding to ganglion cells, astrocytes and some amacrine cells, is supplied by the superficial vascular complex (SVC), which comprise both the nerve fibre layer vascular plexus and the SCP. The inner nuclear layer on OCT consists of the bipolar, horizontal and amacrine cells. It is supplied by the deep vascular complex (DVC) that comprise a combination of ICP and DCP. The outer retina consists of photoreceptors and is mainly supplied by the choroid. Oxygen delivery models of the retina have shown that the photoreceptors and their axons may receive up to 15% of their needs from the retinal capillaries (Birol et al., 2007).

When we consider structure-function correlation, the macula is a specialised region of the retina. It is responsible for the highest resolution of visual acuity and is located temporal to the optic nerve. Cone density peaks sharply in the foveola, the central region of the macula, and decreases rapidly into the periphery (Curcio et al., 1990). There is also a high prevalence of midget circuitry cells at the margin of the fovea (Provis et al., 2005). The locus of fixation is within the average-sized FAZ and not necessarily at the foveola. Structurally, there are remarkable differences in retinal cellular layers and retinal capillary networks between the macular region and other retinal regions, resulting in thicker macula than the rod-dominated peripheral retina. The greater numbers and density of ganglion cells and the more synaptic interaction result in a thicker IPL. Similarly, the larger number of ganglion cell axons also contribute to the thicker NFL, explaining the thicker layers around the fovea (Huber et al., 2010). Despite these neurosensory changes, the centre of the macula is generally avascular, surrounded by circularly arranged capillaries delimitating the FAZ and is nourished by the choriocapillaris (Provis et al., 2013). Therefore, this limited blood supply needs to meet the demands of the high rate of oxygen consumption of the retinal neurons (Joyal et al., 2018). One compensatory mechanism of this vascular compromise is the autoregulation of the retinal vasculature, a phenomenon known as neurovascular coupling (Kur et al., 2012). For example, the retinal arterioles and perhaps the capillaries dilate and increase blood flow locally to compensate for changes in neuronal activity in response to a visual stimulus. These adaptive mechanisms within a relatively compromised blood supply make the central macula vulnerable to insults within the microenvironment.

These anatomical considerations are critical to our understanding of structure-function correlation in DMI. In particular, this emphasises that visual acuity is not an ideal endpoint

Author Manuscript Author Manuscript Author Manuscript Author Manuscript

for clinical trials evaluating interventions to prevent or delay the progression of retinal capillary loss in DMI.

3. Retinal oxygen metabolism

The study of retinal oxygen (O_2) flux has greatly enhanced our understanding of how oxygen delivery is regulated in the retina. The inner retinal circulation and choroidal blood flow together regulate how oxygen reaches the different metabolic units of the retina. The research in this area has also greatly improved our understanding of how these metabolic units utilise oxygen under different lighting conditions. Using intraretinal micro-electrodes to measure the gradient of retinal oxygen in various animal models under different perturbations, Linsenmeier and his colleagues, as well as Cringle and Yu, have pioneered this field over the last 3+ decades (Yu and Cringle, 2001). Understanding the regulation of oxygen in the diabetic retina remains a highly important and quite understudied area. Tools to measure retinal oxygen in vivo in humans are currently limited to reflectance-based oximetry measurements, which have important limitations. Also, these are rarely coupled with blood flow imaging, making their interpretation challenging. This topic, as well as the tools to measure oxygen in vivo, has been explored in greater detail by Linsenmeier et al. (Linsenmeier and Zhang, 2017).

Using oxygen-sensitive micro-electrodes inserted into the living animal retina remains the most accurate and direct experimental tool that informs our understanding. In various models, including the macaque retina, the closest to the human retina, the oxygen gradients in the outer retina are now well documented and understood (Linsenmeier and Zhang, 2017). The overall gradients are quite similar, with minor differences across species. Overall, the inner segment of the photoreceptor (with its high mitochondrial content) is the major oxygen consumer of the outer avascular retina. A steep gradient of oxygen profile from the choroid, along with very low, single-digit PO_2 in the dark, supports this conclusion. In the dark-adapted retina, there is a second gradient towards the photoreceptors from the inner retina in all these models, which, though it is less steep than the choroidal gradients, does indicate a dependence of the photoreceptors on the deep capillary circulation, especially in their highly metabolic dark-adapted state. This fraction of retinal capillary contribution to the dark-adapted photoreceptor oxygen demands is estimated at 15% in the macaque (Birol et al., 2007).

Modelling inner retinal O_2 consumption has been less well studied and is generally hampered by the difficulty in accurately tracking the location of the inner retinal capillaries using the intraretinal electrode approach. A 3-dimensional model, which would require additional information about these capillaries and their proximity to the electrodes, has not been feasible, although various lines of evidence suggest that the inner retina consumes about the same amount of oxygen as the photoreceptors (Braun et al., 1995; Medrano and Fox, 1995).

The high rate of oxygen demand of the photoreceptors and the clinical observation that patients with co-existent end-stage retinitis pigmentosa (complete loss of photoreceptors) and diabetes do not manifest diabetic retinopathy prompted Arden to suggest that preventing

Author Manuscript Author Manuscript Author Manuscript Author Manuscript

dark adaptation could be a potential therapeutic avenue to decrease the burden of retinopathy. To test this hypothesis, the CLEOPATRA Study randomised patients with non-centre-involved DMO to light-emitting masks or sham masks. Unfortunately, the study found no significant benefit at two years (Sivaprasad et al., 2018). Some limitations of such studies include the impossibility of masking patients and clinicians to the intervention group, as well as the overall low compliance with mask-wearing revealed by this study. More recently, another randomised controlled trial also failed to show benefit for twice daily application of a 90-sec photobiomodulation mask (670 nm, low emission) in centre-involved DMO with good vision (Writing et al., 2021). Other considerations for the lack of benefit may be related to the effect of light on the retina of humans. Notably, compared to the cat retina (50% decreased demand), the light had a smaller effect on the metabolic oxygen rate in the outer retina of the macaque (Birol et al., 2007). Furthermore, the degree of photoreceptor hypoxia in DMO may be highly variable, and thus DMI may be a better target population to apply these interventions in clinical trials.

In addition to their high metabolic demand, one of the intriguing theories proposed by Kern and colleagues suggests that photoreceptors are the main source of the inflammatory burden in the diabetic retina due to their oxidative stress, exacerbating and perhaps even initiating the diabetic microvascular compromise. To test their hypothesis, they studied the vascular and inflammatory changes in mice with or without diffusely absent photoreceptors (toxic or genetic) phenotype (Du et al., 2013). They showed that superoxide generation by diabetic mice is generally greater in the dark, a finding completely abrogated in diabetic mice without photoreceptors. They also showed that the inflammatory cytokines iNOS and ICAM1 were reduced in diabetic retinas with photoreceptor degeneration. They further expanded their findings in an ex vivo and in vitro model where they showed that photoreceptors released inflammatory mediators that could activate leucocytes and lead to endothelial cell death (Tonade et al., 2016).

3.1. Retinal vascular response to systemic hypoxia

As discussed in the next section, evidence of hypoxia in the human diabetic retina is largely based on indirect clues in early DR and less reliably on the vitreous PO_2 measurements in advanced stages of PDR. To model the effect of hypoxia in the retinal and choroidal circulation, one approach has been the use of controlled systemic hypoxic exposure. The important caveat to these experiments and how they may or may not relate to DR is that the choroid is largely unable to compensate for systemic hypoxia with a significant decrease in the choroidal PO_2 consistently seen in animal experiments, placing the photoreceptors at significant hazard with functional changes seen in the ERG c-wave, especially in the dark-adapted retina (Linsenmeier and Braun, 1992; Moret et al., 1992; Pournaras, 1995). Interestingly, because the retinal vasculature can adapt to a hypoxic inspired PO_2 by increasing blood flow, the inner retina is protected from PO_2 compromise, and the b-wave of the ERG does not change until the inspired PO_2 falls to 40 mmHg in the cat (Linsenmeier and Steinberg, 1986; Linsenmeier and Steinberg, 1986; Yancey and Linsenmeier, 1989; Eperon et al., 1975; Cheng et al., 2016; Enroth-Cugell and Harding, 1980; Linsenmeier and Braun, 1992).

Author Manuscript Author Manuscript Author Manuscript Author Manuscript

3.2. Oxygen measurements in human DR

The direct evidence (via measurements) of retinal hypoxia in human DR is still quite limited, particularly in the early stages of DR. In contrast, eyes undergoing vitrectomy for advanced PDR complications, such as vitreous haemorrhage and macular detachment, show that the intra-operative vitreous PO_2 was lower than that in the normal control eyes (Holekamp et al., 2006; Lange et al., 2011). While the mid-vitreous PO_2 has been used in these studies as a surrogate for retinal PO_2, it is generally thought to be a suboptimal reflection of retinal PO_2 for two reasons. First, the optical probes used are quite large, and hence they can miss focal changes. Second, the PO_2 gradients are primarily modulated by the proximity to retinal arterioles/venules, making their interpretation extremely complex (Alder et al., 1991; Alder and Cringle, 1985; Buerk et al., 1993; Petropoulos et al., 2013; Lange et al., 2011; Faberowski et al., 1989). As a case in point, when the surgeons measured the PO_2 from the same subjects closer to the retinal surface near the superficial arterioles and the macula, they found that these measurements were significantly higher in their diabetic subjects than in controls (Lange et al., 2011). Whether these high measurements reflected un-utilised O_2 being diffused into the vitreous by the already dysfunctional neurons or the eyes had gone from a hypoxic phase into a compensatory phase remains to be tested. The evidence from studies that measured the vitreous PO_2 directly over preretinal neovascular lesions further compounded this issue because these measurements were significantly higher than other areas in the macula or peripheral retina (lasered or un-lasered) (Maeda and Tano, 1996).

3.3. The effect of panretinal photocoagulation (PRP) on retinal oxygen

The efficacy of PRP in DR is mainly empirical and may be scientifically reasoned by the improved oxygen flow to the inner retina due to ablating the high-oxygen demanding rods and the subsequent thinning and increased proximity of the inner retina to the choroid. While this theoretical reasoning has never been directly proven in human subjects, using laser treatment in the normal cat, the Linsenmeier group has shown that oxygen flow to the inner retina indeed increases directly overlying these photoreceptor-ablating lesions (Budzynski et al., 2008). Interestingly, when these authors performed another model to understand better the effect of laser on the adjacent unablated retina, they found that the relatively increased inner retinal O_2 did not extend beyond 50–90 μm from these laser lesions. Together, they suggested a need for a very tight placement of these PRP lesions for the treatment to be efficient if PRP benefits are solely related to inner retinal oxygen, which remains an open question (Budzynski et al., 2008).

3.4. Oxygen in DR animal models

As outlined in the next section, the animal models used for DR suffer many limitations in replicating human DR stages, especially leakage and neovascularisation. To model the earlier stages of DR, rodents, especially the rat STZ model of type 1 diabetes, show evidence of capillary loss and leakage (Robinson et al., 2012). Investigators have measured the intraretinal PO_2 in the STZ-rats with somewhat inconsistent findings, which could be partially explained by rodent strain differences, a critically important consideration in rodent models of DR. However, the inner retinal PO_2 increased in the STZ-rats after three months

Author Manuscript Author Manuscript Author Manuscript Author Manuscript

of diabetes (Engerman and Kern, 1995; Hammes, 2005; Kern and Engerman, 1996a, 1996b; Yu et al., 2019).

4. Alterations in the neurovascular unit in diabetes

4.1. Hyperglycaemia induced neurodegeneration initiating vasoregression

When all changes within the neuro-glial-vasculature complex in diabetes are taken together, the evidence to date suggests that the retina goes through a series of events in diabetes, including early neurodegeneration, vascular hyperpermeability, vasoregression and ischaemia. Consequently, neurodegeneration and compensatory neovascularisation develop in the background of chronic hyperglycaemia (Hammes et al., 2011; Antonetti et al., 2012). The link between chronic hyperglycaemia and neurodegeneration have been investigated at length. Whilst the hyperglycaemia-induced release of reactive oxygen species (ROS) from mitochondrial has a significant deleterious effect on the retina, activation of protein kinase C (PKC), formation of advanced glycation end products (AGEs) and increased flux through the polyol pathway are also contributory factors. Hyperglycaemia also results in a decrease in neurotrophic factors and anti-inflammatory cytokines, especially from microglia. An increase in glutamate results in excitotoxic cell death, glial activation related inflammation and release of toxic chemicals and growth factors. These adverse events of hyperglycaemia on the neurons and glia can lead to increased vascular permeability, vasoregression and further neurodegeneration (Hammes et al., 2011; Antonetti et al., 2012; Kim et al., 2016b; Sohn et al., 2016; Moran et al., 2016). Nevertheless, chronic hyperglycaemia may not be the only factor that causes retinal neurodegeneration in the diabetic retina. Loss of insulin receptors, prolactin, glucagon and lipid byproducts, inflammation, overexpression of growth factors in diabetes can also cause retinal neurodegeneration (Stitt et al., 2016).

More studies are required to understand how these neurodegenerative changes affect the macula, particularly the fovea, to cause functional changes. In particular, as the inner retina is thinner in the fovea, the role of photoreceptor related oxidative stress may be relevant (Du et al., 2013). There is evidence that impaired dark adaptation, decreased contrast sensitivity, multifocal ERG deficits and reduced oscillatory potentials are present before the onset of visible retinal vascular changes (Lorenzi and Gerhardinger, 2001). These suggest abnormalities in both the outer and inner retina, but only inner retinal thinning is confirmed on OCT (Sohn et al., 2016). Changes in outer retinal thickness remain equivocal. It may be because not all these functional changes translate into measurable thinning of the retina (Park et al., 2020), in keeping with rat models of diabetes where both functional and nonvascular changes are seen early in the inner retina (Robinson et al., 2012). However, the EUROCONDOR study suggests that a significant proportion of individuals do not have any multifocal ERG deficits in eyes with early DR. The finding points to the fact that some eyes may progress to diabetic microvascular changes before neuronal changes. Alternatively, multifocal ERG may not be sensitive enough to isolate focal deficits in retinal neurons or the study period was too short (Santos et al., 2017).

Author Manuscript Author Manuscript Author Manuscript Author Manuscript

4.2. Vasoregression followed by vasoproliferation

Vasoregression can occur early before visible vascular changes, as evidenced by capillary cell loss on OCTA. Both endothelial cells and pericytes are by themselves vulnerable to the insults of chronic hyperglycaemia, including accumulation of mitochondrial ROS, inflammation, glucose modified extracellular matrix, decrease in endothelial progenitor cells and abnormal guidance cues from stressed neurons (Hammes et al., 2011). Endothelial cells may lose the integrity of their tight junctions due to an increase in vascular growth factors and cytokines, and together with an increase in endocytosis, resulting in the breakdown of the blood-retinal barrier before cell death. Both pericyte cell death and their migration away from endothelial cells further contribute to the loss of structural support for the microvasculature (Pfister et al., 2008; Moran et al., 2016).

As the duration of diabetes increases, the continued impaired nutrition and oxygen delivery, reduced pH, accumulation of pro-inflammatory cytokines, ROS and growth factors, alongside the metabolic dysequilibrium and excitotoxicity, all lead to further neurodegeneration. Furthermore, retinal ganglion cells activate endoplasmic reticulum stressors and suppress the natural repair process of the local immune system. These may be visualised on OCT as further inner retinal thinning and disorganisation termed as disorganisation of the inner retinal layers (DRIL).

Following a phase of vasoregression, vasoproliferation occurs as a compensatory mechanism to capillary nonperfusion caused by vasoregression. Although pathological neovascularisation occurs, revascularisation of the areas of capillary nonperfusion is rarely seen. In addition, macular neovascularisation is rare even in eyes with significant macular nonperfusion. Vasorepulsive factors such as semaphorins (SEMA3a) and the presence of pigment epithelium-derived factor (PEDF) have been identified in the retina. However, whether these factors are more concentrated at the macula remains unclear (Sapieha et al., 2010).

4.3. Retinal blood flow and blood velocity

Retinal microvasculopathy in DR ultimately compromises retinal blood perfusion. Retinal blood flow and blood velocity in diabetes have been studied extensively using various techniques, including FA with videography, laser Doppler flowmetry, Doppler OCT, ultrasound-based colour Doppler imaging, adaptive optics scanning laser ophthalmoscope (AOSLO), and OCTA.

Despite the wide range of techniques, the course of changes in retinal blood flow and blood velocity across DR severity are still relatively controversial. What is generally agreed upon is that more advanced DR stages are associated with reduced retinal blood flow in the setting of severe capillary nonperfusion. Most of these studies agree that retinal blood flow is significantly decreased in eyes with severe non-proliferative diabetic retinopathy (NPDR) and PDR (Grunwald et al., 1993; Kohner, 1993; Nagaoka et al., 2010; Srinivas et al., 2017). In early DR and especially in eyes without clinically observable DR, the findings have been more controversial. Whilst some studies suggested a decreased blood flow in these eyes, others showed that the blood flow and the blood velocity were increased

Author Manuscript Author Manuscript Author Manuscript Author Manuscript

in eyes without clinically evident DR (Cuypers et al., 2000; Palochak et al., 2019). These controversies may also relate to the general limitations and the highly variable (temporal and spatial) resolution of the methodologies used in the past. For example, colour Doppler ultrasonographic evaluation of blood flow has been limited to the global measurements of the large retrobulbar vasculature. In contrast, AOSLO technology (depending on the approach) can measure the capillary flow velocity in the individual retinal arterioles and venules, all the way down to the individual capillaries. Therefore, one would expect that the ability to discern potentially subtle changes in the earliest stages of DR requires techniques with the highest resolution and sensitivity.

One model for the progression of DR based on retinal blood flow suggested that there was an increase in retinal blood velocity and blood flow in the early stages of diabetes to meet the metabolic demand of the retina and to compensate for initial focal capillary closure (Palochak et al., 2019; Rosen et al., 2019). With the further capillary loss, these mechanisms ultimately reach their limit, at which point blood flow declines, leading to progressive ischaemia and damage, along with profoundly decreased blood flow and blood velocity in the more advanced stages of DR.

4.4. Capillary perfusion defects

Ischaemic injury in retinal tissue is associated with spatial redistribution and closure of retinal capillaries. Macular capillary loss causes enlargement of the intervening non-perfused neural tissue. Although there is general variation in the spatial organisation of the retinal capillaries in the different plexus based on the oxygen diffusion capacity, the threshold of intercapillary distances has been considered to be 30 μm, which is consistent with the AOSLO studies (Arthur et al., 2019; Burns et al., 2019). Compared to the lateral resolution of OCTA, which is limited by the optical aberrations of the eye (20 μm), the exquisite lateral resolution of AOSLO permits an accurate assessment of the normal capillary free zones in the retina (Arthur et al., 2019; Burns et al., 2019).

Recently, several OCTA studies quantified the area of retinal capillary nonperfusion (see section 6 for details). These studies have revealed that the capillary nonperfusion area is increased in DR and is associated with the severity of DR (Agemy et al., 2015). In addition, non-perfused areas in the DCP may be associated with macular photoreceptor disruption in DMI (Nesper et al., 2017b). The area and location of the retinal capillary nonperfusion could be a useful biomarker in DR. New tools to quantify and standardise these measurements are needed to make these biomarkers more clinically relevant.

4.5. Foveal avascular zone

The FAZ is a capillary free zone centred at the fovea. Although the normal FAZ shows great variability in healthy populations, there is extensive literature regarding the formation and enlargement of irregular FAZ after the loss of capillaries in DR (Bresnick et al., 1984). In study cohorts comparing FAZ abnormalities in various severity levels of DR, the FAZ area is associated with the severity of DR (Mansour et al., 1993). Recent OCTA studies have shown that FAZ enlargement occurs even before the appearance of clinical DR (Takase et al., 2015b). This observation suggests that the central macular capillaries

Author Manuscript Author Manuscript Author Manuscript Author Manuscript

are more susceptible to diabetes-related stress than any other part of the retina. Oxidative stress, hypoxia, inflammation, and other systemic parameters all induce endothelial cell apoptosis, and the FAZ may be more susceptible to these stressors in some individuals. However, when we consider the FAZ area in people with PDR, not all PDR eyes with similar peripheral capillary nonperfusion have a large FAZ, suggesting that there are other local factors that determine the capillary layer loss at the foveal margin. Amongst several theories explaining the FAZ development, both anti-angiogenic and axon guidance factors are contributory factors (Kozulin et al., 2009). The balance between the anti-angiogenic factors and the angiogenic factors is critical. The vascular endothelial growth factor (VEGF) favours anti-angiogenesis at the FAZ, repelling vascular growth towards the fovea. The pigment epithelium-derived growth factor (PEDF) performs anti-angiogenic effects by inducing the Fas/Fas ligand-mediated apoptotic pathway, which targets the endothelial cells of the immature vessels. Alterations of this ratio may be of significance in a stressed retina. In a VEGF stimulated environment, PEDF induces apoptosis of endothelial cells through several molecular pathways that involve Fas, PPARγ, ERK and Wnt signalling. Another molecule that may be responsible for vasoregression of the FAZ before DR is angiopoietin-2 (Ang2) because Ang2 can cause vessel regression and endothelial cell death in the absence of VEGF (Lobov et al., 2002; Volpert et al., 2002). Ang2 is also associated with reducing and propelling pericyte migration (Hammes et al., 2004). Finally, the role of leukostasis in the pathogenesis of an enlarged and irregular FAZ has not been fully explored, although leukostasis is a well-established trigger for retinal capillary nonperfusion (Campochiaro, 2015).

4.6. Choriocapillaris and choroid

The choroid is the least studied vascular bed in DMI, although the choriocapillaris predominantly supplies the outer retina. In addition, the foveola is dependent solely on the choroid. Imaging the choroid remains a challenge. On indocyanine angiography, early hypofluorescent spots followed by later hyperfluorescent spots of choroidal nonperfusion is associated with the severity levels of DR (Hua et al., 2013). However, the FAZ outline or area on FA do not correlate with OCT-based choroid changes, including choroidal volume, thickness, and choroidal vascularity index (Sidorczuk et al., 2021). Multiple explanations have been put forward to explain the unparalleled FAZ changes and the choroidal parameters. Several phenomena have been observed. Firstly, the choroidal changes occur earlier than retinal changes (Nesper et al., 2017a). Secondly, the choroid in DR is also affected by autonomic neuropathy. Thirdly, the choroidal changes may be more pronounced in the periphery. Lastly, inter-individual regional variability of the choriocapillaris and the technical challenges of imaging the choroid may confound the current observations. In contrast to ICG that generally does not provide decent images of the choriocapillaris, using OCTA allows better visualisation and evaluation of the choroidal layer. However, studies are scarce regarding diabetic choroidopathy at present. The lower signal penetration and higher susceptibility to shadow artefacts of the widely available spectral-domain OCTA devices have been particularly daunting. For imaging the choroid, especially in eyes with macular thickening or exudates, swept-source devices have better penetration and higher image quality and reliability (Lane et al., 2016).

Author Manuscript Author Manuscript Author Manuscript Author Manuscript

5. DR histology and animal models relating to clinical features

5.1. Pericytes

The classic histopathological studies in the 1960s showed that pericyte loss and basement membrane thickening are some of the earliest changes in DR (Cogan and Kuwabara, 1963; Cogan et al., 1961). Retinal capillary walls are composed of endothelial cells tubes surrounded by a basement membrane and a dense network of perivascular cells, the pericytes. Retinal pericytes are contractile and play an important role in regulating blood flow by maintaining the neurovascular unit and providing mechanical strength to the vessel walls by stabilising the endothelial cells. Retinal pericytes are also essential components of the inner blood-retinal barrier (Armulik et al., 2011; Klaassen et al., 2013). These cells surround the retinal capillary lumen and are also attached to the glial cells. The loss of pericytes and the thickening of the basement membrane lead to the change in vascular wall stiffness and occlusive angiopathy, ultimately leading to tissue hypoxia and damage. In addition, pericytes control endothelial cell integrity via secretory signals and direct cell-cell contact. Reduced pericyte-endothelial cell contact causes the release of inflammatory cytokines, the increase of leukocyte-endothelial cell adhesion and entrapment (Chibber et al., 2007), and platelet hyperactivity that might lead to the occlusion of the retinal capillaries (Kaur et al., 2018).

Pericyte loss is also thought to contribute to the formation of microaneurysms. In a mouse model where pericytes were depleted from the inner retinal vessels, the endothelial cell proliferated and resulted in aneurysm-like structures (Ogura et al., 2017). These facts agree with the histological finding in the human retina, where endothelial cell proliferation occurs in retinal microaneurysms (Cogan and Kuwabara, 1963).

Furthermore, pericyte loss also leads to increased retinal vascular permeability. In mouse models, a deficiency in pericytes induces endothelial cell inflammation, perivascular macrophage infiltration, and VEGF overexpression, thereby increasing the vascular permeability (Hellström et al., 2001; Ogura et al., 2017; Park et al., 2017).

These studies suggest that pericyte loss contributes to the clinical findings in DR, such as microaneurysms, leakage, capillary nonperfusion area, and intraretinal microvascular abnormalities. However, vasoregression of the FAZ in the absence of DR may be better explained by direct hyperglycaemia-induced oxidative stress, causing pericyte loss and focal acellular non-perfused capillaries in the FAZ before diffuse destruction in the rest of the retina (Hammes et al., 2011).

The retinal vascular endothelial cells on the luminal side directly contact the blood and form the inner blood-retinal barrier. The pericytes modulate blood flow, and the tight junctions between the endothelial cells regulate vascular permeability. In diabetes, these cells are lost, resulting in acellular capillaries; they also migrate and proliferate, resulting in neovascularisation.

Author Manuscript Author Manuscript Author Manuscript Author Manuscript

5.2. Loss of neurovascular coupling

Neurovascular coupling is a regulatory mechanism designed to adjust the retinal blood flow to a defined region of the neural retina (Newman, 2013). The neurovascular unit comprises neurons, glial cells, pericytes, astrocytes, microglia, and retinal blood vessels. Intricate mechanisms that control the interactions of these cells tightly regulate the process of neurovascular coupling and retinal blood flow. Newman et al. showed that glial cells played an important role in signalling between neurons and blood vessels (Metea and Newman, 2007). In diabetic animal models, aberrant neurovascular coupling was associated with reduced light-evoked vasodilation in the retinal vasculature without losing retinal neurons or vascular responsiveness (Mishra and Newman, 2010). In addition, the response of retinal vessels diameters to flicker stimulation was abnormal in patients with diabetes and even in those without clinically detectable DR (Bek et al., 2008; Garhöfer et al., 2004; Lecleire-Collet et al., 2011; Mandecka et al., 2007). Interestingly, a recent OCTA study showed that acute glucose ingestion in healthy subjects affected neurovascular coupling during dark to light adaption (Kwan et al., 2020). In aggregate, these studies suggest that neurovascular coupling may be highly sensitive to glucose and the derangements in neurovascular coupling precede visible vascular changes in DR, vascular hyperpermeability and capillary loss.

5.3. Choroidal changes

Choroidal changes may precede any DR and explain some cases of visual loss in people with diabetes without DR, although this is very rare. Histopathologically, diabetic choroid may show extensive capillary dropout, intrachoroidal neovascularisation, arteriosclerotic arteries, and thickened basement membranes (Cao et al., 1998; Hidayat and Fine, 1985). Choroidal blood flow was also reduced in diabetic mice (Muir et al., 2012). In addition, increased VEGF could be detected in the endothelium of choriocapillaris in the diabetic human choroid (Lutty et al., 1996). The exact relation between diabetic choroidopathy and DR is not well-defined. More specifically, the role of focal choriocapillaris dysfunction or deficit at the fovea and its contribution to vision-threatening DMI is poorly understood.

5.4. Histological changes in animal models

There have been various models to mimic DR, but their major limitation is the inability to create severe stages of human DR, especially neovascularisation. Furthermore, these models are limited by inconsistency, especially in rodents where strain differences make their features highly variable (Robinson et al., 2012).

To model type 1 DM, there are a variety of chemically induced models, of which STZ-induced DM has been the most commonly used in rodents. Depending on the dose and animal, hyperglycaemia onset occurs within a few days in this model. In the STZ-induced diabetic mice, astrocyte activation and increased astrocyte number were observed at week four to five of hyperglycaemia (Feit-Leichman et al., 2005; Kumar and Zhuo, 2010). Retinal ganglion cells (RGCs) reduction started from the sixth week (Martin et al., 2004), though others have failed to replicate this finding (Feit-Leichman et al., 2005; Asnaghi et al., 2003; Gastinger et al., 2006).

Author Manuscript Author Manuscript Author Manuscript Author Manuscript

For vascular changes, increased vascular permeability was observed earliest on the eighth day of hyperglycaemia (Kim et al., 2009), and vascular leakage was recorded from month two (Kim et al., 2012). However, these features can be highly variable depending on the mouse strains used. Researchers have reported thickening of the capillary basal lamina after 17 weeks of hyperglycaemia (Kuiper et al., 2008), while retinal acellular capillaries and pericyte ghosts were demonstrated after 6–9 months of hyperglycaemia in these mice (Feit-Leichman et al., 2005; Zheng et al., 2007a).

More notable changes have been reported in the STZ-rat models, where biochemical modifications begin to appear between 1 and 2 months after the onset of hyperglycaemia. In contrast to mice, rats require lower doses of STZ to develop diabetes (Lai and Lo, 2013). The onset of retinal lesions differs between rat strains, but several observable phenotypes, including vascular leakage, start around two weeks after diabetes onset. Diabetes-induced non-vascular changes (neuronal and glial) were reported to occur before developing changes in vascular cells and might contribute to the pathology of the vascular disease in this model (Barber et al., 1998; Kohzaki et al., 2008). However, there were variations in the reported retinal biochemistry and histopathological response to diabetes between species and even within the same species, as shown by a systematic study of the early stages of DR in three different rat strains (Sprague Dawley, Lewis, and Wistar). After eight months of diabetes, Lewis rats showed the most loss of retinal capillaries and RGCs, whereas Wistar rats showed degeneration of the capillaries without significant neurodegeneration, and Sprague Dawley rats showed no lesions at this time point (Kern et al., 2010).

In addition to the chemically induced type-1 DR model, transgenic DR animal models are also available. The Ins2Akita mouse harbouring a missense mutation in the Insulin 2 gene is a model for type 1 diabetes. The Ins2Akita mouse helps study the early progression of DR, and the loss of RGCs could be detected in a short period at 8–12 weeks (Robinson et al., 2012). Reactive microglia and decreased RGCs in the peripheral retina were observed as early as eight weeks of diabetes (Barber et al., 2005). Decreased thickness of the IPL and INL in the peripheral region was recorded at 22 weeks. Concerning vascular changes, significant increases in vascular permeability were seen when measured at 12 weeks of hyperglycaemia, and increased acellular capillaries were observed at 31–36 weeks (Barber et al., 2005; Gastinger et al., 2008). The NOD mice, in which an autoimmune process destroys the pancreatic β-cells, showed apoptosis of pericytes, endothelial cells and RGCs at four weeks (Li and Sun, 2010). Retinal capillary basement membrane thickening started at the fourth week, whereas vasoconstriction and degeneration of major vessels with abnormal microvessels formation could be detected at approximately four months of hyperglycaemia (Shaw et al., 2006).

To study type 2 diabetes, Db/db mice are often used. The Db/db mice spontaneously develop type 2 diabetes and severe obesity due to leptin receptor deficiency, with the biochemical onset of diabetes at 4–8 weeks of age. Db/db mice have also been used to study the early features of DR. After six weeks of hyperglycaemia, the reduction in the RGCs, as well as in the thickness of the central retina and the INL, was identified (Tang et al., 2011). The pericyte loss was observed after 18 weeks (Midena et al., 1989), whilst glial cells activated at 13 months of the onset of hyperglycaemia (Cheung et al., 2005). The capillary basement

Author Manuscript Author Manuscript Author Manuscript Author Manuscript

membrane thickening was demonstrated at 14 weeks (Clements et al., 1998), while acellular capillaries (Midena et al., 1989) and vessel leakage (Cheung et al., 2005) were traced at 26 weeks.

Disappointingly, none of these rodent models advance to proliferative disease. Instead, the Akimba mouse model and the oxygen-induced retinopathy (OIR) model are often used to simulate advanced DR. Akimba mouse is generated by crossing the Ins2Akita mouse (Rakoczy et al., 2010) with the Akimba (trVEGF029) mouse, a transgenic mouse model of non-diabetic neovascularisation due to transient overexpression of human VEGF. Akimba mice exhibit uneven retinal thickness, retinal oedema, and reduced photoreceptor layer thickness. With time, retinal detachment develops at eight weeks of age, and reduced RGCs number and neural retinal thickness can be found at 24 weeks. Capillary dropout, microaneurysm, vascular leakage, vascular dilation, retinal bleeding, and neovascularisation were observed in this model at eight weeks (Rakoczy et al., 2010).

The OIR model is also used to model retinal neovascularisation, though this is a neonatal model used to replicate neonatal retinopathy of prematurity. The OIR model exposes the pups to hyperoxic conditions when the retinal vasculature is still developing (at postnatal day 7). During this exposure, vaso-obliteration occurs in the pre-existing retinal vasculature. After five days of this exposure, the pups are returned to room air, resulting in hypoxic conditions of the retina, hence the growth of blood vessels and neovascularisation in the retina. These models of OIR exhibit neovascularisation and nonperfusion, and the maximum severity of neovascularisation is reached at five days post-return to room air exposure (at postnatal day 17) (Stahl et al., 2010; Zhang et al., 2017). Interestingly, these vascular changes regress spontaneously with the resumption of normal revascularisation of the retina over the following days. While these models do not have hyperglycaemia as a prominent feature, they have been used to study the angiogenic phase of ischaemic retinopathies.

Higher-order mammals, including dogs, cats, monkeys, have also been used for studying diabetic retinopathy. These models have shown many similarities to the pathology of DR in humans, and the larger eyes allow easier in vivo studies. Pancreatectomised cats exhibited microaneurysms after 5 years, intraretinal haemorrhage at 6.5 years, capillary nonperfusion and intraretinal microvascular abnormalities (IRMAs) at 7.5 years, and neovascularisation at 8.5 years following the surgery (Hatchell et al., 1995; Mansour et al., 1990). In the galactose-induced dog model, pericyte loss was found at about 1.5 years, and the destruction of endothelial cells was observed at 2 years of feeding with galactose (Kador et al., 1995). Microaneurysm formation and dot and blot haemorrhages were documented from about 2.5 years following galactose feeding, and acellular capillaries were reported at 3 years (Kador et al., 2007). Abnormalities in intraretinal microvessels, occlusion of arterioles, large arteriovenous shunts, and node formation on arterial and arteriolar walls were also shown after about 5 years of intervention (Cusick et al., 2003; Kador et al., 1995). In monkeys, STZ injection or pancreatectomy, which results in insulin dependency and hyperglycaemia, was used to model type 1 diabetics. These monkeys do not show any significant DR signs until 5 years of hyperglycaemia, and the ischaemic signs, such as microaneurysms, capillary dropout and cotton-wool spots, were observed between 6 and 15 years of diabetes (Tso et al., 1988). Monkeys that spontaneously develop type 2 diabetes have also been used.

Author Manuscript Author Manuscript Author Manuscript Author Manuscript

In this model, intraretinal haemorrhage, microaneurysms, cotton-wool spots, nonperfusion area, and IRMAs were observed following at least 3–8 years of diabetes (Kim et al., 2004).

6. Evaluation of DMI with FA and OCTA

6.1. Dye-based angiography

As the first imaging modality used to identify DMI, FA remains the current gold standard for diagnosing DMI (1991; Bresnick et al., 1984; Mansour et al., 1993). The presence and the severity of DMI are determined by assessing the best available early FA frames (defined as frames taken between 13 and 28 s from the injection of fluorescein dye) (Sakata et al., 2007).

In the Early Treatment for Diabetic Retinopathy Study (ETDRS), DMI was determined by three characteristics: FAZ size, outline, and capillary loss in the central subfield. The grading of FAZ size was only applicable to eyes in which the capillary outline was regular (round or oval). Eyes were graded using a reference circle with a radius of 300 μm- Grade 0: the size of the FAZ was less than the area of the reference circle, Grade 1: the size of FAZ was equal to the reference circle, Grade 2: the size of the FAZ was greater than the reference circle but less than a circle of 500 μm radius, Grade 3: the size of FAZ was greater than or equal to a circle of 500 μm radius, and Grade 8: where the FAZ size could not be graded.

In cases where the area could not be graded due to an irregular outline from partial destruction of the surrounding capillaries, the following grading was used- Grade 0: the outline of FAZ was normal, Grade 1: questionable (the outline was relatively round or oval, but irregularities were visible), Grade 2: the outline was definitely destroyed for less than half of the original circumference, Grade 3: the outline was destroyed for half or more of the original circumference, Grade 4: the capillary outline was completely destroyed, and Grade 8: the outline could not be graded. The grading of capillary loss had five levels: 0 (absent), 1 (questionable, Q), 2 (definitely present, D), 3 (moderate, M), 4 (severe, S). These gradings were defined by comparisons to the standard photographs (1991).

While FA remains the gold standard imaging modality for assessing the macular capillary network and DMI (1991; Spaide et al., 2015b), this modality is limited by some shortcomings. Firstly, FA is an invasive technique that requires the intravenous injection of dye. The risk of allergic reactions limits its utility in repeated examinations (Karhunen et al., 1986; Kornblau and El-Annan, 2019; Yannuzzi et al., 1986). Owing to this practical shortcoming, DMI has not been studied in pivotal epidemiologic studies of DR (Bresnick et al., 1984; Klein et al., 1992; Varma et al., 2004).

Secondly, FA only provides a two-dimensional image of retinal capillaries and cannot differentiate the three capillary networks within the retina. Precisely, observations from FA correspond mainly to the superficial capillary network. Deeper capillary networks are not well visualised with FA (Mendis et al., 2010; Spaide et al., 2015b; Weinhaus et al., 1995), and capillaries in the RNFL were seen four times more clearly than capillaries found in the deepest vascular plane (Weinhaus et al., 1995). This poor visualisation of deeper capillary networks is attributed to the light scattering in the retina, resulting in image

Author Manuscript Author Manuscript Author Manuscript Author Manuscript

degradation (Gorrand, 1979; Mendis et al., 2010). Overall, it is essential to visualise all levels of capillary flow to adequately assess the perfusion, especially in conditions like DR. Specific to DMI, the differential in perfusion between capillary layers is crucial in identifying different vascular phenotypes.

Lastly, there are limited quantitative parameters for evaluating DMI based on FA. Potentially useful metrics provided by FA, such as blood flow velocity as described by Arend et al., require custom software and complicated calculations (Arend et al., 1991). Such measurements are designed for use by reading centres but not practical for clinical application. An additional limitation is that few commercial devices have incorporated such software for clinical use. Conrath et al. attempted to simplify these methods by examining the association between ETDRS FAZ qualitative measures and the more complex quantitative metrics, such as the FAZ size and the perimeter ascertained by the manual segmentation of the FAZ. They concluded that the qualitative and the quantitative parameters were well correlated with each other and with DR severity (Conrath et al., 2005a). However, other studies using simplified DMI grading schemes showed varying results (1995; Chung et al., 2008; Mitchell et al., 2011).

6.2. OCT angiography

As mentioned earlier, OCTA can compute *en face* images of the retina vasculature by mapping the movement of red blood cells over time from volumetric OCT scans. Briefly, the differences in motion (motion contrast) are detected by comparing changes between B scans at the same location. Coupled with image processing algorithms, OCTA allows the acquisition of high-resolution depth-resolved images of the retina vasculature. OCTA has several advantages over FA. Most importantly, its non-invasive nature permits easy and practical repeated measurements, providing longitudinal information. Another advantage is the ability to analyse the retinal capillary beds within individual retina layers (Spaide et al., 2015a) (Spaide et al., 2018). The two commonly segmented layers by most commercially available OCTA instruments are the SCP and the DCP in the macular area. Histologically, the SVC correlates to the superficial vascular plexus and is composed of arteries, arterioles, capillaries, venules and veins in the ganglion cell layer. The DVC comprises the intermediate capillary plexus (ICP) and the deep capillary plexus (DCP). It correlates to the capillary network between the inner plexiform layer and the inner nuclear layer border (Spaide et al., 2015a). Data of the volumetric scans derived from the repeated B-scans can be segmented into the desired histological layers, and the angiogram of different retinal capillary plexuses can be visualised. As the cross-sectional structural scans are intrinsically and simultaneously acquired with the *en face* scans, the cross-sectional and the *en face* images can be correlated to ensure the accurate presentation of the angiogram (Spaide et al., 2018).

Several studies have reported the importance of differentiating the SCP and DCP in DMI. Early studies showed that poor visual acuity was associated with reduced perfusion in both the SCP and DCP (Freiberg et al., 2016; Samara et al., 2017). Further analysis, however, showed that poor vision was independently associated with reduced DCP perfusion alone regardless of the perfusion of the SCP (Dupas et al., 2018; Tang et al., 2020). Other

Author Manuscript Author Manuscript Author Manuscript Author Manuscript

investigators have reported an association between reduced retinal sensitivity and reduced vessel density in the DCP (Pereira et al., 2019; Tsai et al., 2020).

These structural-functional correlations are supported by histologic studies, which have demonstrated a higher vulnerability of the DCP to endothelial injury (Borrelli et al., 2019). Furthermore, ischaemic changes in the DCP were more likely to result in photoreceptor disruptions than changes in the SCP (Scarinci et al., 2015, 2016). Early histological work on primates showed that the DCP was critical in supplying the metabolic needs of photoreceptors (Birol et al., 2007; Usui et al., 2015). Ischaemic retinopathies, including DR, may compromise the metabolic needs of the outer retina (Grunwald et al., 1984) and, in particular, result in damage to the photoreceptors that reside in the watershed zone between the retinal and choroidal circulation.

There is, however, variability in the association and importance between the DCP and the DR severity (Agemy et al., 2015; Durbin et al., 2017; Li et al., 2019; Nesper et al., 2017a; Onishi et al., 2018; Sambhav et al., 2017; Tang et al., 2020; Zhang et al., 2016b). Some investigators hypothesise that early changes affect the DCP before the SCP. This finding is supported by the reports that the DCP was more strongly associated with the DR severity (Nesper et al., 2017a; Sambhav et al., 2017; Tang et al., 2020). However, others showed that both the SCP and DCP perfusion were equally associated with the DR severity (Agemy et al., 2015; Li et al., 2019; Zhang et al., 2016b). Conversely, some studies have shown that the SCP correlated best to the disease severity (Durbin et al., 2017; Ong et al., 2020). These discrepancies may be due to several factors. To begin, despite the better visualisation of the deeper vascular networks in the retina, the SCP still provides the best quality scans. The DCP is often plagued with artefacts from various sources, which result in inaccurate quantification. In addition, due to the layer segmentation border, the third vascular plexus, also known as the ICP, is indistinguishable from the DCP. This ambiguity introduces another potential confounder to the true effect of diabetes on the various capillary plexus (Casselholmde Salles et al., 2016).

There are disadvantages in OCTA imaging modality, which currently limit its use in clinical practice (Spaide et al., 2015a, 2018). Briefly, the interpretability of images is made difficult by the inherent technology and artefacts, and the resultant false signals can be divided into two categories. The first is “false negative flow”, where low OCTA signals suggest no flow, but the flow actually exists. The reason is that the generated signal is too weak over the time interval measured for flow to be considered present. Signals can also be attenuated by media opacities or from structures such as pigment in the retinal pigment epithelium (RPE). The second is “false positive flow”, where the OCTA signal is high enough to be considered flow present when there is actually none. The false-positive signals can result from noise in the image, projection artefacts or motion artefacts (Spaide et al., 2018).

It is also important for readers to note that differences exist between OCTA systems, leading to variations in findings and interpretation of OCTA images (Corvi et al., 2018; Spaide et al., 2018b; Tan et al., 2018). The two most commonly used platforms are spectral-domain (SD)-OCT and swept-source (SS)-OCT. The SS-OCT platforms utilise a longer wavelength of light, allowing for deeper scans with better penetration of retinal

Author Manuscript Author Manuscript Author Manuscript Author Manuscript

tissue (Spaide et al., 2018b). The scanning speed is also different. The commercially available SD-OCTA instruments scan at around 60–85,000 A-scans per second, whereas the SS-OCTA instruments capture 100–200,000 A-scans per second. In research settings, OCTA at mega-hertz scanning speed is also available (Migacz et al., 2019; Mohler et al., 2015; Reznicek et al., 2014, 2015). Different platforms use different algorithms to detect flow, either decorrelation detection by amplitude, phase, or both. The heterogeneity in these properties explains the resolution variation when the same eye is imaged using different systems. In addition, different software, artefact handling strategies and preset segmentation options can further affect the output (Spaide et al., 2018). These differences extend as far as nomenclature describing similar quantitative metrics.

Some investigators have compared the repeatability, reproducibility and agreement between different commercially available platforms. These attempts were performed on a small number of healthy individuals. Corvi et al. compared vessel density, fractal dimensions and the FAZ size of the superficial and deep capillary plexus on 7 OCTA devices. Significant differences were found between the devices for most of the measurements. The authors concluded that a comparison between instruments is almost impossible, and the set of measurements from various instruments are not interchangeable (Corvi et al., 2018). In contrast, Munk et al. found no significant differences in software-generated vessel density amongst four platforms. In addition, they ranked these platforms according to the number of artefacts, FAZ discernibility, vessel continuity and the number of vessel bifurcations. Three independent retinal experts scored these parameters and ranked each platform. They concluded that the Zeiss platform was superior in all of these parameters, but each platform had its strengths and weaknesses (Munk et al., 2017). In addition to vessel density, other investigators have also evaluated the variability in FAZ measurements between machines in healthy volunteers. Magrath et al. and Mihailovic et al. found that significant variability exists between platforms, and comparison between platforms should be considered with caution (Magrath et al., 2017; Mihailovic et al., 2018).

In essence, quantitative readouts from each platform should be assessed with the strengths and weaknesses in mind. Readers should understand these factors before accepting the device-generated results.

6.3. Quantitative endpoints

Quantitative measures are important for a standardised definition, longitudinal follow-ups as well as treatment guidance. Several parameters associated with DMI can be assessed quantitatively. The FAZ size is the main parameter that can be evaluated quantitatively based on both FA and OCTA. In addition, quantitative assessments of several other parameters based on OCTA have been reported (Table 1).

6.3.1. Quantitative assessment of DMI on FA—Following the detailed classification of DMI by the ETDRS study group, several studies have used a variety of methods, including quantification of the FAZ size and qualitative grading of the FAZ outline to compare diabetes versus controls as well as between eyes with increasing DR severity

Author Manuscript Author Manuscript Author Manuscript Author Manuscript

(Arend et al., 1991; Bresnick et al., 1984; Conrath et al., 2005b; Mansour et al., 1993; Sim et al., 2013b). Most of these studies relied on manual segmentation to outline the FAZ.

In addition to the FAZ size, Bresnick et al. used other quantitative markers such as the circumference, the longest diameter, and the mean diameter of the FAZ to assess the differences between eyes with DR and controls. They determined that eyes with DR had a larger FAZ circumference compared to controls. The finding was expected since an increase in the FAZ margin irregularity would have a more significant effect on the circumference of the FAZ rather than the area. In this study, no FAZ quantitative metrics were associated with the increasing severity of DR (Bresnick et al., 1984). This finding contrasts with a study by Mansour et al., who reported that the increasing mean FAZ size was associated with the DR severity. They also found that irregular FAZ contour, as defined qualitatively by irregular margins with prominent notching, interdigitations and budding, was also associated with eyes with DR versus controls (29.2% in eyes with DR vs 3.7% in control eyes) (Mansour et al., 1993). However, other quantitative FA metrics, such as capillary blood flow velocity, failed to correlate with the DR severity grades. In another study, the perifoveal intercapillary area (PICA) and the FAZ area were significantly associated with DR severity. However, additional highly labour-intensive manual measurements were required to delineate PICA (Arend et al., 1991).

For the evaluation of progressive changes in the FAZ size, some investigators have developed custom software. Sim et al. graded all images at all time points using qualitative and quantitative metrics. Qualitatively, DMI was assessed in this study based on the ETDRS criteria and classified as none, questionable, mild, moderate, or severe. Quantitatively, analysis of all FA was performed on a validated grading software platform that facilitates measurements of the FAZ. The FAZ was manually delineated and measured as square millimetres. Overall, the authors showed a 5–10% increase in the FAZ size per year in eyes with established DMI, and a more severe baseline DMI grade was associated with a more rapid enlargement of the FAZ size. The DMI progression, in terms of the FAZ size, was also predictive of progressive vision loss (Sim et al., 2013a).

6.3.2. Quantitative assessment of DMI on OCTA—In addition to the FAZ size, many other OCTA-based quantitative parameters have been proposed as useful biomarkers for evaluating DMI. While many potential quantifiable parameters can be generated from OCTA, clinically meaningful biomarkers should specifically reflect the pathophysiological changes in diabetic macula ischaemia.

Generally speaking, quantification in OCTA for DMI can be divided into the quantification of perfusion versus the quantification of nonperfusion. Perfusion quantification can be further subdivided into two broad categories: metrics describing the flow (Nesper et al., 2017a; Rosen et al., 2019) and metrics describing the vascular patterns (Alam et al., 2017; Tang et al., 2017). The quantification of nonperfusion can be categorised by location. For example, metrics at the FAZ refer to the area, the perimeter and the acircularity index, whereas metrics outside the FAZ indicate the intercapillary area (Schottenhamml et al., 2016) and the percent area of nonperfusion (PAN) (Nesper et al., 2017a) (Fig. 2). Among the many parameters described below, only vessel density, perfusion density and the FAZ

Author Manuscript Author Manuscript Author Manuscript Author Manuscript

area are commonly available in the devices. Manual adjustment of the preset segmentation of cross-section retinal layers in terms of contour, depth and boundary can be made in all commercially available platforms. Similarly, the FAZ outline can be manually adjusted on the enface image. These adjustments, in turn, will affect the quantitative readouts of the parameters mentioned above.

6.3.2.1. Metrics of perfusion

6.3.2.1.1. Quantification of flow.: The quantification of flow on OCTA is not well defined and generally is interpreted as a measure of the flow signal detected on OCTA. The terminology and definitions of some metrics of flow quantification are variable according to the instrument manufacturers or the investigators. For the purpose of clarity, these terms, definitions and origins have been summarised in Table 2. In this review, we have defined perfusion density (PD) as the total area of perfused vasculature per unit area in a region of interest. Vessel length density (VLD) is defined as the total length of perfused vasculature per unit area in a region of interest. Some commercial OCTA devices have built-in software for 'vessel density'. The VD in the Zeiss platform measures the VLD as defined above, while the VD in the Topcon and Optovue platforms measures PD as defined above.

6.3.2.1.2. Perfusion density (PD).: Perfusion density can be more precisely quantified in OCTA than FA as the vessels are not obscured by leakage (Nesper et al., 2017c). Most commercially available OCTA instruments have incorporated automated algorithms to generate perfusion density readout (Figs. 3 and 4).

Alternatively, the OCTA images can be exported to generate a perfusion density map with additional processing, generally starting with enhancement and binarisation of the OCTA *en face* images. The methodology for the following steps is variable but adheres to basic principles to mitigate the signal-to-noise ratio in order to differentiate, as best as possible, the true vessels from the background noise. One technique applied by Hwang et al. took reference from the average flow signal in the control eyes to detect the perfusion areas (Hwang et al., 2016). The other method by Jia et al. defined flow as the pixel intensity above the averaged pixel intensity of the FAZ. As the averaged pixel intensity of the FAZ was presumed to have no vascular flow, it was representative of background noise (Jia et al., 2015).

There is currently no standardised definition of perfusion density, and several measures have been used to reflect this entity. One method to quantify perfusion density is to measure the proportion of vessel pixels (that represent perfusion) versus the area of interest. This area of interest could be the entire *en face* image or the parafoveal area, another commonly used area of interest, defined as an annulus centred on the fovea with the inner and outer ring diameters of 1 and 3 mm. This method takes into account larger and smaller vessels, and the quantification measure will reflect as such.

Multiple studies have used perfusion density as a metric of association between the levels of DR severity and controls. Generally, the perfusion density decreases from controls to patients with diabetes without DR and declines even more in increasing DR severity levels. There is some variability in results due to different methodology, but most report a similar

Author Manuscript Author Manuscript Author Manuscript Author Manuscript

trend (Agemy et al., 2015; Al-Sheikh et al., 2016; Kim et al., 2016a; Salz et al., 2016; Samara et al., 2017; Zahid et al., 2016).

6.3.2.1.3. Vessel length density (VLD).: Vessel length density, in contrast to perfusion density, is another metric to quantify flow. This metric measures the density of the perfused pixel length rather than the density of the perfused pixel area. This process involves converting each vessel regardless of size to one-pixel width or "skeletonisation". The ratio of the pixels representing the total skeletonised vessel length to the pixels representing the area of interest is then presented as the "vessel length density". Both PD and VLD metrics have been used in various studies. The difference is that PD allows larger vessels to count toward the total measure of flow, whereas large and small vessels carry the same weight in VLD (Figs. 3 and 4). It is also important to note that the nomenclature used by various devices for the same parameter may vary.

6.3.2.1.4. Perfused capillary density (PCD).: Perfused capillary density is defined as the vessel density that excludes the non-capillary blood vessels. This metric is assessed by subtracting the pixels representing non-capillary blood vessels based on an arbitrary pixel intensity defined by the authors from the entire OCTA image. The subsequent subtracted image is binarised, and pixels representing capillaries are quantified as a ratio to the total parafoveal area (Rosen et al., 2019). Rosen et al. showed that the PCD was a much more sensitive marker to detect the difference between DR severities (Rosen et al., 2019).

6.3.2.1.5. Adjusted flow index (AFI).: This metric is a surrogate marker for blood flow in an individual OCTA scan. By using phantom studies, Tokayer et al. showed that OCTA imaging with the split-detection algorithm exhibited a linear relationship between the pixel intensity and the flow speed, which was within a relevant range for measuring physiologic retinal blood flow. Notably, this relationship was saturated at higher speeds, with a plateau-like configuration at lower speeds (Tokayer et al., 2013). To calculate the AFI, the image is first adjusted for noise, and then the pixel intensity for the vessels is converted into an index, which can be taken as a marker for flow (Nesper et al., 2017a).

6.3.2.1.6. Fractal dimension (FD).: The degree of complexity of natural objects or shapes is described by the parameter "fractal dimension" (FD), which is less than the spatial dimension subtended by the pattern. Formulas exist for mathematical models of fractals. However, in nature, a simple method to measure the FD of a two-dimensional shape, also the method used in most studies, is to divide the pattern into a grid of squares (box-counting). The number of boxes at a particular scale that has part of the pattern in it is counted. This count is repeated when the scale of the squares of the grid is increased. The FD for normal retinal vasculature based on colour fundus photography has been found to be approximately 1.7. In relation to DMI, the box-counting method has been used by most studies that measure FD on OCTA, and changes secondary to ischaemia is hypothesised to reduce the FD as a result of the reduction in the vessel density (Tang et al., 2017, 2020; Zahid et al., 2016). Interestingly, in one cross-sectional study, FD was shown to worsen with the progression of DR but with a relative improvement in the panretinal photocoagulation

Author Manuscript Author Manuscript Author Manuscript Author Manuscript

(PRP) treated eyes, suggesting vascular remodelling following the therapy (Fayed et al., 2019).

6.3.2.1.7. Vessel tortuosity.: In a tube model, the vessel tortuosity did not begin until a critical pressure of transmural pressure was reached (Kylstra et al., 1986). Compared to large vessels, smaller vessels might be more sensitive to hemodynamic changes. Vessel tortuosity has been used by some studies to determine the complexity of the vasculature on OCTA. This metric is defined quantitatively as the ratio of the geodesic distance (the minimum length) of a skeletonised vessel to the Euclidean distance (the shortest linear distance) between the two ends of the same vessel. Lee et al. found that the vessel tortuosity increased with worsening DR severity. However, in this cross-sectional case-control study, the prior treatment history of the participants was unclear; hence the reduction in vessel tortuosity could have been confounded by the prior treatments in eyes with PDR (Lee et al., 2018). In a different study, the SCP large vessel tortuosity was found to increase with increasing DR severity. It was also worst in PDR but improved with PRP, suggesting this metric may be a useful marker for disease severity as well as treatment response (Fayed et al., 2019).

6.3.2.1.8. Vessel diameter index (VDI).: The vessel diameter index (VDI) is calculated as the area occupied by the blood vessels from the binarised image over the total length of the blood vessels from the skeletonised image, representing the average vessel calibre of the blood vessels. Increased VDI was shown to be correlated with higher fasting glucose levels (Alam et al., 2017; Tang et al., 2017).

6.3.2.2. Metrics of nonperfusion

6.3.2.2.1. Foveal avascular zone (FAZ).: In DR, the enlargement of the FAZ occurs after the loss of capillaries in the adjacent vessels; therefore, the most common approach is to measure the area of the FAZ. There is a significant correlation between the FAZ size on OCTA (SCP) and FA, with studies reporting intraclass correlation coefficient (ICC) of 0.885–0.9 (Cennamo et al., 2015a; La Mantia et al., 2019; Shahlaee et al., 2016). Due to the non-invasive nature of OCTA, this modality has been used to evaluate patients with diabetes without clinical DR. In these asymptomatic patients with no clinically visible DR, a significantly enlarged FAZ compared to healthy controls has been reported by many investigators (de Carlo et al., 2015; Di et al., 2016; Takase et al., 2015a). A significant correlation between the OCTA FAZ area and visual acuity in patients with DR has also been established (Balaratnasingam et al., 2016). Several metrics have been used to characterise the FAZ. These include the FAZ area, perimetry, and acircularity index (Fig. 4).

6.3.2.2.2. FAZ area and perimeter.: The FAZ area on OCTA is a measure that is most closely related to the original measure of DMI as described by the ETDRS investigators. While in the ETDRS, the FAZ area was measured using a standard grid overlaid on the FA, advances in imaging software have allowed for much more accurate measurements of the FAZ area. The difference in the definition of an enlarged FAZ is the most notable discrepancy between FA and OCTA measurements. In the ETDRS study, an enlarged FAZ size was defined as any FAZ area larger than the reference circle of radius 300 μm, equating to 0.28 mm^2. In contrast, OCTA studies of normal eyes suggest that the upper range of the

Author Manuscript Author Manuscript Author Manuscript Author Manuscript

FAZ size was about 0.5 mm^2 (Magrath et al., 2017; Samara et al., 2015, 2017). There are several reasons for this difference. First, OCTA signal derived from flow threshold may not detect all the parafoveal vessels, resulting in a larger than actual FAZ area. Second, different platforms and patient characteristics, such as ethnicity, axial length, age and gender, may also affect the normal FAZ size (Iafe et al., 2016; Sampson et al., 2017; You et al., 2019). The definition of an enlarged FAZ on OCTA may be considered as a threshold of at least two standard deviations more than the average FAZ measured on OCTA. This consideration was the strategy adopted by the diabetic retinopathy clinical research network in selecting the central subfield thickness threshold for centre-involved diabetic macular oedema in clinical trials (Diabetic Retinopathy Clinical Research et al., 2012; Diabetic Retinopathy Clinical Research et al., 2012).

The FAZ area can be calculated by manually delineating the FAZ detected on OCTA. Early OCTA studies established that manual segmentation resulted in a good agreement of the FAZ area between the graders (de Carlo et al., 2015; Takase et al., 2015a). This agreement was largely due to the high-contrast images of the foveal capillaries acquired on OCTA beyond what could be appreciated on FA (Al-Sheikh et al., 2016; Bhanushali et al., 2016; de Carlo et al., 2015; Freiberg et al., 2016; Samara et al., 2015; Takase et al., 2015a). Subsequent measures of the FAZ area can be quantified by pixels, which can be converted to square millimetres based on a set magnification factor. Likewise, the FAZ perimeter can be derived from the manually delineated length.

With the advent of sophisticated imaging recognition techniques and algorithms, semi-automated methods have been developed to quantify the FAZ area and associated parameters. For example, several studies required manually defining the “seed point”, the fovea centre, and some suggested using either an active contour model (Chan and Vese, 1999) or a region growing algorithm (Tang et al., 2017) to delineate the FAZ automatically.

Lu et al. developed a fully automated algorithm by defining the seed point as the centre of the image (assuming this was the fovea centre). Similarly, applying an active contour model (GGVF snake algorithm) could automatically delineate the FAZ showing a good agreement with manual segmentation (Lu et al., 2018). Despite these new FAZ detection techniques, the interpretation of capillary dropout associated with an enlarged FAZ can still be challenging, as illustrated in Fig. 5.

6.3.2.2.3. FAZ acircularity index and circularity index (FAZ-AI and FAZ-CI).: The FAZ acircularity index (FAZ-AI) is defined as the ratio of the perimeter of the FAZ to the perimeter of a circle with an equal area, whereas the FAZ circularity index (FAZ-CI) is quantified as 4π times the ratio of the FAZ area to the perimeter squared. A perfect circle will have a CI and an AI of 1 or 100%. When the shape is less circular, the CI will go down whilst the AI will go up. To evaluate the FAZ circularity, the FAZ needs to be outlined either automatically or manually. Some commercially available OCTA instruments automatically outline the FAZ (which may also be manually adjusted) and provide automated FAZ circularity assessment.

Author Manuscript Author Manuscript Author Manuscript Author Manuscript

Shiihara et al. showed that the shape of the FAZ might better characterise the FAZ as heterogeneity exists in the size of FAZ among the normal population. Assessment of the FAZ circularity might be more informative of disease-induced microvascular changes than the FAZ area because once the obstruction of the innermost capillaries surrounding the fovea occurs, the FAZ adopts an irregular shape (Shiihara et al., 2018). The other advantage of using circularity is its robust nature and is not affected by the ocular magnification and the image scaling.

6.3.2.2.4. Intercapillary area/avascular area.: Several OCTA parameters have been used to quantify macular ischaemia on OCTA by assessing the spaces between the vessels. These include perifoveal intercapillary area, total avascular area (TAA) and extrafoveal avascular area (EAA). These measures address vascular changes in the perifoveal and the parafoveal areas, offering complementary and additional information to the FAZ (Lu et al., 2018).

Perifoveal intercapillary area (PICA) is determined by finding the connected components between the vessels of a binarised image. Schottenhamml et al. assessed the means of the 10 and 20 largest PICAs, either including and excluding the FAZ, showing that all four metrics were good in differentiating DR severity, but the mean of the ten largest PICAs offered the best discrimination (Schottenhamml et al., 2016). Krawitz et al. evaluated PICAs by the perfusion standard deviation mapping approach on OCTA. They showed that the PICAs were associated with the severity of DR using this method. However, in this study, they only studied the SCP layer (Krawitz et al., 2018).

The TAA and EAA are defined as the total non-flow areas and the total non-flow area outside a 1-mm-diameter circle centred on the fovea. Various techniques may be applied to differentiate the background noise from the true non-flow signals. Lu et al. showed that the EAA was more sensitive than the FAZ size in differentiating DR severity (Lu et al., 2018).

6.3.2.2.5. Percent area of nonperfusion (PAN).: The metric “percent area of nonperfusion” attempts to improve detection by distinguishing the vessels and the nonperfusion areas from the background noise. It is calculated based on the pixel intensity binarised by a global threshold in each eye. Mean noise pixel intensity (background intensity) within the FAZ is obtained, and all pixels with the intensity above the background intensity are considered “vessels.” The pixels with the intensity below the background intensity are considered “nonperfusion” (Nesper et al., 2017a).

6.3.2.2.6. Geometric perfusion deficits (GPD).: Chen et al. recently quantified geometric perfusion deficits (GPDs) by thresholding the capillary perfusion distance (30 μm) in the SCP and DCP layers after excluding the FAZ. The 30-μm threshold represents the physiologic vessel-free area and the theoretical oxygen diffusion distance, beyond which the tissue would be ischaemic (Arthur et al., 2019; Burns et al., 2019). These authors showed that the GPD was significantly higher in the DR eyes than in the normal eyes. They also showed that GPD had superior repeatability to vessel density (Chen et al., 2021).

Author Manuscript Author Manuscript Author Manuscript Author Manuscript

6.4. Technical considerations for DMI assessment on OCTA

Most of the assessed parameters are based on *en face* OCTA images generated by assigning flow signals to the preset boundaries of the retinal layers, thereby investigating the capillary plexuses of interest. These boundaries are based on the histological understanding of the normal eyes. Therefore, potential inaccuracies exist in segmentation if the layers differ from the expected thickness due to disease or normal variation. Moreover, co-existent DMO presents specific challenges to the assessment of DMI using OCTA. Variations in the quantification of the FAZ area may also result from different outlines selected (Fig. 5). Furthermore, developmentally and histopathologically, the macula has three vascular plexuses located within the inner two-thirds of the retina. Most commercial software uses arbitrary boundaries to split these plexuses into “superficial and deep”, without general agreement on the segmentation boundaries, creating potential variabilities in these plexuses. Importantly, the intermediate plexus has generally been shown to change in a similar direction to the deep plexus, and thus incorporating the ICP with the SCP may create unwanted confounding effects (Campbell et al., 2017b; Cuenca et al., 2020; Spaide et al., 2018b).

6.4.1. Eyes with DMO—*En face* OCTA imaging provides abundant information regarding the perfusion of the segmented layer of interest. However, this is dependent on accurate segmentation, which is difficult in the case of a diseased eye even with meticulous manual adjustment of the segmentation. In the context of DMI, this is especially challenging as often these eyes have concurrent DMO (Fig. 6). DMO is characterised by the presence of cysts or fluid in various retinal compartments that distorts the normal anatomy, making it almost impossible for current algorithms based on normal retinal architecture to segment retinal layers of interest correctly. As a result of this incorrect segmentation, improvement in perfusion may be observed with the resolution of DMO. This misinterpretation is because the retinal cysts appear avascular on DMO, and when the cysts disappear as the DMO resolves, the OCTA device mistakenly interpreted it as an improvement of perfusion (Fig. 6) (Spaide et al., 2018a).

6.4.2. Eyes with DRIL—Segmentation generally works well in eyes with normal retina architecture, but it may be less effective when applied to eyes with disrupted anatomy, as in the case of eyes with DMI.

Disorganisation of the retinal inner layers (DRIL) may be present in diabetic eyes (Fig. 7). By definition, the boundaries of the RGCL/IPL, the INL, and the outer plexiform layer (OPL) become indistinct in these eyes (Vujosevic et al., 2018, 2019a). Focal or diffuse thinning of one or more retinal layers may co-exist, further complicating the process. These structural changes can lead to inaccuracies when preset segmentation boundaries are applied. Layers may be segmented to be too thin or thick, and sometimes the layers are missing. This “misinterpretation” of segments compounds the errors of visualisation and quantification of vasculature in each layer of interest (Fig. 6).

In both DMO and DRIL, the segmentation artefact can be overcome by viewing the OCTA B-scans to ensure that segmentation boundaries are correctly placed. Most commercially

Author Manuscript Author Manuscript Author Manuscript Author Manuscript

available software allows manual correction of the segmentation boundaries in cases of algorithm failure, but this process can be time-consuming and not practical in a clinical setting (Spaide et al., 2018a).

6.4.3. Other sources of artefacts on OCTA—Various other artefacts exist that interfere with the interpretability and quantification of OCTA. Generally, the DCP is more prone to artefacts than the SCP due to lower signal strength which may result from a variety of reasons, including media opacity (shadow), astigmatism, defocus or incorrect positioning of the OCT instrument. OCTA signal attenuated by the above-mentioned reasons or other insults is usually coupled with higher background noise. The lower signal-to-noise ratio creates images in which the minor details cannot be differentiated from the background noise. The ratio is especially critical in quantifying capillary networks in DMI as minute capillaries in the perifoveal area may be lost in the background noise (Spaide et al., 2015a).

Various commercial instruments have both an indicator of signal strength as well as compensating proprietary algorithms to denoise the OCTA images. Multiple image averaging is another potential technique to decrease the speckle noise, thereby enhancing OCTA images. This technique has been well established in enhanced OCT B-scans (Sakamoto et al., 2008; Sander et al., 2005) and applied to OCTA to optimise image quality (Spaide and Ledesma-Gil, 2020; Uji et al., 2018). This technique may be technically challenging and requires post-acquisition manipulation of the OCTA scans. In addition, averaged images may result in loss or addition of information.

Projection artefact results in false flow signals from a more superficial layer (e.g. SCP) being detected in the deeper layers due to reflection from a highly reflective deeper layer (e.g. RPE) (Campbell et al., 2017a). Projection of the SCP can lead to erroneously high vessel density in the DCP. These shortcomings can be mitigated by software correction techniques that suppress the projections, including the use of subtraction algorithms (Zhang et al., 2015, 2016a).

Motion artefacts can also result in widespread decorrelation and shearing or gaps in the entire *en face* image. These movements can result from either gross eye movements or minute movements secondary to saccades or loss of fixation. Motion artefacts, in general, result in poor quality images that may be unusable due to the loss of information. When quantifying, motion artefacts lead to missing signals in the particular B-scan involved. Currently, motion artefacts are corrected by eye-tracking. With such techniques, corrective measures can be taken, and areas affected by motion artefacts can be rescanned. Several scan quality parameters such as fine vessel visibility, centration, tilt and motion artefacts were found to affect the repeatability of retinal capillary measurements necessary for accurately assessing the retinal vasculature (Fenner et al., 2018). A recent study by Holman et al. showed that the three most prevalent artefacts for OCTA were motion, shadow and defocus artefacts. Further operator acquisition training was found to be sufficient to overcome these artefacts (Holmen et al., 2020).

While artefact removal and denoising have the advantage of producing OCTA images with higher resolution, they may also introduce errors. This disadvantage of artefact removal,

Author Manuscript Author Manuscript Author Manuscript Author Manuscript

especially the denoising technique, is that the important information from small vessels may be lost inadvertently, resulting in an inaccurate interpretation of areas of nonperfusion. Likewise, projection artefact removal may subtract true flow signal in the deeper layers in areas mistakenly taken as the projection from the more superficial layers. Lastly, while motion artefacts can be overcome by repeating the scans in the affected areas, this process may lengthen the time to acquire the OCTA image (Spaide et al., 2015a; Spaide et al., 2018a).

Overall, each of the features assessed with OCTA detailed above is substantiated by the hypothesised pathophysiology of DMI. However, different parameters may be affected more during different stages of the disease. They may all constitute a part of the overall measure of DMI with no singular metric that appears to be superior. Furthermore, there are technical considerations, particularly related to quantification, that are specific to each parameter. The ideal metric should consider the mechanistic pathophysiology and the impact of ischaemia on the retina. This may not exist in one measure; hence we suggest that a variety of measures should be taken into account to reflect both the perfused and non-perfused measures. They should also be easily attainable and simply quantifiable. In addition, these metrics should also be applicable to relevant layers of the retina, especially the DCP, which has shown to be an important layer that affects functional outcomes. Specific to diabetes, imaging parameters should also be interpreted in the context of other mechanisms of vision loss in DR, in which ischaemia is just one of the mechanisms. Others include vascular permeability, inflammation, and neurodegeneration. Shortcomings of OCTA should be considered. These include image quality, artefacts, and reproducibility, especially if OCTA is used to track longitudinal changes. Obtaining good quality OCTA in a clinical setting may also be challenging in the presence of media opacity or DMO that may affect accurate segmentation. The post-processing of OCTA images can be very complex in determining the actual quantitative metrics, which may not be immediately accessible to most clinicians.

6.5. Generalised arteriolar narrowing and DMI

Eyes with more severe DMI have a narrower arteriolar calibre and an increased FAZ size. More than ¾th of the subjects with narrow arterioles may have DMI, and the arteriole calibre is reversely correlated with the severity of DR and DR-associated co-morbidities (Liew et al., 2015). The correlation between macular capillary loss and venular calibre has not been reported.

6.6. Generalisability of DMI to other causes of macular ischaemia

Macular ischaemia may be consequent to several vascular diseases. While DMI is a gradual process, retinal vein occlusions (RVO) are acute events, in which macular ischaemia occurs more rapidly and visual loss is more common. The RVO studies suggested that the DCP correlated better with the degree of ischaemic damage and visual acuity than the SCP (Chung et al., 2018; Nobre Cardoso et al., 2016; Samara et al., 2016; Suzuki et al., 2016). It is unclear whether the anatomical configuration of the DCP makes it more vulnerable to acute ischaemia than SCP. Whilst DCP ischaemia may disrupt the photoreceptor layer on OCT, DRIL may indicate the SCP is also significantly affected during the ischaemia

Author Manuscript Author Manuscript Author Manuscript Author Manuscript

(Moussa et al., 2019; Wakabayashi et al., 2017). It is likely that various phenotypes may emerge based on the degree of SCP and DCP involvement in macular ischaemia due to various retinal diseases (Moein et al., 2018).

7. Functional correlates of DMI

7.1. Prevalence of DMI and its relation to visual acuity

DMI is usually a presumptive diagnosis for unexplained visual loss in people with DR, especially in the absence of DMO or neovascularisation (Arend et al., 1995) (Sim et al., 2013b). Therefore, the prevalence of DMI in a population with diabetes is dependent on the DR severity grade of the population, definition and grading of DMI, and the device used to assess DMI (Sim et al., 2013b).

In eyes with DMO, the presence of DMI is a common cause for non-resolving macular oedema, recurring macular oedema, and visual impairment. Eyes with DMO improve with anti-VEGF therapy both in terms of visual acuity and resolution of macular fluid. Nevertheless, improvement in central macular thickness with anti-VEGF therapy only modestly correlates with visual acuity gains. Co-existent DMI may be one of the reasons, although it is challenging to quantify DMI pre and post anti-VEGF therapy for DMO. Large prospective studies such as the RESTORE study did not find a clear association between reduced treatment effect and increasing DMI. However, those observations were based on simplified schemes for grading DMI on FA (Gerendas et al., 2018).

Multiple studies have found that visual function is affected in DMI (Arend et al., 1995, 1997; Bresnick et al., 1975; Onishi et al., 2018; Tyrberg et al., 2008; Unoki et al., 2007). However, the exact point at which DMI becomes the predominant factor that determines vision loss in the natural history of DR is unknown. Although rare, there have been some reports of spontaneous reperfusion in diabetic patients following prolonged ischaemia (Takahashi et al., 1998). The relative severity of ischaemia between the SCP, DCP and choriocapillaris may affect visual function differently. Furthermore, other structural changes such as DMO and neuronal loss may also affect visual function. We propose a scheme in which DMI alone or complicated with DMO and/or neuronal loss may ultimately result in visual loss (Fig. 7). Traditional testing with visual acuity may not be sensitive enough to reflect the impact of DMI, further complicating the assessment of functional correlates of DMI. Other functional evaluations, such as microperimetry, may be more reliable to assess structure-function correlation.

7.2. Correlation of DMI phenotypes with functional assessments

The level of functional impairment may vary according to the severity as well as the phenotype of DMI. Currently, these variations within DMI may explain the challenge to decipher the proportion of patients who lose vision due to DMI even in eyes previously treated with panretinal photocoagulation. Moreover, the combination of neuronal changes such as DRIL (Moore et al., 1999) and thicker central retinal thickness (CRT) in eyes due to DMO may also contribute to poor visual acuity in eyes with an enlarged FAZ or increased PICAs (Moein et al., 2018). When DMI is defined by an enlarged or an irregular FAZ in

Author Manuscript Author Manuscript Author Manuscript Author Manuscript

patients with DR, the reports on the relation between DMI and visual acuity is conflicting (Sim et al., 2013b) (Fig. 8). As both the SCP and DCP changes are observed in DMI and negatively impact visual acuity, one crucial question is whether the contribution proportion of these plexus influences the severity of the functional loss.

Several reports have shown that the visual loss in diabetic eyes correlated more with the alterations in the DCP than in the SCP (DaCosta et al., 2020; Gill et al., 2017; Samara et al., 2017). However, when considered together, the length of the photoreceptor layer disruption, the DRIL length, and the FAZ circularity are all independent determinants of visual acuity (Endo et al., 2021). When linking the association between these structural or vascular changes with visual acuity, decreased vessel density in the DCP by itself is sufficient to cause visual impairment, independent of the presence of DRIL. In contrast, in eyes with DRIL alone without photoreceptor disturbance, the SCP is generally affected. However, eyes that have perfusion deficits in both the SCP and DCP appear to have a more functional loss, probably due to both inner and outer retina disturbance (Hsiao et al., 2020; Moein et al., 2018). What adds to this complexity is that the role of choriocapillaris in DMI related visual loss needs to be explored, too, as photoreceptors are located in the watershed zone between the outer retina and choroid, further increasing its vulnerability to ischaemia (Birol et al., 2007; Iwasaki and Inomata, 1986; Linsenmeier and Zhang, 2017; Park et al., 2016).

7.2.1. Phenotypes of DMI—There are likely to be various clinical phenotypes of DMI that may explain the degree of visual function losses. If the SCP is more compromised than the DCP, the eyes are likely to manifest as DRIL and an enlarged FAZ, while eyes with insufficient DCP are likely associated with ellipsoid disruption. However, due to the complex relationship between the SCP and the DCP through the intermediate plexus, the relative involvement of the SCP and the DCP may explain various structure-function phenotypes. Eyes with co-existent DRIL and photoreceptor disturbance probably have a more severe localised compromise of the retinal circulation (Nesper et al., 2017a). Hence, several distinctive phenotypes of DMI can be derived from the layer by layer analysis on OCTA based on the changes observed in the SCP and the DCP (Abdelshafy and Abdelshafy, 2020; Dupas et al., 2018; Samara et al., 2015).

7.2.1.1. Generalised DMI.: A generalised reduction of vessel density is observed in both the SCP and DCP (Fig. 9). This global reduction is often accompanied by structural OCT changes such as DRIL or outer retinal atrophy (Spaide, 2015). This phenotype may result in direct functional loss, as studies have demonstrated a correlation between a lower VD in both layers with poor vision in eyes with no DMO (Hsiao et al., 2020). Even in eyes with concurrent DMO, investigators have observed that imaging metrics of both the vascular capillary perfusion and the nonperfusion are independently correlated with visual acuity, in addition to the presence of macular oedema and photoreceptor disruption (Hsiao et al., 2020). Whether these phenotypes represent stages along a fixed progression pattern has not been studied.

7.2.1.2. Predominant DCP-ischaemia.: In this phenotype of DMI observed on OCTA, there is a greater reduction in the vessel density in the DCP compared to the SCP (Fig. 10).

Author Manuscript Author Manuscript Author Manuscript Author Manuscript

An overall reduction in the DCP may be a better predictor for DR severity and risk of visual acuity loss due to its contribution of blood supply to the photoreceptors (Abdelshafy and Abdelshafy, 2020; Bhardwaj et al., 2018; Carnevali et al., 2017; Chen et al., 2017; Dupas et al., 2018). Foveal microstructural changes in the outer retinal layers such as subfoveal loss of integrity or reflectivity of the ellipsoid zone correlate with zones of capillary nonperfusion in eyes with DR without DMO, particularly with the areas of DCP capillary nonperfusion (Balaratnasingam et al., 2016; Dmuchowska et al., 2014; Lee et al., 2013; Scarinci et al., 2015, 2016; Yeung et al., 2009). Therefore, a decrease in blood flow in the DCP in DMI may also be responsible for the decrease in visual function (Nesper et al., 2017a). Furthermore, histological studies have shown that the DCP may be more vulnerable to endothelial injury due to ischaemia (Moore et al., 1999). However, foveal cones solely depend on the choroid for nutrition (Nickla and Wallman, 2010). Therefore, visual acuity may not be affected. Microperimetry may be a better visual function test in these circumstances.

An additional mechanism through which the predominant DCP ischaemic phenotype may lead to functional loss is the propensity to develop recurrent or persistent DMO. Spaide et al. showed that the VD mismatch between the DCP and the SCP was associated with the recurrence or persistence of oedema. This phenomenon was demonstrated by the proximity between the areas of DCP VD loss and the areas of fluid accumulation (Spaide, 2015). This mismatch and resultant worsening of oedema have also been shown in eyes with branch retinal vein occlusion, with increased DCP to SCP VD loss being more resistant to treatment (Yeung et al., 2019). The proposed mechanism for this persistent oedema was the relative mismatch and subsequent outflow reduction through the DCP, exacerbating fluid accumulation (Spaide, 2015). The severity and phenotype of DMI may further affect the visual outcome of DMO therapy.

7.2.1.3. Predominant SCP-ischaemia.: This phenotype, which mainly involves the SCP and spares the DCP, may represent a milder or earlier stage of the disease (Fig. 11). The functional impact of this phenotype can be expected to be less severe, although most eyes with DMI are of this phenotype.

7.2.2. Methods of evaluation of function—Conventionally, visual acuity tests for high contrast macular function may not be an optimal measure of visual function in several macular diseases. Visual acuity loss represents a late stage of functional impairment and may not be deranged in the earlier subclinical stages of diseases. Earlier and better sensitive measures such as impaired contrast sensitivity, colour vision loss, and electroretinographic changes may be detected in eyes with preserved visual acuity (Tzekov and Arden, 1999). Only advanced stages of DMI are associated with poor visual acuity.

Changes in multifocal electroretinogram (mfERG) have been reported even in mild DR. A longer FAZ diameter is associated with an increase in the implicit time of the innermost concentric rings and the third concentric ring in the first-order kernel mfERG. Moreover, a larger sum of the FAZ and the perifoveal inter-capillary area is also correlated with an increasing implicit time of mfERG. These findings suggest that the neuronal changes due to DMI may cause focal functional deficits before reducing the visual acuity (Molina-Martin et al., 2018; Midena et al., 2021; Santos et al., 2017; Simo et al., 2019).

Author Manuscript Author Manuscript Author Manuscript Author Manuscript

Microperimetry allows an accurate topographic correlation between the anatomical lesions in the fundus and the corresponding visual function (Molina-Martin et al., 2018). In DR, a dissociation between microperimetry and visual acuity increases with the severity of DR, suggesting that microperimetry may show focal deficits of visual function in areas of macular capillary nonperfusion before visual acuity is compromised, serving as a predictor of visual function and a superior measure of disease progression over visual acuity (Parravano et al., 2010). Reduced retinal sensitivity has been correlated with increasing DR severity. Also, compromised sensitivity corresponds to a reduced perifoveal vessel density and an enlarged FAZ area (Tsai et al., 2020; Pereira et al., 2019). Reduction of vessel density in the SCP and the DCP is independently associated with the worsening of the retinal sensitivity (Pereira et al., 2019; Scarinci et al., 2019; Tsai et al., 2020). In addition, Pereira et al. and Moen et al. have reported a correlation between retinal sensitivity and the area of DRIL on OCT (Moein et al., 2018; Pereira et al., 2019). In eyes with DMO and DMI, anti-VEGF injections can significantly improve the sensitivity without accompanying significant visual acuity improvement (Pereira et al., 2019). Reduced light sensitivity in the ischaemic macula may be explained by a dysfunction of retinal ganglion cells, explaining the loss of contrast sensitivity (Arend et al., 1997). These changes may precede visual acuity changes.

The lateral resolution of OCT is currently limited to ~20 μm, while adaptive optics has a much higher lateral resolution and allows us to image the photoreceptor cells. Both increased cone spacing on adaptive optics and decreased outer retinal reflectivity on OCT correspond to focal deficits of retinal sensitivity on microperimetry and reduced amplitudes on mfERG (Nesper et al., 2017b). In DR, a reduced perifoveal photoreceptor density and a deviation from the normal cone packing arrangement have been reported (Lombardo et al., 2014, 2016; Tam et al., 2012). The presence of photoreceptor pathology on adaptive optics also correlates with DR severity (Lombardo et al., 2016; Tam et al., 2012). Photoreceptor abnormalities on adaptive optics are also observed in areas of nonperfusion in the DCP (Nesper et al., 2017b).

Further structure-function correlation studies need to be done to accurately identify the clinical endpoints that can be utilised in clinical trials on novel agents to treat DMI or to decrease its progression. In this regard, advances in automatic measurements of perfusion indices on OCTA may aid as a non-invasive modality for diagnosing DMI and monitoring DMI progression.

7.3. Visual impairment due to DMI and DMO

While current therapy for vision-threatening DR mainly targets PDR and DMO, the underlying pathogenesis of DR is not fully addressed by laser photocoagulation or anti-VEGF therapy. As discussed in section 4.1, microvascular changes in response to hyperglycaemia play a central role in the pathogenesis of DR and its complications. Luminal narrowing has been shown to result from endothelial cell hypertrophy in the deep capillary plexus due to VEGF overexpression (Hofman et al., 2001). In addition to VEGF, other cytokines, including TNF-α and inducible nitric oxide synthase, have been proposed to mediate the tissue injury due to ischaemia through inflammation and neurotoxicity (Lam

Author Manuscript Author Manuscript Author Manuscript Author Manuscript

et al., 1999). One of the effects of VEGF is to increase ICAM-1 expression in the retinal capillary endothelial cells, leading to leukocyte plugging (Zheng et al., 2007b; Joussen et al., 2002; Miyamoto et al., 2000; Nishiwaki et al., 2003). The leukocytes adhere to the vasculature through CD18 and remodel it through Fas ligand (FasL)-mediated endothelial cell apoptosis. These early changes are responsible for ischaemia observed in DR. Ischaemia alone may lead to functional loss, as detailed in sections 7.1 and 7.2. In addition, a subset of eyes with DMI may develop DMO and suffer accelerated visual loss.

We propose that DMO may be a result of DMI. This proposal is supported by studies of the underlying pathophysiology. Ischaemia, which can initiate endothelial cell injury, can lead to progressive disruption of the blood-retinal barrier due to the breakdown of tight junctions and increased vascular permeability. Recruitment of inflammatory cytokines further exacerbates the increase in vascular permeability, leading to hypersecretion of transudation and exudation and accumulation of extracellular fluid. An additional mechanism outlined in section 7.2.1.2 also suggests that the mismatch in the decrease of vessel density in the DCP and the SCP may result in further loss of outflow from the DCP, thereby exacerbating the imbalance between production and clearance of fluid. According to Starling law, the mismatch results in extracellular fluid accumulation in the retina (Daruich et al., 2018). Developing therapies to address DMI may therefore reduce the incidence of DMO.

Despite the availability of anti-VEGF therapy as a treatment for DMO, the response is variable. Persistent macular oedema has been reported in 40% of the eyes after initiation of 6 monthly ranibizumab in protocol I, and 16% met the definition of chronic persistent macular oedema at year 3 (Bressler et al., 2016). The degree of underlying DMI may influence the responsiveness of DMO (Daruich et al., 2018; Joe et al., 2019; Touhami et al., 2021). It has been proposed that eyes with predominant inflammatory components may show a better response to steroids than to anti-VEGF. We propose that eyes with more severe DMI may recruit a more inflammatory response, which in turn show a less favourable response to anti-VEGF therapy alone. In addition, the persistence of DMI despite the resolution of oedema may limit the visual improvement that can be achieved with anti-VEGF therapy.

7.4. Visual impairment resulting from DMI and inner retinal neuronal changes

Ischaemia of the SCP may affect the inner retina preferentially and manifest as loss of neuronal cells and the development of DRIL. Even in the early response to ischaemia, changes in the neuronal cells are observed, including retinal ganglion cell and cholinergic amacrine cell loss, an increase of apoptosis, and glial activation (Lam et al., 1999; Nemiroff et al., 2016). As discussed in section 5.2, loss of neurovascular coupling can further perpetuate the cycle of worsening DMI, neuronal loss, and DMO.

Clinically, Unoki et al. have demonstrated that the inner retinal is thinner in the area of diabetic capillary nonperfusion than that in the normal retina (Cennamo et al., 2015b). In addition, structural changes in the ganglion cell layer are also seen on OCT in DMI eyes (Byeon et al., 2009). On OCTA, a decreased VD correlates with a thinner macular ganglion-cell inner plexiform layer (Tang et al., 2017). These findings corroborate histological evidence of ganglion cell loss, inner nuclear layer attenuation, and capillary network

Author Manuscript Author Manuscript Author Manuscript Author Manuscript

hyalinisation due to the ischaemic damage of the perifoveal vascular plexus (Bek, 1994). DRIL (see section 6.4.2) is also visualised well on OCT and is characterised by difficulty distinguishing among the ganglion cell layer, IPL, INL and OPL (Balaratnasingam et al., 2016). The association of DRIL with visual impairment is well established (Arend et al., 1995, 1997; Mitchell et al., 2011; Sim et al., 2013b; Tyrberg et al., 2008; Unoki et al., 2007). Although neuronal stretch from DMO may result in DRIL (Sun et al., 2014, 2015), ischaemia in areas of DRIL is likely to play a key role in its pathogenesis. This proposal is reinforced by the observations that the VD is lower in areas of DRIL, and DRIL is associated with an enlarged FAZ (Moein et al., 2018; Onishi et al., 2018). However, not all capillary nonperfusion areas are associated with DRIL (Fig. 12), suggesting that vascular changes precede DRIL, and there may be a threshold for capillary nonperfusion to develop DRIL (Nicholson et al., 2015) (Fig. 13). The presence of DRIL on OCT indicates a derangement in the visual transduction pathways in the retina and may interfere with the optical transmission from photoreceptors to ganglion cells (Scarinci et al., 2015). DRIL correlates with poor visual acuity and final visual outcomes in DMO eyes. Visual acuity change with time is associated with the change of DRIL from baseline (Balaratnasingam et al., 2016; Sun et al., 2014, 2015). DRIL also correlates with increasing DR severity, which in turn may be associated with decreasing FAZ circularity. It seems that alterations in the SCP predominate and precede DRIL in the inner retina.

8. DMI as a novel treatment endpoint

8.1. Potential options for preventing or treating DMI

At present, there are no preventive or treatment options for DMI. Some proposed therapies have targeted neurodegeneration, vasoregression or pathological neovascularisation to combat ischaemia (Moran et al., 2016). However, all three aspects are unlikely to be reversed or prevented by a single agent. Most therapies for retinal neovascularisation also adversely affect neuronal survival. Another challenge is that although animal models show that some therapeutic options may be beneficial, they fail when translated to human clinical trials. Furthermore, studies on animal models indicate that therapies preventing neurodegeneration and vasoregression are best given in the stage of NPDR. Therefore, these therapies need to be patient-friendly both in terms of delivery and treatment frequency and, most importantly, safe as these are likely to be life-long therapies. Control of hyperglycaemia remains a key preventative and treatment option irrespective of disease severity level.

8.1.1. Targeting neurodegeneration—As there is significant evidence that retinal neurodegeneration precedes vasoregression, several researchers have been investigating the role of neuroprotectors and perhaps vasoprotection in the early stages of diabetic retinopathy. These therapeutic options have been delivered via different routes. Although nearly all have shown promise in animal studies, we either need more confirmatory data in animals, especially the *Ins2Akita* mouse, as it is an excellent model to explore the molecular mechanisms implicated in the initiation and early progression of DR or have sufficient data to be translated to humans (Barber et al., 2005). However, several of these agents have failed to show sufficient neuroprotection when tested individually, probably due to the complex

Author Manuscript Author Manuscript Author Manuscript Author Manuscript

nature of neuronal cell loss in diabetes. Although some of these options have already proven unsuccessful in humans, the recent availability of OCT and OCTA may allow us to investigate the local effects of these agents and better interrogate disease mechanisms. Investigational neuroprotective agents include brimonidine, somatostatin, local insulin delivery, memantine targeting glutamate related excitotoxicity, and local delivery of PEDF, brain-derived neurotrophic factor (BDNF) and nerve growth factor (NGF) as neurotrophic agents (Simo et al., 2019; Stem and Gardner, 2013). Intravitreal administration of BDNF to diabetic rats improved survival of both amacrine cells and ganglion cells while NGF prevented ganglion cell apoptosis (Hammes et al., 1995; Seki et al., 2004). A combination of tauroursodeoxycholic acid (a bile acid derivative that can suppress endoplasmic reticulum stress) and citicoline (an intermediate molecule in the metabolism of phosphatidyl choline) are currently being investigated. Combinations of these neuroprotectors are worth exploring in early diabetes (Oshitari, 2022). However, whether these agents can reverse or delay the progression of vasoregression in diabetes needs to be evaluated as an endpoint in clinical trials, but this will require long-term follow-up.

8.1.2. Anti-inflammatory effects—Several inflammatory cytokines are upregulated early in the retina in diabetes (Koleva-Georgieva et al., 2011). Agents blocking these cytokines have been explored individually, but combining them may augment the anti-inflammatory response. Although VEGF is an inflammatory cytokine, the effects of blocking it in combination with other blockers such as TNF-α, IL-1β, IL-6 still need to be investigated in concomitant DMO and DMI. Non-steroidal anti-inflammatory agents have been investigated mainly as anti-permeability agents, but they are unlikely to affect vasoregression (Thagaard et al., 2021). Fenofibrate is a peroxisome proliferator-activated receptor alpha (PPARα) that lowers lipids and decreases oxidative stress with anti-inflammatory and anti-apoptotic activity. Its multimodal effects on retinal neuroprotection have to be re-investigated based on the evidence provided by the FIELD and ACCORD studies (Group et al., 2010; Keech et al., 2007). Similarly, calcium dobesilate have pleiotropic effects such as anti-inflammatory, anti-apoptotic and antioxidant actions in both retinal neurons and microvasculature, and it also has anti-vascular hyperpermeability effects. Other options include insulin growth factor 1 (IGF-1), erythropoietin (EPO), and secretogranin III (Scg3) protects both the neurons and the vasculature. However, the timing of these therapies is critical as they only have a short period from neurodegeneration to vasoregression to pathological neovascularisation pathway (see section 8.1.8).

8.1.3. Oxygen therapy—It has been hypothesised that hypoxia in DMI can lead to osmotic leakage, and hence, oxygen inhalation can be used to improve oedema (Stefansson, 2006; Sharifipour et al., 2011; Nguyen et al., 2004). Moreover, oxygen therapy also reduces VEGF levels by reducing hypoxia (Stefansson, 2006). The reduction of retinal thickness due to the decrease in vascular leakage after oxygen therapy may also help in improving oxygen delivery to the inner retinal layers from the choroidal circulation (Nguyen et al., 2004). However, this is not a practical option for managing DMI, and this has not been explored any further.

Author Manuscript Author Manuscript Author Manuscript Author Manuscript

8.1.4. Semaphorins (SEMA)—Interest in axonal guidance cues and their effect on vaso-obliteration and vaso-proliferation has influenced research on semaphorins in DMI. Axonal guidance cues belong to four major classes: netrins, semaphorins, slits, and ephrins. These may be attractive or repulsive neuronal cues, and the pathways are complex due to the dual functions of some of these cues. Some may also alter the behaviour of blood vessels (Sakurai et al., 2012). These cues can stimulate angiogenesis or augment the actions of VEGF but, more importantly, prevent the revascularisation of the ischaemic retina (Carmeliet and Tessier-Lavigne, 2005). When we consider this relationship to DMI, spatiotemporal distributions and dysfunction of these cues and their receptors may explain why new vessels that develop at the margins of capillary nonperfusion do not grow into the ischaemic areas but instead grow towards the vitreous (Fig. 14). The altered retinal environment in diabetes induced by oxidative stress, hypoxia and inflammation affects the dynamics of these cues. Semaphorins are a new group of proteins that is associated with diabetic neurodegeneration and vascular dysfunction. They regulate endothelial cell migration and revascularisation of ischaemic tissue. They are also upregulated in DR. Class III semaphorin SEMA3A is secreted by retinal ganglion cells in the early stages of DR, and levels of SEMA3A have been demonstrated to be significantly raised in the vitreous of patients with DMO and PDR (Cerani et al., 2013; Dejda et al., 2014). SEMA3A has a role in the apoptosis of retinal neurons and inflammation associated with retinopathy; hence blocking of SEMA3A may have a potential role in reversing the breakdown in the blood-retinal barrier and hyperpermeability (Cerani et al., 2013).

On the contrary, class III semaphorin SEMA3E, an anti-angiogenic molecule, is secreted by severely ischaemic retinal neurons and normalises the retinal revascularisation by suppressing vascular outgrowth (Fukushima et al., 2011). SEMA3E also activates PLexinD1 to selectively target retinal neonascularisation without adversely affecting the normal repair of the retinal microvasculature. Levels of SEMA3E have been shown to be reduced in the vitreous of advanced DR patients; hence there may be a potential therapeutic benefit in treating retinal neovascularisation (Fukushima et al., 2011). Ongoing studies (Fukushima et al., 2011) are likely to elucidate the role of semaphorin and the neuropilin pathway as therapeutic interventions in DMI (ClinicalTrials.gov: NCT04424290 and NCT04919499).

8.1.5. Angiopoietin/Tie signalling pathway—The Angiopoietin/Tie signalling pathway regulates vascular haemostasis and controls vessel permeability, inflammation and angiogenic responses. In healthy tissues, the binding of Ang-1 to the Tie2 receptor stabilises endothelial cells. In pathologic conditions, however, increased levels of Ang-2 act as a competitive inhibitor for Tie2 binding. Displacement of Ang-1 leads to weakening of the integrity of endothelial cell junctions and contribute to vascular instability.

Vascular endothelial-protein tyrosine phosphatase (VE-PTP) is a phosphatase that inactivates Tie2 through dephosphorylation. VE-PTP is increased in the hypoxic retina. In animal models, VE-PTP suppresses retinal neovascularisation in mice with ischaemic retinopathy. Subcutaneous injections of AKB-9778, a small molecule that competitively inhibits VE-PTP, led to reduced macular oedema in patients with DMO. However, the phase 2 TIME-2b study did not meet the primary endpoint of 2-step reduction in diabetic retinopathy severity score (ClinicalTrials.gov: NCT02050828).

Author Manuscript Author Manuscript Author Manuscript Author Manuscript

Faricimab is a novel, humanised, bispecific, immunoglobulin G monoclonal antibody designed for intraocular use via intravitreal injection. It independently binds and neutralises both Ang2 and VEGF-A (Regula et al., 2016). Recent evidence assessing the use of faricimab in eyes with DMO has shown favourable vision gains and durability outcomes. Ang2 negatively regulates the Ang/Tie pathway by competitively binding to Tie2, inducing endothelial cell activation and destabilisation. The resultant overexpression of molecules such as ICAM-1 and VCAM-1 leads to increased transmigration of macrophages and other inflammatory cells, pericyte detachment, and endothelial barrier breakdown. The proposed effect of faricimab as an Ang2 inhibitor offers the potential for further vessel stabilisation. In a post-hoc analysis of the phase 2 BOULEVARD study, a higher proportion of faricimab-treated eyes achieved retinal stability (defined as central subfield thickness [CST] ≤ 325 μm and maintaining this to week 24) at every time point studied. Retinal stability was also achieved earlier in faricimab-treated eyes than in ranibizumab-treated eyes, and a dose-dependent relationship was demonstrated. In the phase 3 YOSEMITE/RHINE studies, a higher proportion of faricimab-treated eyes achieved protocol defined retinal stability (CST ≤325 μm) than aflibercept-treated eyes. This effect is particularly important in DMO as it may address the underlying pathology affecting the blood vessels (Heier et al., 2021; Joussen et al., 2021). In the preclinical mouse model of spontaneous choroidal neovascularisation, dual inhibition of Ang2 and VEGF-A led to a sustained reduction in vascular leakage and the amount of microglial and macrophage activation. The proposed vascular stabilisation mechanism through the Tie2 pathway may have benefits for DMI.

8.1.6. Anti-VEGF therapy—It is well-established that VEGF-A is an important developmental and growth factor for physiological and pathological angiogenesis. The standard treatment for DMO is anti-VEGF therapy as VEGF is the main driver of increased vascular permeability in the diabetic retina. It also modulates retinal neovascularisation, although the effects are short-lived. There has been significant debate on its role in retinal ischaemia. Moreover, VEGF is a survival factor for retinal microvasculature and retinal neurons and is expressed in retinal neurons, glia and retinal pigment epithelium (Cervia et al., 2012; Witmer et al., 2003). It binds mainly to VEGFR2 to promote the integrity of the inner blood-retinal barrier and endothelial migration. Therefore, it appears counter-intuitive to postulate that anti-VEGF agents have a protective effect on DMI.

8.1.7. Placental growth factor (PlGF)—As a member of the VEGF family, it binds to VEGFR. It is secreted by the ganglion cells and is highly expressed in the inner retina in the vasoregression phase and decrease in early neurodegeneration, suggesting an early beneficial effect (Shih et al., 2003). However, the fact that aflibercept improves DMO and hampers vasoproliferation by blocking both VEGF-A and PIGF, suggesting that the initial beneficial effect of PIGF as a neuroprotective agent may be outweighed by its vasoproliferative effect at a later stage of the disease.

8.1.8. Drugs that may be a double-edged sword—Erythropoietin (EPO) is an ischaemia-induced growth factor that reduces VEGF and Ang-2 levels in STZ-diabetic rats and reduces vasoregression if given low doses. However, if given after vasoregression, it stimulates neovascularisation. This dual function is a double-edged sword, making it

Author Manuscript Author Manuscript Author Manuscript Author Manuscript

a challenge to use in clinical practice. Similarly, retinal PEDF secreted by the RPE and Müller cells is decreased in diabetes; however, studies in animal models suggest they may have therapeutic value in decreasing neurodegeneration, vascular hyperpermeability, inflammation and neovascularisation by suppressing the Wnt signalling pathway (Barnstable and Tombran-Tink, 2004; Moran et al., 2016). Therefore, anti-PDGF in the diabetic retina may effectively regress neovascularisation, but it may also adversely affect neuronal survival (Robbins et al., 1994).

8.1.9. Integrins—Integrins mediate the adhesion of endothelial cells to the extracellular matrix. They are heterodimeric, consisting of α and β units. They regulate the survival, proliferation and migration of endothelial cells. Integrins $\alpha_v\beta_3$ and $\alpha_v\beta_5$ are upregulated in endothelial cells in PDR (Campochiaro, 2007). Their role in DMI needs to be explored.

8.2. Cell-based therapy

Although this may be a potential treatment option for retinal ischaemia, there are significant challenges with cell-based therapy in diabetic retinopathy, especially in homing the stems cells to the damaged tissue effectively. As several vascular and non-vascular cells are affected in the diabetic retina, direct replacement by multipotent cells that can regenerate to multiple cell types may be more promising. Recent studies on adult mesenchymal stem cells (MSC), endothelial progenitor cells (EPCs), adipose stromal cells (ASC) and undifferentiated induced pluripotent stem cells (iPSC) have shown that cell-based therapies may be viable options for regeneration of damaged tissue in animal models (Park, 2016).

Adult mesenchymal stem cells are most researched probably due to the absence of ethical concerns, easy harvesting, low immunogenicity and tumorigenesis risks, multipotent differentiation ability, and a marked ability to home to injury sites. These cells are harvested from mature organs such as bone marrow or adipose tissue and have been successfully delivered by intravitreal, subretinal or intravenous routes in retinal degeneration or acute ischaemia-reperfusion murine models. Animal models used in adult mesenchymal stem cells therapies for NPDR (vasoregression) include streptozotocin administered C57BL6 mice; Hes5-GFP transgenic mice; glial fibrillary acidic protein (GFAP)-STAT3-cKO mice and nonobese diabetic (NOD) mice. For PDR, rats with raised intraocular pressures induced retinal ischaemia, OIR, and Akimba mice have been used (Fiori et al., 2018). However, the regenerative capacity of these cells is a paracrine trophic effect on the ischaemic or degenerating retina by secreting both neuroprotective and angiogenic factors. Their ability to regenerate to the damaged cell type is limited, and there is only a small window of opportunity when there are sufficient existing viable cells. Their immunomodulatory property may also be an advantage in retinal ischaemia. However, these cells can also cause neovascularisation and other adverse cell proliferation, although the diabetic milieu may not be conducive (Park, 2016).

A pilot clinical trial on intravenous administration of autologous bone marrow MSCs was evaluated to treat 15 PDR or 19 NPDR. Only NPDR showed a macular thickness reduction and a significant visual acuity improvement (Gu et al., 2018).

Author Manuscript Author Manuscript Author Manuscript Author Manuscript

Other adult cells are the EPCs from blood or bone marrow (Lois et al., 2014). Vascular injury can cause circulating angiogenic factors to increase and activate metalloproteinases, which stimulates the proliferation and mobilisation of EPC to the circulation and then to the ischaemic retina. However, diabetes can reduce the numbers and function of EPCs, whereas statins and angiotensin II receptor antagonists enhance their numbers in circulation. Intravitreal and intravenous delivery of human $CD34^+$ EPC from the peripheral blood and bone marrow into animal models of diabetes or acute ischaemia-reperfusion injury have shown that EPCs rapidly home into the ischaemic retinal area, although the regrafting was low. A large trial is investigating the ACE/ACE2 ratio within blood EPC over four years in people with different severity levels of NPDR and control to evaluate whether EPCs can be used to predict DR (ClinicalTrials.gov: NCT02119689).

These EPCs also have a paracrine effect and secrete both angiogenic and neurotrophic factors. In addition, their properties include immunosuppression and prevention of apoptosis of mature endothelial cells caused by oxidative stress. In a Phase 1 trial of intravitreal injection of autologous bone marrow-derived $CD34^+$ EPC into human eyes with irreversible vision loss due to retinal degeneration and ischaemia, the safety profile was good with functional and structural improvement up to 6 months. An ongoing clinical trial is evaluating the role of fenofibrate in increasing circulating EPC levels in DR (ClinicalTrials.gov: NCT01927315). Another clinical trial is investigating the safety and efficacy of autologous $CD34^+$ stem cells isolated from bone marrow at six months in 15 patients with irreversible blindness due to various retinal conditions, including DR.

Endothelial colony-forming cells (ECFCs) or outgrowth endothelial cells (OECs) are subpopulations of EPC. The ECFCs do not regraft or proliferate well but secrete IL-8 to promote vascular repair. The OECs were found to be effective in reversing capillary nonperfusion in an animal model of retinal ischaemia. They proliferated well and regenerated well with minimal adverse neovascularisation.

Undifferentiated and multipotent adipose tissue may also serve as pericyte precursors. They also have a paracrine effect, secrete anti-apoptotic factors and improve endothelial cell survival. These cells have been administered intravitreally and intravenously into animal models of oxygen-induced retinopathy and diabetic retinopathy with good perivascular integration, improved ERG, improved vascular permeability and reduced apoptosis.

Undifferentiated iPSC also showed a paracrine effect when injected subretinally into a rat model of acute ischaemia-reperfusion injury but without engraftment. There is an ongoing clinical trial (ClinicalTrials.gov: NCT03403699) investigating whether iPSC derived from peripheral blood cells of subjects with diabetes and age-matched controls could be injected into murine and primate model to evaluate the ability of mesoderm cells to generate endothelial cells and pericytes in areas of degenerated capillaries and enhance vessel formation.

Embryonic stem cells and iPSC cells from cord blood performed better than iPSC from adult cells in homing, engraftment and vascular repair in an ischaemia-reperfusion model.

Author Manuscript Author Manuscript Author Manuscript Author Manuscript

Ongoing cell-based therapy trials include those evaluating various delivery routes for nonperfusion retinopathies (ClinicalTrials.gov: NCT03011541 and NCT 03981549).

9. Remaining questions and future research direction

In this review, we summarised the findings from basic science work to support that DMI is an early and critical component of functional loss in DR. DMI alone can lead to a variable degree of visual loss, which may be explained by the phenotypes of DMI. DMI may also lead to visual loss through promoting the development of DMO and neurodegeneration. Activation of inflammatory responses in response to DMI may further exacerbate DMO. Hence, the severity of underlying DMI also likely influence the responsiveness of DMO to anti-VEGF therapy. We propose that DMI should be systematically evaluated in every DR assessment and its presence considered as VTDR.

Although DMI has long been recognised as a manifestation of diabetic eye disease, it has not been routinely assessed nor considered a treatment endpoint. With advances in imaging techniques, particularly with the rapid uptake of OCTA in clinical practices, DMI can now be assessed much more readily. With therapies in development that can target or reverse microvascular changes, DMI is a potential novel therapeutic target, in addition to DMO and DR. However, any future therapeutic trials aiming to evaluate DMI will require a thorough understanding of the natural history and progression pattern of DMI in prospective datasets. Whether all cases of DMI progress or some may spontaneously recover remains unknown. Whether there is a threshold of DMI associated with a worse prognosis also remains to be determined.

Currently, OCTA appears to be the most promising imaging modality for evaluating DMI. However, the definition of DMI, the nomenclature, and the normative values will need to be standardised. Efforts should be devoted to harmonising measurements derived from different commercially available instruments (Fawzi, 2017; Cheung and Wong, 2018). However, this is likely not possible for all parameters, considering the differences in the technologies used by different manufacturers. Lessons can be learnt from the early days of incorporation of OCT into clinical trials. For example, various OCT-based metrics were used, such as centre point thickness, central retinal thickness, central subfield thickness, and central macular thickness. Standardisation of definition was eventually introduced to ensure that results from clinical trials and research studies can be compared. In addition, variations between various spectral-domain commercial instruments exist due to differences in the boundaries used. Formula to convert between instruments eventually led to the ability to combine and utilise data acquired from different clinical sites using different instruments. A multidisciplinary panel of retinal imaging experts have been formed to decide on a list of key descriptors of OCTA in neovascular age-related macular degeneration (Mendonca et al., 2021). Similar efforts to standardise the nomenclature and definition of various OCTA parameters for assessing DMI will be required. To this end, we have highlighted the variabilities in currently used taxonomy and proposed a system for nomenclature towards standardisation.

With the recognition of the importance of DMI, future research work should be directed to address the molecular basis of DMI. Therapies targeting VEGF appear only to address

Author Manuscript Author Manuscript Author Manuscript Author Manuscript

a limited component of this complex disease. However, further work to understand the natural progression of DMI and the functional impact is necessary for guiding the selection of suitable clinical endpoints for these therapeutic trials. Many considerations are similar to those in clinical trials for geographic atrophy (Cheung et al., 2021). For example, is it possible to repair or regenerate damaged vasculature, especially in diabetic individuals? Should new therapies aim to reverse DMI, or is slowing its progression adequate? What is the threshold of DMI that should be targeted for intervention? Is there a point of no return for DMI? Nonetheless, the authors believe future therapies should aim at improving our current option by stabilising the retinal vasculature, addressing inflammation, and offering neuroprotection.

Acknowledgements

Sobha Sivaprasad and Wei-Shan Tsai are supported by the ORNATE-India grant: GCRF UKR1 (MR/P027881/1).

CMG Cheung is supported by the National Medical Research Council Singapore Open Fund Large Collaborative Grant: NMRC/LCG/004/2018.

KYC Teo is supported by the National Medical Research Council Singapore Transition Award.

Abbreviations

AFI	Adjusted flow index
Ang2	Angiopoietin-2
AOSLO	Adaptive optics scanning laser ophthalmoscope
DCP	Deep capillary plexus
DM	Diabetic mellitus
DMI	Diabetic macular ischaemia
DMO	Diabetic macular oedema
DR	Diabetic retinopathy
DRIL	Disorganisation of the retinal inner layers
DVC	Deep vascular complex
EAA	Extrafoveal avascular area
ETDRS	Early Treatment for Diabetic Retinopathy Study
FA	Fluorescein angiography
FAZ	Foveal avascular zone
FAZ-AI	Foveal avascular zone acircularity index
FAZ-CI	Foveal avascular zone circularity index

Author Manuscript Author Manuscript Author Manuscript Author Manuscript

FD	Fractal dimension
GPD	Geometric Perfusion Deficits
ICP	Intermediate capillary plexus
INL	Inner nuclear layer
IPL	Inner plexiform layer
mfERG	Multifocal electroretinogram
NPDR	Non-proliferative diabetic retinopathy
OCT	Optical coherence tomography
OCTA	Optical coherence tomography angiography
OPL	Outer plexiform layer
PAN	Percent area of nonperfusion
PCD	Perfused capillary density
PD	Perfusion density
PDR	Proliferative diabetic retinopathy
PEDF	Pigment epithelium-derived growth facto
PICA	Perifoveal intercapillary area
PRP	Panretinal photocoagulation
RGCL	Retinal ganglion cell layer
RNFL	Retinal nerve fibre layer
SCP	Superficial capillary plexus
SEMA	Semaphorin
SVC	Superficial vascular complex
TAA	Total avascular areas
VD	Vessel density
VDI	Vessel diameter index
VEGF	Vascular endothelial growth factor
VLD	Vessel length density
VTDR	Vision-threatening diabetic retinopathy

Author Manuscript Author Manuscript Author Manuscript Author Manuscript

References

Diabetic Retinopathy Clinical Research, N., Elman MJ., Aiello LP., Beck RW., Bressler NM., Bressler SB., Edwards AR., Ferris FL 3rd., Friedman SM., Glassman AR., Miller KM., Scott IU., Stockdale CR., Sun JK, 2010. Randomized trial evaluating ranibizumab plus prompt or deferred laser or triamcinolone plus prompt laser for diabetic macular edema. Ophthalmology 117, 1064–1077 e1035. [PubMed: 20427088]

Abdelshafy M, Abdelshafy A, 2020. Correlations between optical coherence tomography angiography parameters and the visual acuity in patients with diabetic retinopathy. Clin. Ophthalmol. 14, 1107–1115. [PubMed: 32425497]

Agemy SA, Scripsema NK, Shah CM, Chui T, Garcia PM, Lee JG, Gentile RC, Hsiao Y-S, Zhou Q, Ko T, 2015. Retinal vascular perfusion density mapping using optical coherence tomography angiography in normals and diabetic retinopathy patients. Retina 35, 2353–2363. [PubMed: 26465617]

Aiello LP, Cahill MT, Wong JS, 2001. Systemic considerations in the management of diabetic retinopathy. Am. J. Ophthalmol. 132, 760–776. [PubMed: 11704039]

Al-Sheikh M, Akil H, Pfau M, Sadda SR, 2016. Swept-source OCT angiography imaging of the foveal avascular zone and macular capillary network density in diabetic retinopathy. Investig. Ophthalmol. Vis. Sci. 57, 3907–3913. [PubMed: 27472076]

Alam M, Thapa D, Lim JI, Cao D, Yao X, 2017. Quantitative characteristics of sickle cell retinopathy in optical coherence tomography angiography. Biomed. Opt Express 8, 1741–1753. [PubMed: 28663862]

Alder VA, Cringle SJ, 1985. The effect of the retinal circulation on vitreal oxygen tension. Curr. Eye Res. 4, 121–129. [PubMed: 3987345]

Alder VA, Yu DY, Cringle SJ, Su EN, 1991. Changes in vitreal oxygen tension distribution in the streptozotocin diabetic rat. Diabetologia 34, 469–476. [PubMed: 1916051]

Antonetti DA, Klein R, Gardner TW, 2012. Diabetic retinopathy. N. Engl. J. Med. 366, 1227–1239. [PubMed: 22455417]

Arend O, Wolf S, Jung F, Bertram B, Postgens H, Toonen H, Reim M, 1991. Retinal microcirculation in patients with diabetes mellitus: dynamic and morphological analysis of perifoveal capillary network. Br. J. Ophthalmol. 75, 514–518. [PubMed: 1911651]

Arend O, Wolf S, Harris A, Reim M, 1995. The relationship of macular microcirculation to visual acuity in diabetic patients. Arch. Ophthalmol. 113, 610–614. [PubMed: 7748131]

Arend O, Remky A, Evans D, Stuber R, Harris A, 1997. Contrast sensitivity loss is coupled with capillary dropout in patients with diabetes. Investig. Ophthalmol. Vis. Sci. 38, 1819–1824. [PubMed: 9286271]

Armulik A, Genové G, Betsholtz C, 2011. Pericytes: developmental, physiological, and pathological perspectives, problems, and promises. Dev. Cell 21, 193–215. [PubMed: 21839917]

Arthur E, Elsner AE, Sapoznik KA, Papay JA, Muller MS, Burns SA, 2019. Distances from capillaries to arterioles or venules measured using OCTA and AOSLO. Investig. Ophthalmol. Vis. Sci. 60, 1833–1844. [PubMed: 31042789]

Asnaghi V, Gerhardinger C, Hoehn T, Adeboje A, Lorenzi M, 2003. A role for the polyol pathway in the early neuroretinal apoptosis and glial changes induced by diabetes in the rat. Diabetes 52, 506–511. [PubMed: 12540628]

Balaratnasingam C, Inoue M, Ahn S, McCann J, Dhrami-Gavazi E, Yannuzzi LA, Freund KB, 2016. Visual acuity is correlated with the area of the foveal avascular zone in diabetic retinopathy and retinal vein occlusion. Ophthalmology 123, 2352–2367. [PubMed: 27523615]

Barber AJ, Lieth E, Khin SA, Antonetti DA, Buchanan AG, Gardner TW, 1998. Neural apoptosis in the retina during experimental and human diabetes. Early onset and effect of insulin. J. Clin. Invest. 102, 783–791. [PubMed: 9710447]

Barber AJ, Antonetti DA, Kern TS, Reiter CE, Soans RS, Krady JK, Levison SW, Gardner TW, Bronson SK, 2005. The Ins2Akita mouse as a model of early retinal complications in diabetes. Investig. Ophthalmol. Vis. Sci. 46, 2210–2218. [PubMed: 15914643]

Author Manuscript Author Manuscript Author Manuscript Author Manuscript

Barnstable CJ, Tombran-Tink J, 2004. Neuroprotective and antiangiogenic actions of PEDF in the eye: molecular targets and therapeutic potential. Prog. Retin. Eye Res. 23, 561–577. [PubMed: 15302351]

Bek T, 1994. Transretinal histopathological changes in capillary-free areas of diabetic retinopathy. Acta Ophthalmol. 72, 409–415. [PubMed: 7825403]

Bek T, Hajari J, Jeppesen P, 2008. Interaction between flicker-induced vasodilatation and pressure autoregulation in early retinopathy of type 2 diabetes. Graefe's archive for clinical and experimental ophthalmology = Albrecht von Graefes Archiv fur klinische und experimentelle Ophthalmologie, 246, 763–769.

Bhanushali D, Anegondi N, Gadde SG, Srinivasan P, Chidambara L, Yadav NK, Sinha Roy A, 2016. Linking retinal microvasculature features with severity of diabetic retinopathy using optical coherence tomography angiography. Investig. Ophthalmol. Vis. Sci 57, OCT519–525. [PubMed: 27472275]

Bhardwaj S, Tsui E, Zahid S, Young E, Mehta N, Agemy S, Garcia P, Rosen RB, Young JA, 2018. Value of fractal analysis of optical coherence tomography angiography in various stages of diabetic retinopathy. Retina 38, 1816–1823. [PubMed: 28723846]

Birol G, Wang S, Budzynski E, Wangsa-Wirawan ND, Linsenmeier RA, 2007. Oxygen distribution and consumption in the macaque retina. Am. J. Physiol. Heart Circ. Physiol. 293, H1696–H1704. [PubMed: 17557923]

Borrelli E, Sacconi R, Brambati M, Bandello F, Querques G, 2019. In vivo rotational three-dimensional OCTA analysis of microaneurysms in the human diabetic retina. Sci. Rep. 9, 16789. [PubMed: 31728070]

Braun RD, Linsenmeier RA, Goldstick TK, 1995. Oxygen consumption in the inner and outer retina of the cat. Investig. Ophthalmol. Vis. Sci. 36, 542–554. [PubMed: 7890485]

Bresnick GH, De Venecia G, Myers FL, Harris JA, Davis MD, 1975. Retinal ischemia in diabetic retinopathy. Arch. Ophthalmol. 93, 1300–1310. [PubMed: 1200895]

Bresnick GH, Condit R, Syrjala S, Palta M, Groo A, Korth K, 1984. Abnormalities of the foveal avascular zone in diabetic retinopathy. Arch. Ophthalmol. 102, 1286–1293. [PubMed: 6477244]

Bressler SB, Ayala AR, Bressler NM, Melia M, Qin H, Ferris FL 3rd, Flaxel CJ, Friedman SM, Glassman AR, Jampol LM, Rauser ME, 2016. Diabetic retinopathy clinical research, N., persistent macular thickening after ranibizumab treatment for diabetic macular edema with vision impairment. JAMA Ophthalmol. 134, 278–285. [PubMed: 26746868]

Budzynski E, Smith JH, Bryar P, Birol G, Linsenmeier RA, 2008. Effects of photocoagulation on intraretinal PO2 in cat. Investig. Ophthalmol. Vis. Sci. 49, 380–389. [PubMed: 18172116]

Buerk DG, Shonat RD, Riva CE, Cranstoun SD, 1993. O2 gradients and countercurrent exchange in the cat vitreous humor near retinal arterioles and venules. Microvasc. Res. 45, 134–148. [PubMed: 8361397]

Burns SA, Elsner AE, Sapoznik KA, Warner RL, Gast TJ, 2019. Adaptive optics imaging of the human retina. Prog. Retin. Eye Res. 68, 1–30. [PubMed: 30165239]

Byeon SH, Chu YK, Lee H, Lee SY, Kwon OW, 2009. Foveal ganglion cell layer damage in ischemic diabetic maculopathy: correlation of optical coherence tomographic and anatomic changes. Ophthalmology 116, 1949–1959 e1948. [PubMed: 19699533]

Campbell J, Zhang M, Hwang T, Bailey S, Wilson D, Jia Y, Huang D, 2017a. Detailed vascular anatomy of the human retina by projection-resolved optical coherence tomography angiography. Sci. Rep. 7, 1–11. [PubMed: 28127051]

Campbell JP, Zhang M, Hwang TS, Bailey ST, Wilson DJ, Jia Y, Huang D, 2017b. Detailed vascular anatomy of the human retina by projection-resolved optical coherence tomography angiography. Sci. Rep. 7, 42201. [PubMed: 28186181]

Campochiaro PA, 2007. Molecular targets for retinal vascular diseases. J. Cell. Physiol. 210, 575–581. [PubMed: 17133346]

Campochiaro PA, 2015. Molecular pathogenesis of retinal and choroidal vascular diseases. Prog. Retin. Eye Res. 49, 67–81. [PubMed: 26113211]

Cao J, McLeod S, Merges CA, Lutty GA, 1998. Choriocapillaris degeneration and related pathologic changes in human diabetic eyes. Arch. Ophthalmol. 116, 589–597. [PubMed: 9596494]

Author Manuscript Author Manuscript Author Manuscript Author Manuscript

Carmeliet P, Tessier-Lavigne M, 2005. Common mechanisms of nerve and blood vessel wiring. Nature 436, 193–200. [PubMed: 16015319]

Carnevali A, Sacconi R, Corbelli E, Tomasso L, Querques L, Zerbini G, Scorcia V, Bandello F, Querques G, 2017. Optical coherence tomography angiography analysis of retinal vascular plexuses and choriocapillaris in patients with type 1 diabetes without diabetic retinopathy. Acta Diabetol. 54, 695–702. [PubMed: 28474119]

Casselholmde Salles M, Kvanta A, Amren U, Epstein D, 2016. Optical coherence tomography angiography in central retinal vein occlusion: correlation between the foveal avascular zone and visual acuity. Investig. Ophthalmol. Vis. Sci. 57, OCT242–246. [PubMed: 27409478]

Cennamo G, Vecchio EC, Finelli M, Velotti N, de Crecchio G, 2015a. Evaluation of ischemic diabetic maculopathy with Fourier-domain optical coherence tomography and microperimetry. Can. J. Ophthalmol. 50, 44–48. [PubMed: 25677282]

Cennamo G, Vecchio EC, Finelli M, Velotti N, de Crecchio G, 2015b. Evaluation of ischemic diabetic maculopathy with Fourier-domain optical coherence tomography and microperimetry. Can. J. Ophthalmol. 50, 44–48. [PubMed: 25677282]

Cerani A, Tetreault N, Menard C, Lapalme E, Patel C, Sitaras N, Beaudoin F, Leboeuf D, De Guire V, Binet F, Dejda A, Rezende FA, Miloudi K, Sapieha P, 2013. Neuron-derived semaphorin 3A is an early inducer of vascular permeability in diabetic retinopathy via neuropilin-1. Cell Metabol. 18, 505–518.

Cervia D, Catalani E, Dal Monte M, Casini G, 2012. Vascular endothelial growth factor in the ischemic retina and its regulation by somatostatin. J. Neurochem. 120, 818–829. [PubMed: 22168912]

Chan T, Vese L, 1999. An active contour model without edges. International Conference on Scale-Space Theories in Computer Vision. Springer, pp. 141–151.

Chen Q, Ma Q, Wu C, Tan F, Chen F, Wu Q, Zhou R, Zhuang X, Lu F, Qu J, Shen M, 2017. Macular vascular fractal dimension in the deep capillary layer as an early indicator of microvascular loss for retinopathy in type 2 diabetic patients. Investig. Ophthalmol. Vis. Sci. 58, 3785–3794. [PubMed: 28744552]

Chen S, Moult EM, Zangwill LM, Weinreb RN, Fujimoto JG, 2021. Geometric perfusion deficits: a novel OCT angiography biomarker for diabetic retinopathy based on oxygen diffusion. Am. J. Ophthalmol. 222, 256–270. [PubMed: 32918905]

Cheng RW, Yusof F, Tsui E, Jong M, Duffin J, Flanagan JG, Fisher JA, Hudson C, 2016. Relationship between retinal blood flow and arterial oxygen. J. Physiol. 594, 625–640. [PubMed: 26607393]

Cheung CMG, Wong TY, 2018. Clinical use of optical coherence tomography angiography in diabetic retinopathy treatment: ready for showtime? JAMA Ophthalmol. 136, 729–730. [PubMed: 29801085]

Cheung AK, Fung MK, Lo AC, Lam TT, So KF, Chung SS, Chung SK, 2005. Aldose reductase deficiency prevents diabetes-induced blood-retinal barrier breakdown, apoptosis, and glial reactivation in the retina of db/db mice. Diabetes 54, 3119–3125. [PubMed: 16249434]

Cheung CMG, Pearce E, Fenner B, Sen P, Chong V, Sivaprasad S, 2021. Looking ahead: visual and anatomical endpoints in future trials of diabetic macular ischemia. Ophthalmologica. Journal international d'ophtalmologie. International journal of ophthalmology. Zeitschrift fur Augenheilkunde, 244, 451–464. [PubMed: 33626529]

Chibber R, Ben-Mahmud BM, Chibber S, Kohner EM, 2007. Leukocytes in diabetic retinopathy. Curr. Diabetes Rev. 3, 3–14. [PubMed: 18220651]

Chung EJ, Roh MI, Kwon OW, Koh HJ, 2008. Effects of macular ischemia on the outcome of intravitreal bevacizumab therapy for diabetic macular edema. Retina 28, 957–963. [PubMed: 18698297]

Chung CY, Tang HHY, Li SH, Li KKW, 2018. Differential microvascular assessment of retinal vein occlusion with coherence tomography angiography and fluorescein angiography: a blinded comparative study. Int. Ophthalmol. 38, 1119–1128. [PubMed: 28550346]

Clements RS Jr., Robison WG Jr., Cohen MP, 1998. Anti-glycated albumin therapy ameliorates early retinal microvascular pathology in db/db mice. J. Diabet. Complicat. 12, 28–33.

Author Manuscript Author Manuscript Author Manuscript Author Manuscript

Cogan DG, Kuwabara T, 1963. Capillary shunts IN the pathogenesis OF diabetic retinopathy. Diabetes 12, 293–300. [PubMed: 14081839]

Cogan DG, Toussaint D, Kuwabara T, 1961. Retinal vascular patterns. IV. Diabetic retinopathy. Arch. Ophthalmol. 66, 366–378. [PubMed: 13694291]

Conrath J, Giorgi R, Raccah D, Ridings B, 2005a. Foveal avascular zone in diabetic retinopathy: quantitative vs qualitative assessment. Eye 19, 322–326. [PubMed: 15258601]

Conrath J, Giorgi R, Ridings B, Raccah D, 2005b. Metabolic factors and the foveal avascular zone of the retina in diabetes mellitus. Diabetes Metab. 31, 465–470. [PubMed: 16357790]

Corvi F, Pellegrini M, Erba S, Cozzi M, Staurenghi G, Giani A, 2018. Reproducibility of vessel density, fractal dimension, and foveal avascular zone using 7 different optical coherence tomography angiography devices. Am. J. Ophthalmol. 186, 25–31. [PubMed: 29169882]

Cuenca N, Ortuno-Lizaran I, Sanchez-Saez X, Kutsyr O, Albertos-Arranz H, Fernandez-Sanchez L, Martinez-Gil N, Noailles A, Lopez-Garrido JA, Lopez-Galvez M, Lax P, Maneu V, Pinilla I, 2020. Interpretation of OCT and OCTA images from a histological approach: clinical and experimental implications. Prog. Retin. Eye Res. 77, 100828. [PubMed: 31911236]

Curcio CA, Sloan KR, Kalina RE, Hendrickson AE, 1990. Human photoreceptor topography. J. Comp. Neurol. 292, 497–523. [PubMed: 2324310]

Cusick M, Chew EY, Ferris F 3rd, Cox TA, Chan CC, Kador PF, 2003. Effects of aldose reductase inhibitors and galactose withdrawal on fluorescein angiographic lesions in galactose-fed dogs. Arch. Ophthalmol. 121, 1745–1751. [PubMed: 14662595]

Cuypers MH, Kasanardjo JS, Polak BC, 2000. Retinal blood flow changes in diabetic retinopathy measured with the Heidelberg scanning laser Doppler flowmeter. Graefe's archive for clinical and experimental ophthalmology = Albrecht von Graefes Archiv fur klinische und experimentelle Ophthalmologie, 238, 935–941.

DaCosta J, Bhatia D, Talks J, 2020. The use of optical coherence tomography angiography and optical coherence tomography to predict visual acuity in diabetic retinopathy. Eye 34, 942–947. [PubMed: 31591506]

Daruich A, Matet A, Moulin A, Kowalczuk L, Nicolas M, Sellam A, Rothschild PR, Omri S, Gelize E, Jonet L, Delaunay K, De Kozak Y, Berdugo M, Zhao M, Crisanti P, Behar-Cohen F, 2018. Mechanisms of macular edema: beyond the surface. Prog. Retin. Eye Res. 63, 20–68. [PubMed: 29126927]

de Carlo TE, Chin AT, Bonini Filho MA, Adhi M, Branchini L, Salz DA, Baumal CR, Crawford C, Reichel E, Witkin AJ, Duker JS, Waheed NK, 2015. Detection of microvascular changes in eyes of patients with diabetes but not clinical diabetic retinopathy using optical coherence tomography angiography. Retina 35, 2364–2370. [PubMed: 26469537]

Dejda A, Mawambo G, Cerani A, Miloudi K, Shao Z, Daudelin JF, Boulet S, Oubaha M, Beaudoin F, Akla N, Henriques S, Menard C, Stahl A, Delisle JS, Rezende FA, Labrecque N, Sapieha P, 2014. Neuropilin-1 mediates myeloid cell chemoattraction and influences retinal neuroimmune crosstalk. J. Clin. Invest. 124, 4807–4822. [PubMed: 25271625]

Di G, Weihong Y, Xiao Z, Zhikun Y, Xuan Z, Yi Q, Fangtian D, 2016. A morphological study of the foveal avascular zone in patients with diabetes mellitus using optical coherence tomography angiography. Graefe's archive for clinical and experimental ophthalmology = Albrecht von Graefes Archiv fur klinische und experimentelle Ophthalmologie, 254, 873–879.

Diabetic Retinopathy Clinical Research, N., Elman MJ., Qin H., Aiello., Beck RW., Bressler NM., Ferris FL 3rd., Glassman AR, Maturi RK., Melia M., 2012. Intravitreal ranibizumab for diabetic macular edema with prompt versus deferred laser treatment: three-year randomized trial results. Ophthalmology 119, 2312–2318. [PubMed: 22999634]

Dmuchowska DA, Krasnicki P, Mariak Z, 2014. Can optical coherence tomography replace fluorescein angiography in detection of ischemic diabetic maculopathy? Graefe's archive for clinical and experimental ophthalmology = Albrecht von Graefes Archiv fur klinische und experimentelle Ophthalmologie, 252, 731–738.

Du Y, Veenstra A, Palczewski K, Kern TS, 2013. Photoreceptor cells are major contributors to diabetes-induced oxidative stress and local inflammation in the retina. Proc. Natl. Acad. Sci. U.S.A. 110, 16586–16591. [PubMed: 24067647]

Author Manuscript Author Manuscript Author Manuscript Author Manuscript

Dupas B, Minvielle W, Bonnin S, Couturier A, Erginay A, Massin P, Gaudric A, Tadayoni R, 2018. Association between vessel density and visual acuity in patients with diabetic retinopathy and poorly controlled type 1 diabetes. JAMA Ophthalmol. 136, 721–728. [PubMed: 29800967]

Durbin MK, An L, Shemonski ND, Soares M, Santos T, Lopes M, Neves C, Cunha-Vaz J, 2017. Quantification of retinal microvascular density in optical coherence tomographic angiography images in diabetic retinopathy. JAMA ophthalmology 135, 370–376. [PubMed: 28301651]

Endo H, Kase S, Tanaka H, Takahashi M, Katsuta S, Suzuki Y, Fujii M, Ishida S, Kase M, 2021. Factors based on optical coherence tomography correlated with vision impairment in diabetic patients. Sci. Rep. 11, 3004. [PubMed: 33542264]

Engerman RL, Kern TS, 1995. Retinopathy in animal models of diabetes. Diabetes Metab. Rev. 11, 109–120. [PubMed: 7555563]

Enroth-Cugell C, Harding TH, 1980. Summation of rod signals within the receptive field centre of cat retinal ganglion cells. J. Physiol. 298, 235–250. [PubMed: 7359397]

Eperon G, Johnson M, David NJ, 1975. The effect of arterial PO2 on relative retinal blood flow in monkeys. Invest. Ophthalmol. 14, 342–352. [PubMed: 1126823]

Faberowski N, Stefansson E, Davidson RC, 1989. Local hypothermia protects the retina from ischemia. A quantitative study in the rat. Investig. Ophthalmol. Vis. Sci. 30, 2309–2313. [PubMed: 2807788]

Fawzi AA, 2017. Consensus on optical coherence tomographic angiography nomenclature: do we need to develop and learn a new language? JAMA Ophthalmol. 135, 377–378. [PubMed: 28301649]

Fayed AE, Abdelbaki AM, El Zawahry OM, Fawzi AA, 2019. Optical coherence tomography angiography reveals progressive worsening of retinal vascular geometry in diabetic retinopathy and improved geometry after panretinal photocoagulation. PLoS One 14, e0226629. [PubMed: 31887149]

Feit-Leichman RA, Kinouchi R, Takeda M, Fan Z, Mohr S, Kern TS, Chen DF, 2005. Vascular damage in a mouse model of diabetic retinopathy: relation to neuronal and glial changes. Invest. Ophthalmol. Vis. Sci. 46, 4281–4287. [PubMed: 16249509]

Fenner BJ, Tan GSW, Tan ACS, Yeo IYS, Wong TY, Cheung GCM, 2018. Identification of imaging features that determine quality and repeatability of retinal capillary plexus density measurements in OCT angiography. Br. J. Ophthalmol. 102, 509–514. [PubMed: 28814409]

Fiori A, Terlizzi V, Kremer H, Gebauer J, Hammes HP, Harmsen MC, Bieback K, 2018. Mesenchymal stromal/stem cells as potential therapy in diabetic retinopathy. Immunobiology 223, 729–743. [PubMed: 29402461]

Freiberg FJ, Pfau M, Wons J, Wirth MA, Becker MD, Michels S, 2016. Optical coherence tomography angiography of the foveal avascular zone in diabetic retinopathy. Graefe's archive for clinical and experimental ophthalmology = Albrecht von Graefes Archiv fur klinische und experimentelle Ophthalmologie, 254, 1051–1058.

Fukushima Y, Okada M, Kataoka H, Hirashima M, Yoshida Y, Mann F, Gomi F, Nishida K, Nishikawa S, Uemura A, 2011. Sema3E-PlexinD1 signaling selectively suppresses disoriented angiogenesis in ischemic retinopathy in mice. J. Clin. Invest. 121, 1974–1985. [PubMed: 21505259]

Garhöfer G, Zawinka C, Resch H, Kothy P, Schmetterer L, Dorner GT, 2004. Reduced response of retinal vessel diameters to flicker stimulation in patients with diabetes. Br. J. Ophthalmol. 88, 887–891. [PubMed: 15205231]

Gastinger MJ, Tian N, Horvath T, Marshak DW, 2006. Retinopetal axons in mammals: emphasis on histamine and serotonin. Curr. Eye Res. 31, 655–667. [PubMed: 16877274]

Gastinger MJ, Kunselman AR, Conboy EE, Bronson SK, Barber AJ, 2008. Dendrite remodeling and other abnormalities in the retinal ganglion cells of Ins2 Akita diabetic mice. Invest. Ophthalmol. Vis. Sci. 49, 2635–2642. [PubMed: 18515593]

Gerendas BS, Prager S, Deak G, Simader C, Lammer J, Waldstein SM, Guerin T, Kundi M, Schmidt-Erfurth UM, 2018. Predictive imaging biomarkers relevant for functional and anatomical outcomes during ranibizumab therapy of diabetic macular oedema. Br. J. Ophthalmol. 102, 195–203. [PubMed: 28724636]

Author Manuscript Author Manuscript Author Manuscript Author Manuscript

Gill A, Cole ED, Novais EA, Louzada RN, de Carlo T, Duker JS, Waheed NK, Baumal CR, Witkin AJ, 2017. Visualization of changes in the foveal avascular zone in both observed and treated diabetic macular edema using optical coherence tomography angiography. Int. J. Retina Vitr. 3, 19.

Gorrand JM, 1979. Diffusion of the human retina and quality of the optics of the eye on the fovea and the peripheral retina. Vis. Res. 19, 907–912. [PubMed: 516460]

Group AS, Group AES, Chew EY, Ambrosius WT, Davis MD, Danis RP, Gangaputra S, Greven CM, Hubbard L, Esser BA, Lovato JF, Perdue LH, Goff DC Jr., Cushman WC, Ginsberg HN, Elam MB, Genuth S, Gerstein HC, Schubart U, Fine LJ, 2010. Effects of medical therapies on retinopathy progression in type 2 diabetes. N. Engl. J. Med. 363, 233–244. [PubMed: 20587587]

Grunwald JE, Riva CE, Brucker AJ, Sinclair SH, Petrig BL, 1984. Altered retinal vascular response to 100% oxygen breathing in diabetes mellitus. Ophthalmology 91, 1447–1452. [PubMed: 6084214]

Grunwald JE, Piltz J, Patel N, Bose S, Riva CE, 1993. Effect of aging on retinal macular microcirculation: a blue field simulation study. Investig. Ophthalmol. Vis. Sci. 34, 3609–3613. [PubMed: 8258519]

Gu X, Yu X, Zhao C, Duan P, Zhao T, Liu Y, Li S, Yang Z, Li Y, Qian C, Yin Z, Wang Y, 2018. Efficacy and safety of autologous bone marrow mesenchymal stem cell transplantation in patients with diabetic retinopathy. Cell. Physiol. Biochem. : Int. J. Exp. Med. Cell. Physiol. Biochem. Pharmacol. 49, 40–52.

Hammes HP, 2005. Pericytes and the pathogenesis of diabetic retinopathy. Hormone and metabolic research = Hormon- und Stoffwechselforschung = Hormones et metabolisme, 37 (Suppl. 1), 39–43. [PubMed: 15918109]

Hammes HP, Federoff HJ, Brownlee M, 1995. Nerve growth factor prevents both neuroretinal programmed cell death and capillary pathology in experimental diabetes. Mol. Med. 1, 527–534. [PubMed: 8529118]

Hammes HP, Lin J, Wagner P, Feng Y, Vom Hagen F, Krzizok T, Renner O, Breier G, Brownlee M, Deutsch U, 2004. Angiopoietin-2 causes pericyte dropout in the normal retina: evidence for involvement in diabetic retinopathy. Diabetes 53, 1104–1110. [PubMed: 15047628]

Hammes HP, Feng Y, Pfister F, Brownlee M, 2011. Diabetic retinopathy: targeting vasoregression. Diabetes 60, 9–16. [PubMed: 21193734]

Hatchell DL, Toth CA, Barden CA, Saloupis P, 1995. Diabetic retinopathy in a cat. Exp. Eye Res. 60, 591–593. [PubMed: 7615025]

Hayreh SS, 1963. The central artery OF the retina. Its role IN the blood supply OF the optic nerve. Br. J. Ophthalmol. 47, 651–663. [PubMed: 14211664]

Heier JS, Singh RP, Wykoff CC, Csaky KG, Lai TYY, Loewenstein A, Schlottmann PG, Paris LP, Westenskow PD, Quezada-Ruiz C, 2021. The angiopoietin/tie pathway IN retinal vascular diseases: a review. Retina 41, 1–19. [PubMed: 33136975]

Hellström M, Gerhardt H, Kalén M, Li X, Eriksson U, Wolburg H, Betsholtz C, 2001. Lack of pericytes leads to endothelial hyperplasia and abnormal vascular morphogenesis. J. Cell Biol. 153, 543–553. [PubMed: 11331305]

Hidayat AA, Fine BS, 1985. Diabetic choroidopathy. Light and electron microscopic observations of seven cases. Ophthalmology 92, 512–522. [PubMed: 2582331]

Hofman P, van Blijswijk BC, Gaillard PJ, Vrensen GF, Schlingemann RO, 2001. Endothelial cell hypertrophy induced by vascular endothelial growth factor in the retina: new insights into the pathogenesis of capillary nonperfusion. Arch. Ophthalmol. 119, 861–866. [PubMed: 11405837]

Holekamp NM, Shui YB, Beebe D, 2006. Lower intraocular oxygen tension in diabetic patients: possible contribution to decreased incidence of nuclear sclerotic cataract. Am. J. Ophthalmol. 141, 1027–1032. [PubMed: 16765670]

Holmen IC, Konda SM, Pak JW, McDaniel KW, Blodi B, Stepien KE, Domalpally A, 2020. Prevalence and severity of artifacts in optical coherence tomographic angiograms. JAMA Ophthalmol. 138, 119–126. [PubMed: 31804666]

Hormel TT, Jia Y, Jian Y, Hwang TS, Bailey ST, Pennesi ME, Wilson DJ, Morrison JC, Huang D, 2021. Plexus-specific retinal vascular anatomy and pathologies as seen by projection-resolved optical coherence tomographic angiography. Prog. Retin. Eye Res. 80, 100878. [PubMed: 32712135]

Author Manuscript Author Manuscript Author Manuscript Author Manuscript

Hsiao CC, Yang CM, Yang CH, Ho TC, Lai TT, Hsieh YT, 2020. Correlations between visual acuity and macular microvasculature quantified with optical coherence tomography angiography in diabetic macular oedema. Eye 34, 544–552. [PubMed: 31406356]

Hua R, Liu L, Wang X, Chen L, 2013. Imaging evidence of diabetic choroidopathy in vivo: angiographic pathoanatomy and choroidal-enhanced depth imaging. PLoS One 8, e83494. [PubMed: 24349522]

Huber G, Heynen S, Imsand C, vom Hagen F, Muehlfriedel R, Tanimoto N, Feng Y, Hammes HP, Grimm C, Peichl L, Seeliger MW, Beck SC, 2010. Novel rodent models for macular research. PLoS One 5, e13403. [PubMed: 20976212]

Hwang TS, Gao SS, Liu L, Lauer AK, Bailey ST, Flaxel CJ, Wilson DJ, Huang D, Jia Y, 2016. Automated quantification of capillary nonperfusion using optical coherence tomography angiography in diabetic retinopathy. JAMA Ophthalmol. 134, 367–373. [PubMed: 26795548]

Iafe NA, Phasukkijwatana N, Chen X, Sarraf D, 2016. Retinal capillary density and foveal avascular zone area are age-dependent: quantitative analysis using optical coherence tomography angiography. Investig. Ophthalmol. Vis. Sci. 57, 5780–5787. [PubMed: 27792812]

Iwasaki M, Inomata H, 1986. Relation between superficial capillaries and foveal structures in the human retina. Investig. Ophthalmol. Vis. Sci. 27, 1698–1705. [PubMed: 3793399]

Jia Y, Bailey ST, Hwang TS, McClintic SM, Gao SS, Pennesi ME, Flaxel CJ, Lauer AK, Wilson DJ, Hornegger J, Fujimoto JG, Huang D, 2015. Quantitative optical coherence tomography angiography of vascular abnormalities in the living human eye. Proc. Natl. Acad. Sci. U.S.A. 112, E2395–E2402. [PubMed: 25897021]

Joe AW, Wickremasinghe SS, Gillies MC, Nguyen V, Lim LL, Mehta H, Fraser-Bell S, 2019. Dexamethasone implant for the treatment of persistent diabetic macular oedema despite long-term treatment with bevacizumab. Clin. Exp. Ophthalmol. 47, 287–289. [PubMed: 30084193]

Joussen AM, Poulaki V, Qin W, Kirchhof B, Mitsiades N, Wiegand SJ, Rudge J, Yancopoulos GD, Adamis AP, 2002. Retinal vascular endothelial growth factor induces intercellular adhesion molecule-1 and endothelial nitric oxide synthase expression and initiates early diabetic retinal leukocyte adhesion in vivo. Am. J. Pathol. 160, 501–509. [PubMed: 11839570]

Joussen AM, Ricci F, Paris LP, Korn C, Quezada-Ruiz C, Zarbin M, 2021. Angiopoietin/Tie2 signalling and its role in retinal and choroidal vascular diseases: a review of preclinical data. Eye 35, 1305–1316. [PubMed: 33564135]

Joyal JS, Gantner ML, Smith LEH, 2018. Retinal energy demands control vascular supply of the retina in development and disease: the role of neuronal lipid and glucose metabolism. Prog. Retin. Eye Res. 64, 131–156. [PubMed: 29175509]

Kador PF, Takahashi Y, Wyman M, Ferris F 3rd, 1995. Diabeteslike proliferative retinal changes in galactose-fed dogs. Arch. Ophthalmol. 113, 352–354. [PubMed: 7887849]

Kador PF, Takahashi Y, Akagi Y, Blessing K, Randazzo J, Wyman M, 2007. Age-dependent retinal capillary pericyte degeneration in galactose-fed dogs. J. Ocul. Pharmacol. Therapeut. 23, 63–69.

Karhunen U, Raitta C, Kala R, 1986. Adverse reactions to fluorescein angiography. Acta Ophthalmol. 64, 282–286. [PubMed: 2944349]

Kaur R, Kaur M, Singh J, 2018. Endothelial dysfunction and platelet hyperactivity in type 2 diabetes mellitus: molecular insights and therapeutic strategies. Cardiovasc. Diabetol. 17, 121. [PubMed: 30170601]

Keech AC, Mitchell P, Summanen PA, O'Day J, Davis TM, Moffitt MS, Taskinen MR, Simes RJ, Tse D, Williamson E, Merrifield A, Laatikainen LT, d'Emden MC, Crimet DC, O'Connell RL, Colman PG, investigators F.s., 2007. Effect of fenofibrate on the need for laser treatment for diabetic retinopathy (FIELD study): a randomised controlled trial. Lancet 370, 1687–1697. [PubMed: 17988728]

Kern TS, Engerman RL, 1996a. Capillary lesions develop in retina rather than cerebral cortex in diabetes and experimental galactosemia. Arch. Ophthalmol. 114, 306–310. [PubMed: 8600891]

Kern TS, Engerman RL, 1996b. A mouse model of diabetic retinopathy. Arch. Ophthalmol. 114, 986–990. [PubMed: 8694735]

Author Manuscript Author Manuscript Author Manuscript Author Manuscript

Kern TS, Miller CM, Tang J, Du Y, Ball SL, Berti-Matera L, 2010. Comparison of three strains of diabetic rats with respect to the rate at which retinopathy and tactile allodynia develop. Mol. Vis. 16, 1629–1639. [PubMed: 20806092]

Kim SY, Johnson MA, McLeod DS, Alexander T, Otsuji T, Steidl SM, Hansen BC, Lutty GA, 2004. Retinopathy in monkeys with spontaneous type 2 diabetes. Invest. Ophthalmol. Vis. Sci. 45, 4543–4553. [PubMed: 15557466]

Kim JH, Kim JH, Yu YS, Cho CS, Kim KW, 2009. Blockade of angiotensin II attenuates VEGF-mediated blood-retinal barrier breakdown in diabetic retinopathy. J. Cerebr. Blood Flow Metabol. 29, 621–628.

Kim YH, Kim YS, Roh GS, Choi WS, Cho GJ, 2012. Resveratrol blocks diabetes-induced early vascular lesions and vascular endothelial growth factor induction in mouse retinas. Acta Ophthalmol. 90, e31–37. [PubMed: 21914146]

Kim AY, Chu Z, Shahidzadeh A, Wang RK, Puliafito CA, Kashani AH, 2016a. Quantifying microvascular density and morphology in diabetic retinopathy using spectral-domain optical coherence tomography angiography. Investig. Ophthalmol. Vis. Sci. 57, OCT362–OCT370. [PubMed: 27409494]

Kim K, Yu SY, Kwak HW, Kim ES, 2016b. Retinal neurodegeneration associated with peripheral nerve conduction and autonomic nerve function in diabetic patients. Am. J. Ophthalmol. 170, 15–24. [PubMed: 27381712]

Klaassen I, Van Noorden CJ, Schlingemann RO, 2013. Molecular basis of the inner blood-retinal barrier and its breakdown in diabetic macular edema and other pathological conditions. Prog. Retin. Eye Res. 34, 19–48. [PubMed: 23416119]

Klein R, Klein BE, Moss SE, Linton KL, 1992. The Beaver Dam Eye Study. Retinopathy in adults with newly discovered and previously diagnosed diabetes mellitus. Ophthalmology 99, 58–62. [PubMed: 1741141]

Kohner EM, 1993. The retinal blood flow in diabetes. Diabete Metab. 19, 401–404. [PubMed: 8056118]

Kohzaki K, Vingrys AJ, Bui BV, 2008. Early inner retinal dysfunction in streptozotocin-induced diabetic rats. Invest. Ophthalmol. Vis. Sci. 49, 3595–3604. [PubMed: 18421077]

Koleva-Georgieva DN, Sivkova NP, Terzieva D, 2011. Serum inflammatory cytokines IL-1beta, IL-6, TNF-alpha and VEGF have influence on the development of diabetic retinopathy. Folia Med. 53, 44–50.

Kornblau IS, El-Annan JF, 2019. Adverse reactions to fluorescein angiography: a comprehensive review of the literature. Surv. Ophthalmol. 64, 679–693. [PubMed: 30772364]

Kozulin P, Natoli R, O'Brien KM, Madigan MC, Provis JM, 2009. Differential expression of anti-angiogenic factors and guidance genes in the developing macula. Mol. Vis. 15, 45–59. [PubMed: 19145251]

Krawitz BD, Phillips E, Bavier RD, Mo S, Carroll J, Rosen RB, Chui TYP, 2018. Parafoveal nonperfusion analysis in diabetic retinopathy using optical coherence tomography angiography. Transl Vis Sci Technol 7, 4.

Kuiper EJ, van Zijderveld R, Roestenberg P, Lyons KM, Goldschmeding R, Klaassen I, Van Noorden CJ, Schlingemann RO, 2008. Connective tissue growth factor is necessary for retinal capillary basal lamina thickening in diabetic mice. J. Histochem. Cytochem. 56, 785–792. [PubMed: 18474939]

Kumar S, Zhuo L, 2010. Longitudinal in vivo imaging of retinal gliosis in a diabetic mouse model. Exp. Eye Res. 91, 530–536. [PubMed: 20655908]

Kur J, Newman EA, Chan-Ling T, 2012. Cellular and physiological mechanisms underlying blood flow regulation in the retina and choroid in health and disease. Prog. Retin. Eye Res. 31, 377–406. [PubMed: 22580107]

Kwan CC, Lee HE, Schwartz G, Fawzi AA, 2020. Acute hyperglycemia reverses neurovascular coupling during dark to light adaptation in healthy subjects on optical coherence tomography angiography. Investig. Ophthalmol. Vis. Sci. 61, 38.

Kylstra JA, Wierzbicki T, Wolbarsht ML, Landers MB 3rd, Stefansson E, 1986. The relationship between retinal vessel tortuosity, diameter, and transmural pressure. Graefe's archive for clinical

Author Manuscript Author Manuscript Author Manuscript Author Manuscript

and experimental ophthalmology = Albrecht von Graefes Archiv fur klinische und experimentelle Ophthalmologie, 224, 477–480.

La Mantia A, Kurt RA, Mejor S, Egan CA, Tufail A, Keane PA, Sim DA, 2019. Comparing fundus fluorescein angiography and swept-source optical coherence tomography angiography in the evaluation of diabetic macular perfusion. Retina 39, 926–937. [PubMed: 29346244]

Lai AK, Lo AC, 2013. Animal models of diabetic retinopathy: summary and comparison. J. Diabetes Res. 2013, 106594. [PubMed: 24286086]

Lam TT, Abler AS, Tso M, 1999. Apoptosis and caspases after ischemia-reperfusion injury in rat retina. Investig. Ophthalmol. Vis. Sci. 40, 967–975. [PubMed: 10102294]

Lane M, Moult EM, Novais EA, Louzada RN, Cole ED, Lee B, Husvogt L, Keane PA, Denniston AK, Witkin AJ, Baumal CR, Fujimoto JG, Duker JS, Waheed NK, 2016. Visualizing the choriocapillaris under drusen: comparing 1050-nm swept-source versus 840-nm spectral-domain optical coherence tomography angiography. Investig. Ophthalmol. Vis. Sci. 57, OCT585–590. [PubMed: 27547891]

Lange CAK, Stavrakas P, Luhmann UFO, de Silva DJ, Ali RR, Gregor ZJ, Bainbridge JWB, 2011. Intraocular oxygen distribution in advanced proliferative diabetic retinopathy. Am. J. Ophthalmol. 152, 406–412 e403. [PubMed: 21723532]

Lecleire-Collet A, Audo I, Aout M, Girmens JF, Sofroni R, Erginay A, Le Gargasson JF, Mohand-Saïd S, Meas T, Guillausseau PJ, Vicaut E, Paques M, Massin P, 2011. Evaluation of retinal function and flicker light-induced retinal vascular response in normotensive patients with diabetes without retinopathy. Investig. Ophthalmol. Vis. Sci. 52, 2861–2867. [PubMed: 21282578]

Lee DH, Kim JT, Jung DW, Joe SG, Yoon YH, 2013. The relationship between foveal ischemia and spectral-domain optical coherence tomography findings in ischemic diabetic macular edema. Investig. Ophthalmol. Vis. Sci. 54, 1080–1085. [PubMed: 23329668]

Lee H, Lee M, Chung H, Kim HC, 2018. Quantification of retinal vessel tortuosity in diabetic retinopathy using optical coherence tomography angiography. Retina 38, 976–985. [PubMed: 28333883]

Li CR, Sun SG, 2010. VEGF expression and cell apoptosis in NOD mouse retina. Int. J. Ophthalmol. 3, 224–227. [PubMed: 22553559]

Li L, Almansoob S, Zhang P, Zhou Y.d., Tan Y, Gao L, 2019. Quantitative analysis of retinal and choroid capillary ischaemia using optical coherence tomography angiography in type 2 diabetes. Acta Ophthalmol. 97, 240–246. [PubMed: 30810284]

Liew G, Sim DA, Keane PA, Tan AG, Mitchell P, Wang JJ, Wong TY, Fruttiger M, Tufail A, Egan CA, 2015. Diabetic macular ischaemia is associated with narrower retinal arterioles in patients with type 2 diabetes. Acta Ophthalmol. 93, e45–51. [PubMed: 25613127]

Linsenmeier RA, Braun RD, 1992. Oxygen distribution and consumption in the cat retina during normoxia and hypoxemia. J. Gen. Physiol. 99, 177–197. [PubMed: 1613482]

Linsenmeier RA, Steinberg RH, 1986. Mechanisms of hypoxic effects on the cat DC electroretinogram. Investig. Ophthalmol. Vis. Sci. 27, 1385–1394. [PubMed: 3744728]

Linsenmeier RA, Zhang HF, 2017. Retinal oxygen: from animals to humans. Prog. Retin. Eye Res. 58, 115–151. [PubMed: 28109737]

Lobov IB, Brooks PC, Lang RA, 2002. Angiopoietin-2 displays VEGF-dependent modulation of capillary structure and endothelial cell survival in vivo. Proc. Natl. Acad. Sci. U.S.A. 99, 11205–11210. [PubMed: 12163646]

Lois N, McCarter RV, O'Neill C, Medina RJ, Stitt AW, 2014. Endothelial progenitor cells in diabetic retinopathy. Front. Endocrinol. 5, 44.

Lombardo M, Parravano M, Lombardo G, Varano M, Boccassini B, Stirpe M, Serrao S, 2014. Adaptive optics imaging of parafoveal cones in type 1 diabetes. Retina 34, 546–557. [PubMed: 23928676]

Lombardo M, Parravano M, Serrao S, Ziccardi L, Giannini D, Lombardo G, 2016. Investigation of adaptive optics imaging biomarkers for detecting pathological changes of the cone Mosaic in patients with type 1 diabetes mellitus. PLoS One 11, e0151380. [PubMed: 26963392]

Lorenzi M, Gerhardinger C, 2001. Early cellular and molecular changes induced by diabetes in the retina. Diabetologia 44, 791–804.

Author Manuscript Author Manuscript Author Manuscript Author Manuscript

Lu Y, Simonett JM, Wang J, Zhang M, Hwang T, Hagag AM, Huang D, Li D, Jia Y, 2018. Evaluation of automatically quantified foveal avascular zone metrics for diagnosis of diabetic retinopathy using optical coherence tomography angiography. Investig. Ophthalmol. Vis. Sci. 59, 2212–2221. [PubMed: 29715365]

Lutty GA, McLeod DS, Merges C, Diggs A, Plouet J, 1996. Localization of vascular endothelial growth factor in human retina and choroid. Arch. Ophthalmol. 114, 971–977. [PubMed: 8694733]

Maeda N, Tano Y, 1996. Intraocular oxygen tension in eyes with proliferative diabetic retinopathy with and without vitreous. Graefe's archive for clinical and experimental ophthalmology = Albrecht von Graefes Archiv fur klinische und experimentelle Ophthalmologie, 234 (Suppl. 1), S66–S69.

Magrath GN, Say EAT, Sioufi K, Ferenczy S, Samara WA, Shields CL, 2017. Variability in foveal avascular zone and capillary density using optical coherence tomography angiography machines in healthy eyes. Retina 37, 2102–2111. [PubMed: 27997512]

Mandecka A, Dawczynski J, Blum M, Müller N, Kloos C, Wolf G, Vilser W, Hoyer H, Müller UA, 2007. Influence of flickering light on the retinal vessels in diabetic patients. Diabetes Care 30, 3048–3052. [PubMed: 17728481]

Mansour SZ, Hatchell DL, Chandler D, Saloupis P, Hatchell MC, 1990. Reduction of basement membrane thickening in diabetic cat retina by sulindac. Invest. Ophthalmol. Vis. Sci. 31, 457–463. [PubMed: 2318584]

Mansour AM, Schachat A, Bodiford G, Haymond R, 1993. Foveal avascular zone in diabetes mellitus. Retina 13, 125–128. [PubMed: 8337493]

Martin PM, Roon P, Van Ells TK, Ganapathy V, Smith SB, 2004. Death of retinal neurons in streptozotocin-induced diabetic mice. Invest. Ophthalmol. Vis. Sci. 45, 3330–3336. [PubMed: 15326158]

Medrano CJ, Fox DA, 1995. Oxygen consumption in the rat outer and inner retina: light- and pharmacologically-induced inhibition. Exp. Eye Res. 61, 273–284. [PubMed: 7556491]

Mendis KR, Balaratnasingam C, Yu P, Barry CJ, McAllister IL, Cringle SJ, Yu DY, 2010. Correlation of histologic and clinical images to determine the diagnostic value of fluorescein angiography for studying retinal capillary detail. Investig. Ophthalmol. Vis. Sci. 51, 5864–5869. [PubMed: 20505200]

Mendonca LSM, Perrott-Reynolds R, Schwartz R, Madi HA, Cronbach N, Gendelman I, Muldrew A, Bannon F, Balaskas K, Gemmy Cheung CM, Fawzi A, Ferrara D, Freund KB, Fujimoto J, Munk MR, Querques G, Ribeiro R, Rosenfeld PJ, Sadda SR, Sahni J, Sarraf D, Spaide RF, Schmidt-Erfurth U, Souied E, Staurenghi G, Tadayoni R, Wang RK, Chakravarthy U, Waheed NK, 2021. Deliberations of an international panel of experts on OCT angiography nomenclature of neovascular age-related macular degeneration. Ophthalmology 128, 1109–1112. [PubMed: 33359557]

Metea MR, Newman EA, 2007. Signalling within the neurovascular unit in the mammalian retina. Exp. Physiol. 92, 635–640. [PubMed: 17434916]

Midena E, Segato T, Radin S, di Giorgio G, Meneghini F, Piermarocchi S, Belloni AS, 1989. Studies on the retina of the diabetic db/db mouse. I. Endothelial cell-pericyte ratio. Ophthalmic Res. 21, 106–111. [PubMed: 2734001]

Midena E, Torresin T, Longhin E, Midena G, Pilotto E, Frizziero L, 2021. Early microvascular and oscillatory potentials changes in human diabetic retina: amacrine cells and the intraretinal neurovascular crosstalk. J. Clin. Med. 10.

Migacz JV, Gorczynska I, Azimipour M, Jonnal R, Zawadzki RJ, Werner JS, 2019. Megahertz-rate optical coherence tomography angiography improves the contrast of the choriocapillaris and choroid in human retinal imaging. Biomed. Opt Express 10, 50–65. [PubMed: 30775082]

Mihailovic N, Brand C, Lahme L, Schubert F, Bormann E, Eter N, Alnawaiseh M, 2018. Repeatability, reproducibility and agreement of foveal avascular zone measurements using three different optical coherence tomography angiography devices. PLoS One 13, e0206045. [PubMed: 30335839]

Mishra A, Newman EA, 2010. Inhibition of inducible nitric oxide synthase reverses the loss of functional hyperemia in diabetic retinopathy. Glia 58, 1996–2004. [PubMed: 20830810]

Author Manuscript Author Manuscript Author Manuscript Author Manuscript

Mitchell P, Bandello F, Schmidt-Erfurth U, Lang GE, Massin P, Schlingemann RO, Sutter F, Simader C, Burian G, Gerstner O, Weichselberger A, group R.s., 2011. The RESTORE study: ranibizumab monotherapy or combined with laser versus laser monotherapy for diabetic macular edema. Ophthalmology 118, 615–625. [PubMed: 21459215]

Miyamoto K, Khosrof S, Bursell SE, Moromizato Y, Aiello LP, Ogura Y, Adamis AP, 2000. Vascular endothelial growth factor (VEGF)-induced retinal vascular permeability is mediated by intercellular adhesion molecule-1 (ICAM-1). Am. J. Pathol. 156, 1733–1739. [PubMed: 10793084]

Moein HR, Novais EA, Rebhun CB, Cole ED, Louzada RN, Witkin AJ, Baumal CR, Duker JS, Waheed NK, 2018. Optical coherence tomography angiography to detect macular capillary ischemia in patients with inner retinal changes after resolved diabetic macular edema. Retina 38, 2277–2284. [PubMed: 29068912]

Mohler KJ, Draxinger W, Klein T, Kolb JP, Wieser W, Haritoglou C, Kampik A, Fujimoto JG, Neubauer AS, Huber R, Wolf A, 2015. Combined 60° wide-field choroidal thickness maps and high-definition en face vasculature visualization using swept-source Megahertz OCT at 1050 nm. Investig. Ophthalmol. Vis. Sci. 56, 6284–6293. [PubMed: 26431482]

Molina-Martin A, Perez-Cambrodi RJ, Pinero DP, 2018. Current clinical application of microperimetry: a review. Semin. Ophthalmol. 33, 620–628. [PubMed: 28991503]

Moore J, Bagley S, Ireland G, McLeod D, Boulton ME, 1999. Three dimensional analysis of microaneurysms in the human diabetic retina. J. Anat. 194 (Pt 1), 89–100. [PubMed: 10227670]

Moran EP, Wang Z, Chen J, Sapieha P, Smith LE, Ma JX, 2016. Neurovascular cross talk in diabetic retinopathy: pathophysiological roles and therapeutic implications. Am. J. Physiol. Heart Circ. Physiol. 311, H738–H749. [PubMed: 27473938]

Moret P, Pournaras CJ, Munoz JL, Brazitikos P, Tsacopoulos M, 1992. [Profile of pO2. I. Profile of transretinal pO2 in hypoxia]. Klinische Monatsblatter fur Augenheilkunde 200, 498–499. [PubMed: 1614136]

Moussa M, Leila M, Bessa AS, Lolah M, Abou Shousha M, El Hennawi HM, Hafez TA, 2019. Grading of macular perfusion in retinal vein occlusion using en-face swept-source optical coherence tomography angiography: a retrospective observational case series. BMC Ophthalmol. 19, 127. [PubMed: 31182069]

Muir ER, Renteria RC, Duong TQ, 2012. Reduced ocular blood flow as an early indicator of diabetic retinopathy in a mouse model of diabetes. Investig. Ophthalmol. Vis. Sci. 53, 6488–6494. [PubMed: 22915034]

Munk MR, Giannakaki-Zimmermann H, Berger L, Huf W, Ebneter A, Wolf S, Zinkernagel MS, 2017. OCT-angiography: a qualitative and quantitative comparison of 4 OCT-A devices. PLoS One 12, e0177059. [PubMed: 28489918]

Nagaoka T, Sato E, Takahashi A, Yokota H, Sogawa K, Yoshida A, 2010. Impaired retinal circulation in patients with type 2 diabetes mellitus: retinal laser Doppler velocimetry study. Investig. Ophthalmol. Vis. Sci. 51, 6729–6734. [PubMed: 20631236]

Nemiroff J, Kuehlewein L, Rahimy E, Tsui I, Doshi R, Gaudric A, Gorin MB, Sadda S, Sarraf D, 2016. Assessing deep retinal capillary ischemia in paracentral acute middle maculopathy by optical coherence tomography angiography. Am. J. Ophthalmol. 162, 121–132 e121. [PubMed: 26562176]

Nesper PL, Roberts PK, Onishi AC, Chai H, Liu L, Jampol LM, Fawzi AA, 2017a. Quantifying microvascular abnormalities with increasing severity of diabetic retinopathy using optical coherence tomography angiography. Investig. Ophthalmol. Vis. Sci. 58, BIO307–BIO315. [PubMed: 29059262]

Nesper PL, Scarinci F, Fawzi AA, 2017b. Adaptive optics reveals photoreceptor abnormalities in diabetic macular ischemia. PLoS One 12, e0169926. [PubMed: 28068435]

Nesper PL, Soetikno BT, Zhang HF, Fawzi AA, 2017c. OCT angiography and visible-light OCT in diabetic retinopathy. Vis. Res. 139, 191–203. [PubMed: 28601429]

Newman EA, 2013. Functional hyperemia and mechanisms of neurovascular coupling in the retinal vasculature. J. Cerebr. Blood Flow Metabol. 33, 1685–1695.

Author Manuscript Author Manuscript Author Manuscript Author Manuscript

Nguyen QD, Shah SM, Van Anden E, Sung JU, Vitale S, Campochiaro PA, 2004. Supplemental oxygen improves diabetic macular edema: a pilot study. Investig. Ophthalmol. Vis. Sci. 45, 617–624. [PubMed: 14744906]

Nicholson L, Ramu J, Triantafyllopoulou I, Patrao NV, Comyn O, Hykin P, Sivaprasad S, 2015. Diagnostic accuracy of disorganization of the retinal inner layers in detecting macular capillary non-perfusion in diabetic retinopathy. Clin. Exp. Ophthalmol. 43, 735–741. [PubMed: 25998983]

Nickla DL, Wallman J, 2010. The multifunctional choroid. Prog. Retin. Eye Res. 29, 144–168. [PubMed: 20044062]

Nishiwaki A, Ueda T, Ugawa S, Shimada S, Ogura Y, 2003. Upregulation of P-selectin and intercellular adhesion molecule-1 after retinal ischemia-reperfusion injury. Investig. Ophthalmol. Vis. Sci. 44, 4931–4935. [PubMed: 14578419]

Nobre Cardoso J, Keane PA, Sim DA, Bradley P, Agrawal R, Addison PK, Egan C, Tufail A, 2016. Systematic evaluation of optical coherence tomography angiography in retinal vein occlusion. Am. J. Ophthalmol. 163, 93–107 e106. [PubMed: 26621685]

Ogura S, Kurata K, Hattori Y, Takase H, Ishiguro-Oonuma T, Hwang Y, Ahn S, Park I, Ikeda W, Kusuhara S, Fukushima Y, Nara H, Sakai H, Fujiwara T, Matsushita J, Ema M, Hirashima M, Minami T, Shibuya M, Takakura N, Kim P, Miyata T, Ogura Y, Uemura A, 2017. Sustained inflammation after pericyte depletion induces irreversible blood-retina barrier breakdown. JCI Insight 2, e90905. [PubMed: 28194443]

Ong JX, Kwan CC, Cicinelli MV, Fawzi AA, 2020. Superficial capillary perfusion on optical coherence tomography angiography differentiates moderate and severe nonproliferative diabetic retinopathy. PLoS One 15, e0240064. [PubMed: 33091032]

Onishi AC, Nesper PL, Roberts PK, Moharram GA, Chai H, Liu L, Jampol LM, Fawzi AA, 2018. Importance of considering the middle capillary plexus on OCT angiography in diabetic retinopathy. Investig. Ophthalmol. Vis. Sci. 59, 2167–2176. [PubMed: 29801151]

Oshitari T, 2022. Diabetic retinopathy: neurovascular disease requiring neuroprotective and regenerative therapies. Neural Regen. Res. 17, 795–796. [PubMed: 34472475]

Palochak CMA, Lee HE, Song J, Geng A, Linsenmeier RA, Burns SA, Fawzi AA, 2019. Retinal blood velocity and flow in early diabetes and diabetic retinopathy using adaptive optics scanning laser ophthalmoscopy. J. Clin. Med. 8.

Park SS, 2016. Cell therapy applications for retinal vascular diseases: diabetic retinopathy and retinal vein occlusion. Investig. Ophthalmol. Vis. Sci. 57, ORSFj1–ORSFj10. [PubMed: 27116667]

Park JJ, Soetikno BT, Fawzi AA, 2016. Characterization of the middle capillary plexus using optical coherence tomography angiography in healthy and diabetic eyes. Retina 36, 2039–2050. [PubMed: 27205895]

Park DY, Lee J, Kim J, Kim K, Hong S, Han S, Kubota Y, Augustin HG, Ding L, Kim JW, Kim H, He Y, Adams RH, Koh GY, 2017. Plastic roles of pericytes in the blood-retinal barrier. Nat. Commun. 8, 15296. [PubMed: 28508859]

Park JC, Chen YF, Liu M, Liu K, McAnany JJ, 2020. Structural and functional abnormalities in early-stage diabetic retinopathy. Curr. Eye Res. 45, 975–985. [PubMed: 31847599]

Parravano M, Oddone F, Tedeschi M, Chiaravalloti A, Perillo L, Boccassini B, Varano M, 2010. Retinal functional changes measured by microperimetry in neovascular age-related macular degeneration treated with ranibizumab: 24-month results. Retina 30, 1017–1024. [PubMed: 20224469]

Pereira F, Godoy BR, Maia M, Regatieri CV, 2019. Microperimetry and OCT angiography evaluation of patients with ischemic diabetic macular edema treated with monthly intravitreal bevacizumab: a pilot study. Int. J. Retina Vitr. 5, 24.

Petropoulos IK, Pournaras JA, Stangos AN, Pournaras CJ, 2013. Preretinal partial pressure of oxygen gradients before and after experimental pars plana vitrectomy. Retina 33, 170–178. [PubMed: 22972446]

Pfister F, Feng Y, vom Hagen F, Hoffmann S, Molema G, Hillebrands JL, Shani M, Deutsch U, Hammes HP, 2008. Pericyte migration: a novel mechanism of pericyte loss in experimental diabetic retinopathy. Diabetes 57, 2495–2502. [PubMed: 18559662]

Author Manuscript Author Manuscript Author Manuscript Author Manuscript

Pournaras CJ, 1995. Retinal oxygen distribution. Its role in the physiopathology of vasoproliferative microangiopathies. Retina 15, 332–347. [PubMed: 8545580]

Provis JM, Penfold PL, Cornish EE, Sandercoe TM, Madigan MC, 2005. Anatomy and development of the macula: specialisation and the vulnerability to macular degeneration. Clin. Exp. Optom. 88, 269–281. [PubMed: 16255686]

Provis JM, Dubis AM, Maddess T, Carroll J, 2013. Adaptation of the central retina for high acuity vision: cones, the fovea and the avascular zone. Prog. Retin. Eye Res. 35, 63–81. [PubMed: 23500068]

Rakoczy EP, Ali Rahman IS, Binz N, Li CR, Vagaja NN, de Pinho M, Lai CM, 2010. Characterization of a mouse model of hyperglycemia and retinal neovascularization. Am. J. Pathol. 177, 2659–2670. [PubMed: 20829433]

Regula JT, Lundh von Leithner P, Foxton R, Barathi VA, Cheung CM, Bo Tun SB, Wey YS, Iwata D, Dostalek M, Moelleken J, Stubenrauch KG, Nogoceke E, Widmer G, Strassburger P, Koss MJ, Klein C, Shima DT, Hartmann G, 2016. Targeting key angiogenic pathways with a bispecific CrossMAb optimized for neovascular eye diseases. EMBO Mol. Med. 8, 1265–1288. [PubMed: 27742718]

Reznicek L, Klein T, Wieser W, Kernt M, Wolf A, Haritoglou C, Kampik A, Huber R, Neubauer AS, 2014. Megahertz ultra-wide-field swept-source retina optical coherence tomography compared to current existing imaging devices. Graefe's archive for clinical and experimental ophthalmology = Albrecht von Graefes Archiv fur klinische und experimentelle Ophthalmologie, 252, 1009–1016.

Reznicek L, Kolb JP, Klein T, Mohler KJ, Wieser W, Huber R, Kernt M, Märtz J, Neubauer AS, 2015. Wide-field Megahertz OCT imaging of patients with diabetic retinopathy. J. Diabetes Res. 2015, 305084. [PubMed: 26273665]

Robbins SG, Mixon RN, Wilson DJ, Hart CE, Robertson JE, Westra I, Planck SR, Rosenbaum JT, 1994. Platelet-derived growth factor ligands and receptors immunolocalized in proliferative retinal diseases. Investig. Ophthalmol. Vis. Sci. 35, 3649–3663. [PubMed: 8088954]

Robinson R, Barathi VA, Chaurasia SS, Wong TY, Kern TS, 2012. Update on animal models of diabetic retinopathy: from molecular approaches to mice and higher mammals. Disease models & mechanisms 5, 444–456. [PubMed: 22730475]

Rosen RB, Romo JSA, Krawitz BD, Mo S, Fawzi AA, Linderman RE, Carroll J, Pinhas A, Chui TY, 2019. Earliest evidence of preclinical diabetic retinopathy revealed using optical coherence tomography angiography perfused capillary density. Am. J. Ophthalmol. 203, 103–115. [PubMed: 30689991]

Sakamoto A, Hangai M, Yoshimura N, 2008. Spectral-domain optical coherence tomography with multiple B-scan averaging for enhanced imaging of retinal diseases. Ophthalmology 115, 1071–1078 e1077. [PubMed: 18061270]

Sakata K, Funatsu H, Harino S, Noma H, Hori S, 2007. Relationship of macular microcirculation and retinal thickness with visual acuity in diabetic macular edema. Ophthalmology 114, 2061–2069. [PubMed: 17445900]

Sakurai A, Doci CL, Gutkind JS, 2012. Semaphorin signaling in angiogenesis, lymphangiogenesis and cancer. Cell Res. 22, 23–32. [PubMed: 22157652]

Salz DA, Talisa E, Adhi M, Moult E, Choi W, Baumal CR, Witkin AJ, Duker JS, Fujimoto JG, Waheed NK, 2016. Select features of diabetic retinopathy on swept-source optical coherence tomographic angiography compared with fluorescein angiography and normal eyes. JAMA ophthalmology 134, 644–650. [PubMed: 27055248]

Samara WA, Say EA, Khoo CT, Higgins TP, Magrath G, Ferenczy S, Shields CL, 2015. Correlation of foveal avascular zone size with foveal morphology in normal eyes using optical coherence tomography angiography. Retina 35, 2188–2195. [PubMed: 26469536]

Samara WA, Shahlaee A, Sridhar J, Khan MA, Ho AC, Hsu J, 2016. Quantitative optical coherence tomography angiography features and visual function in eyes with branch retinal vein occlusion. Am. J. Ophthalmol. 166, 76–83. [PubMed: 27038893]

Samara WA, Shahlaee A, Adam MK, Khan MA, Chiang A, Maguire JI, Hsu J, Ho AC, 2017. Quantification of diabetic macular ischemia using optical coherence tomography angiography and its relationship with visual acuity. Ophthalmology 124, 235–244. [PubMed: 27887743]

Author Manuscript Author Manuscript Author Manuscript Author Manuscript

Sambhav K, Abu-Amero KK, Chalam KV, 2017. Deep capillary macular perfusion indices obtained with OCT angiography correlate with degree of nonproliferative diabetic retinopathy. Eur. J. Ophthalmol. 27, 716–729. [PubMed: 28362051]

Sampson DM, Gong P, An D, Menghini M, Hansen A, Mackey DA, Sampson DD, Chen FK, 2017. Axial length variation impacts on superficial retinal vessel density and foveal avascular zone area measurements using optical coherence tomography angiography. Investig. Ophthalmol. Vis. Sci. 58, 3065–3072. [PubMed: 28622398]

Sander B, Larsen M, Thrane L, Hougaard JL, Jorgensen TM, 2005. Enhanced optical coherence tomography imaging by multiple scan averaging. Br. J. Ophthalmol. 89, 207–212. [PubMed: 15665354]

Santos AR, Ribeiro L, Bandello F, Lattanzio R, Egan C, Frydkjaer-Olsen U, Garcia-Arumi J, Gibson J, Grauslund J, Harding SP, Lang GE, Massin P, Midena E, Scanlon P, Aldington SJ, Simao S, Schwartz C, Ponsati B, Porta M, Costa MA, Hernandez C, Cunha-Vaz J, Simo R, 2017. European consortium for the early treatment of diabetic, R. functional and structural findings of neurodegeneration in early stages of diabetic retinopathy: cross-sectional analyses of baseline data of the EUROCONDOR Project. Diabetes 66, 2503–2510. [PubMed: 28663190]

Sapieha P, Hamel D, Shao Z, Rivera JC, Zaniolo K, Joyal JS, Chemtob S, 2010. Proliferative retinopathies: angiogenesis that blinds. Int. J. Biochem. Cell Biol. 42, 5–12. [PubMed: 19836461]

Scarinci F, Jampol LM, Linsenmeier RA, Fawzi AA, 2015. Association of diabetic macular nonperfusion with outer retinal disruption on optical coherence tomography. JAMA Ophthalmol. 133, 1036–1044. [PubMed: 26158562]

Scarinci F, Nesper PL, Fawzi AA, 2016. Deep retinal capillary nonperfusion is associated with photoreceptor disruption in diabetic macular ischemia. Am. J. Ophthalmol. 168, 129–138. [PubMed: 27173374]

Scarinci F, Varano M, Parravano M, 2019. Retinal sensitivity loss correlates with deep capillary plexus impairment in diabetic macular ischemia. J. Ophthalmol. 2019, 7589841. [PubMed: 31737359]

Schottenhamml J, Moult EM, Ploner S, Lee B, Novais EA, Cole E, Dang S, Lu CD, Husvogt L, Waheed NK, 2016. An Automatic, Intercapillary Area Based Algorithm for Quantifying Diabetes Related Capillary Dropout Using OCT Angiography, 36. Retina, Philadelphia, Pa, p. S93.

Seki M, Tanaka T, Nawa H, Usui T, Fukuchi T, Ikeda K, Abe H, Takei N, 2004. Involvement of brain-derived neurotrophic factor in early retinal neuropathy of streptozotocin-induced diabetes in rats: therapeutic potential of brain-derived neurotrophic factor for dopaminergic amacrine cells. Diabetes 53, 2412–2419. [PubMed: 15331553]

Shahlaee A, Pefkianaki M, Hsu J, Ho AC, 2016. Measurement of foveal avascular zone dimensions and its reliability in healthy eyes using optical coherence tomography angiography. Am. J. Ophthalmol. 161, 50–55 e51. [PubMed: 26423672]

Sharifipour F, Soheilian M, Idani E, Azarmina M, Yaseri M, 2011. Oxygen therapy for diabetic macular ischemia: a pilot study. Retina 31, 937–941. [PubMed: 21293317]

Shaw SG, Boden JP, Biecker E, Reichen J, Rothen B, 2006. Endothelin antagonism prevents diabetic retinopathy in NOD mice: a potential role of the angiogenic factor adrenomedullin. Exp. Biol. Med. 231, 1101–1105.

Shih SC, Ju M, Liu N, Smith LE, 2003. Selective stimulation of VEGFR-1 prevents oxygen-induced retinal vascular degeneration in retinopathy of prematurity. J. Clin. Invest. 112, 50–57. [PubMed: 12840058]

Shiihara H, Terasaki H, Sonoda S, Kakiuchi N, Shinohara Y, Tomita M, Sakamoto T, 2018. Objective evaluation of size and shape of superficial foveal avascular zone in normal subjects by optical coherence tomography angiography. Sci. Rep. 8, 1–9. [PubMed: 29311619]

Sidorczuk P, Pieklarz B, Konopinska J, Saeed E, Mariak Z, Dmuchowska D, 2021. Foveal avascular zone does not correspond to choroidal characteristics in patients with diabetic retinopathy: a single-center cross-sectional analysis. Diabetes, Metab. Syndrome Obes. Targets Ther. 14, 2893–2903.

Author Manuscript Author Manuscript Author Manuscript Author Manuscript

Sim DA, Keane PA, Zarranz-Ventura J, Bunce CV, Fruttiger M, Patel PJ, Tufail A, Egan CA, 2013a. Predictive factors for the progression of diabetic macular ischemia. Am. J. Ophthalmol. 156, 684–692. [PubMed: 23891332]

Sim DA, Keane PA, Zarranz-Ventura J, Fung S, Powner MB, Platteau E, Bunce CV, Fruttiger M, Patel PJ, Tufail A, Egan CA, 2013b. The effects of macular ischemia on visual acuity in diabetic retinopathy. Investig. Ophthalmol. Vis. Sci. 54, 2353–2360. [PubMed: 23449720]

Simo R, Hernandez C, Porta M, Bandello F, Grauslund J, Harding SP, Aldington SJ, Egan C, Frydkjaer-Olsen U, Garcia-Arumi J, Gibson J, Lang GE, Lattanzio R, Massin P, Midena E, Ponsati B, Ribeiro L, Scanlon P, Lobo C, Costa MA, Cunha-Vaz J, 2019. European consortium for the early treatment of diabetic, R., effects of topically administered neuroprotective drugs in early stages of diabetic retinopathy: results of the EUROCONDOR clinical trial. Diabetes 68, 457–463. [PubMed: 30389750]

Sivaprasad S, Vasconcelos JC, Prevost AT, Holmes H, Hykin P, George S, Murphy C, Kelly J, Arden GB, Group CS, 2018. Clinical efficacy and safety of a light mask for prevention of dark adaptation in treating and preventing progression of early diabetic macular oedema at 24 months (CLEOPATRA): a multicentre, phase 3, randomised controlled trial. The lancet. Diabetes & endocrinology 6, 382–391. [PubMed: 29519744]

Sohn EH, van Dijk HW, Jiao C, Kok PH, Jeong W, Demirkaya N, Garmager A, Wit F, Kucukevcilioglu M, van Velthoven ME, DeVries JH, Mullins RF, Kuehn MH, Schlingemann RO, Sonka M, Verbraak FD, Abramoff MD, 2016. Retinal neurodegeneration may precede microvascular changes characteristic of diabetic retinopathy in diabetes mellitus. Proc. Natl. Acad. Sci. U.S.A. 113, E2655–E2664. [PubMed: 27114552]

Spaide RF, 2015. Volume-rendered optical coherence tomography of diabetic retinopathy pilot study. Am. J. Ophthalmol. 160, 1200–1210. [PubMed: 26384548]

Spaide RF, Ledesma-Gil G, 2020. Novel method for image averaging of optical coherence tomography angiography images. Retina 40, 2099–2105. [PubMed: 32604340]

Spaide RF, Fujimoto JG, Waheed NK, 2015a. Image artifacts in optical coherence tomography angiography. Retina 35, 2163–2180. [PubMed: 26428607]

Spaide RF, Klancnik JM Jr., Cooney MJ, 2015b. Retinal vascular layers in macular telangiectasia type 2 imaged by optical coherence tomographic angiography. JAMA Ophthalmol. 133, 66–73. [PubMed: 25317692]

Spaide RF, Fujimoto JG, Waheed NK, Sadda SR, Staurenghi G, 2018. Optical coherence tomography angiography. Prog. Retin. Eye Res. 64, 1–55. [PubMed: 29229445]

Srinivas S, Tan O, Nittala MG, Wu JL, Fawzi AA, Huang D, Sadda SR, 2017. Assessment OF retinal blood flow IN diabetic retinopathy using Doppler fourier-domain optical coherence tomography. Retina 37, 2001–2007. [PubMed: 28098726]

Stahl A, Connor KM, Sapieha P, Chen J, Dennison RJ, Krah NM, Seaward MR, Willett KL, Aderman CM, Guerin KI, Hua J, Löfqvist C, Hellström A, Smith LE, 2010. The mouse retina as an angiogenesis model. Invest. Ophthalmol. Vis. Sci. 51, 2813–2826. [PubMed: 20484600]

Stefansson E, 2006. Ocular oxygenation and the treatment of diabetic retinopathy. Surv. Ophthalmol. 51, 364–380. [PubMed: 16818083]

Stem MS, Gardner TW, 2013. Neurodegeneration in the pathogenesis of diabetic retinopathy: molecular mechanisms and therapeutic implications. Curr. Med. Chem. 20, 3241–3250. [PubMed: 23745549]

Stitt AW, Curtis TM, Chen M, Medina RJ, McKay GJ, Jenkins A, Gardiner TA, Lyons TJ, Hammes HP, Simo R, Lois N, 2016. The progress in understanding and treatment of diabetic retinopathy. Prog. Retin. Eye Res. 51, 156–186. [PubMed: 26297071]

Sun JK, Lin MM, Lammer J, Prager S, Sarangi R, Silva PS, Aiello LP, 2014. Disorganization of the retinal inner layers as a predictor of visual acuity in eyes with center-involved diabetic macular edema. JAMA Ophthalmol. 132, 1309–1316. [PubMed: 25058813]

Sun JK, Radwan SH, Soliman AZ, Lammer J, Lin MM, Prager SG, Silva PS, Aiello LB, Aiello LP, 2015. Neural retinal disorganization as a robust marker of visual acuity in current and resolved diabetic macular edema. Diabetes 64, 2560–2570. [PubMed: 25633419]

Author Manuscript Author Manuscript Author Manuscript Author Manuscript

Suzuki N, Hirano Y, Tomiyasu T, Esaki Y, Uemura A, Yasukawa T, Yoshida M, Ogura Y, 2016. Retinal hemodynamics seen on optical coherence tomography angiography before and after treatment of retinal vein occlusion. Investig. Ophthalmol. Vis. Sci. 57, 5681–5687. [PubMed: 27784073]

Takahashi K, Kishi S, Muraoka K, Shimizu K, 1998. Reperfusion of occluded capillary beds in diabetic retinopathy. Am. J. Ophthalmol. 126, 791–797. [PubMed: 9860002]

Takase N, Nozaki M, Kato A, Ozeki H, Yoshida M, Ogura Y, 2015a. Enlargement OF foveal avascular zone IN diabetic eyes evaluated BY en face optical coherence tomography angiography. Retina 35, 2377–2383. [PubMed: 26457396]

Takase N, Nozaki M, Kato A, Ozeki H, Yoshida M, Ogura Y, 2015b. Enlargement of foveal avascular zone in diabetic eyes evaluated by en face optical coherence tomography angiography. Retina 35, 2377–2383. [PubMed: 26457396]

Tam J, Dhamdhere KP, Tiruveedhula P, Lujan BJ, Johnson RN, Bearse MA Jr., Adams AJ, Roorda A, 2012. Subclinical capillary changes in non-proliferative diabetic retinopathy. Optom. Vis. Sci. 89, E692–E703 official publication of the American Academy of Optometry. [PubMed: 22525131]

Tan ACS, Tan GS, Denniston AK, Keane PA, Ang M, Milea D, Chakravarthy U, Cheung CMG, 2018. An overview of the clinical applications of optical coherence tomography angiography. Eye 32, 262–286. [PubMed: 28885606]

Tang L, Zhang Y, Jiang Y, Willard L, Ortiz E, Wark L, Medeiros D, Lin D, 2011. Dietary wolfberry ameliorates retinal structure abnormalities in db/db mice at the early stage of diabetes. Exp. Biol. Med. 236, 1051–1063.

Tang FY, Ng DS, Lam A, Luk F, Wong R, Chan C, Mohamed S, Fong A, Lok J, Tso T, Lai F, Brelen M, Wong TY, Tham CC, Cheung CY, 2017. Determinants of quantitative optical coherence tomography angiography metrics in patients with diabetes. Sci. Rep. 7, 2575. [PubMed: 28566760]

Tang FY, Chan EO, Sun Z, Wong R, Lok J, Szeto S, Chan JC, Lam A, Tham CC, Ng DS, 2020. Clinically relevant factors associated with quantitative optical coherence tomography angiography metrics in deep capillary plexus in patients with diabetes. Eye and vision 7, 7. [PubMed: 32025523]

Thagaard MS, Vergmann AS, Grauslund J, 2021. Topical treatment of diabetic retinopathy: a systematic review. Acta Ophthalmol. 10.1111/aos.14912. In press.

Tokayer J, Jia Y, Dhalla AH, Huang D, 2013. Blood flow velocity quantification using split-spectrum amplitude-decorrelation angiography with optical coherence tomography. Biomed. Opt Express 4, 1909–1924. [PubMed: 24156053]

Tonade D, Liu H, Kern TS, 2016. Photoreceptor cells produce inflammatory mediators that contribute to endothelial cell death in diabetes. Investig. Ophthalmol. Vis. Sci. 57, 4264–4271. [PubMed: 27548900]

Touhami S, Dupas B, Bertaud S, Tadayoni R, Couturier A, 2021. Intravitreal dexamethasone in diabetic macular edema: a way of enhancing the response to anti VEGF in non or poor responders? Ophthalmologica. Journal international d'ophtalmologie. International journal of ophthalmology. Zeitschrift fur Augenheilkunde.

Tsai ASH, Gan ATL, Ting DSW, Wong CW, Teo KYC, Tan ACS, Lee SY, Wong TY, Tan GSW, Gemmy Cheung CM, 2020. Diabetic macular ischemia: correlation of retinal vasculature changes by optical coherence tomography angiography and functional deficit. Retina 40, 2184–2190. [PubMed: 31842192]

Tso MO, Kurosawa A, Benhamou E, Bauman A, Jeffrey J, Jonasson O, 1988. Microangiopathic retinopathy in experimental diabetic monkeys. Trans. Am. Ophthalmol. Soc. 86, 389–421. [PubMed: 2980946]

Tyrberg M, Ponjavic V, Lovestam-Adrian M, 2008. Multifocal electroretinogram (mfERG) in patients with diabetes mellitus and an enlarged foveal avascular zone (FAZ). Documenta ophthalmologica. Adv. Ophthalmol. 117, 185–189.

Tzekov R, Arden GB, 1999. The electroretinogram in diabetic retinopathy. Surv. Ophthalmol. 44, 53–60. [PubMed: 10466588]

Author Manuscript Author Manuscript Author Manuscript Author Manuscript

Uji A, Balasubramanian S, Lei J, Baghdasaryan E, Al-Sheikh M, Borrelli E, Sadda SR, 2018. Multiple enface image averaging for enhanced optical coherence tomography angiography imaging. Acta Ophthalmol. 96, e820–e827. [PubMed: 29855147]

Unoki N, Nishijima K, Sakamoto A, Kita M, Watanabe D, Hangai M, Kimura T, Kawagoe N, Ohta M, Yoshimura N, 2007. Retinal sensitivity loss and structural disturbance in areas of capillary nonperfusion of eyes with diabetic retinopathy. Am. J. Ophthalmol. 144, 755–760. [PubMed: 17868632]

Usui Y, Westenskow PD, Kurihara T, Aguilar E, Sakimoto S, Paris LP, Wittgrove C, Feitelberg D, Friedlander MS, Moreno SK, Dorrell MI, Friedlander M, 2015. Neurovascular crosstalk between interneurons and capillaries is required for vision. J. Clin. Invest. 125, 2335–2346. [PubMed: 25915585]

Varma R, Torres M, Pena F, Klein R, Azen SP, 2004. Los angeles latino eye study, G. prevalence of diabetic retinopathy in adult latinos: the los angeles latino eye study. Ophthalmology 111, 1298–1306. [PubMed: 15234129]

Volpert OV, Zaichuk T, Zhou W, Reiher F, Ferguson TA, Stuart PM, Amin M, Bouck NP, 2002. Inducer-stimulated Fas targets activated endothelium for destruction by anti-angiogenic thrombospondin-1 and pigment epithelium-derived factor. Nat. Med. 8, 349–357. [PubMed: 11927940]

Vujosevic S, Muraca A, Gatti V, Masoero L, Brambilla M, Cannillo B, Villani E, Nucci P, De Cilla S, 2018. Peripapillary microvascular and neural changes in diabetes mellitus: an OCT-angiography study. Investig. Ophthalmol. Vis. Sci. 59, 5074–5081. [PubMed: 30357402]

Vujosevic S, Muraca A, Alkabes M, Villani E, Cavarzeran F, Rossetti L, De Cilla S, 2019a. Early microvascular and neural changes in patients with type 1 and type 2 diabetes mellitus without clinical signs of diabetic retinopathy. Retina 39, 435–445. [PubMed: 29206758]

Vujosevic S, Toma C, Villani E, Gatti V, Brambilla M, Muraca A, Ponziani MC, Aimaretti G, Nuzzo A, Nucci P, De Cilla S, 2019b. Early detection of microvascular changes in patients with diabetes mellitus without and with diabetic retinopathy: comparison between different swept-source OCT-A instruments. J. Diabetes Res. 2019, 2547216. [PubMed: 31281849]

Vujosevic S, Toma C, Villani E, Muraca A, Torti E, Florimbi G, Leporati F, Brambilla M, Nucci P, De Cilla S, 2020. Diabetic macular edema with neuroretinal detachment: OCT and OCT-angiography biomarkers of treatment response to anti-VEGF and steroids. Acta Diabetol. 57, 287–296. [PubMed: 31541333]

Vujosevic S, Cunha-Vaz J, Figueira J, Lowenstein A, Midena E, Parravano M, Scanlon PH, Simo R, Hernandez C, Madeira MH, Marques IP, Martinho AC, Santos AR, Simo-Servat O, Salongcay RP, Zur D, Peto T, 2021. Standardisation of optical coherence tomography angiography imaging biomarkers in diabetic retinal disease. Ophthalmic Res.

Wakabayashi T, Sato T, Hara-Ueno C, Fukushima Y, Sayanagi K, Shiraki N, Sawa M, Ikuno Y, Sakaguchi H, Nishida K, 2017. Retinal microvasculature and visual acuity in eyes with branch retinal vein occlusion: imaging analysis by optical coherence tomography angiography. Investig. Ophthalmol. Vis. Sci. 58, 2087–2094. [PubMed: 28388705]

Weinhaus RS, Burke JM, Delori FC, Snodderly DM, 1995. Comparison of fluorescein angiography with microvascular anatomy of macaque retinas. Exp. Eye Res. 61, 1–16. [PubMed: 7556462]

Witmer AN, Vrensen GF, Van Noorden CJ, Schlingemann RO, 2003. Vascular endothelial growth factors and angiogenesis in eye disease. Prog. Retin. Eye Res. 22, 1–29. [PubMed: 12597922]

Writing C, Kim JE, Glassman AR, Josic K, Melia M, Aiello LP, Baker C, Eells JT, Jampol LM, Kern TS, Marcus D, Martin DF, Salehi-Had H, Shah SN, Stockdale CR, Sun JK, Network DR, 2021. A randomized trial of photobiomodulation therapy for center-involved diabetic macular edema with good visual acuity (protocol AE). Ophthalmology. Retina. l.a.s.N. www.idf.org.

Yancey CM, Linsenmeier RA, 1989. Oxygen distribution and consumption in the cat retina at increased intraocular pressure. Investig. Ophthalmol. Vis. Sci. 30, 600–611. [PubMed: 2703301]

Yannuzzi LA, Rohrer KT, Tindel LJ, Sobel RS, Costanza MA, Shields W, Zang E, 1986. Fluorescein angiography complication survey. Ophthalmology 93, 611–617. [PubMed: 3523356]

Author Manuscript Author Manuscript Author Manuscript Author Manuscript

Yeung L, Lima VC, Garcia P, Landa G, Rosen RB, 2009. Correlation between spectral domain optical coherence tomography findings and fluorescein angiography patterns in diabetic macular edema. Ophthalmology 116, 1158–1167. [PubMed: 19395034]

Yeung L, Wu WC, Chuang LH, Wang NK, Lai CC, 2019. Novel optical coherence tomography angiography biomarker in branch retinal vein occlusion macular edema. Retina 39, 1906–1916. [PubMed: 30028408]

You QS, Chan JCH, Ng ALK, Choy BKN, Shih KC, Cheung JJC, Wong JKW, Shum JWH, Ni MY, Lai JSM, Leung GM, Cheung CMG, Wong TY, Wong IYH, 2019. Macular vessel density measured with optical coherence tomography angiography and its associations in a large population-based study. Investig. Ophthalmol. Vis. Sci. 60, 4830–4837. [PubMed: 31747685]

Yu DY, Cringle SJ, 2001. Oxygen distribution and consumption within the retina in vascularised and avascular retinas and in animal models of retinal disease. Prog. Retin. Eye Res. 20, 175–208. [PubMed: 11173251]

Yu DY, Cringle SJ, Yu PK, Balaratnasingam C, Mehnert A, Sarunic MV, An D, Su EN, 2019. Retinal capillary perfusion: spatial and temporal heterogeneity. Prog. Retin. Eye Res. 70, 23–54. [PubMed: 30769149]

Zahid S, Dolz-Marco R, Freund KB, Balaratnasingam C, Dansingani K, Gilani F, Mehta N, Young E, Klifto MR, Chae B, 2016. Fractal dimensional analysis of optical coherence tomography angiography in eyes with diabetic retinopathy. Investig. Ophthalmol. Vis. Sci. 57, 4940–4947. [PubMed: 27654421]

Zhang A, Zhang Q, Wang RK, 2015. Minimizing projection artifacts for accurate presentation of choroidal neovascularization in OCT micro-angiography. Biomed. Opt Express 6, 4130–4143. [PubMed: 26504660]

Zhang M, Hwang TS, Campbell JP, Bailey ST, Wilson DJ, Huang D, Jia Y, 2016a. Projection-resolved optical coherence tomographic angiography. Biomed. Opt Express 7, 816–828. [PubMed: 27231591]

Zhang M, Hwang TS, Dongye C, Wilson DJ, Huang D, Jia Y, 2016b. Automated quantification of nonperfusion in three retinal plexuses using projection-resolved optical coherence tomography angiography in diabetic retinopathy. Investig. Ophthalmol. Vis. Sci. 57, 5101–5106. [PubMed: 27699408]

Zhang P, Wang H, Cao H, Xu X, Sun T, 2017. Insulin-like growth factor binding protein-related protein 1 inhibit retinal neovascularization in the mouse model of oxygen-induced retinopathy. J. Ocul. Pharmacol. Therapeut. 33, 459–465.

Zheng L, Du Y, Miller C, Gubitosi-Klug RA, Kern TS, Ball S, Berkowitz BA, 2007a. Critical role of inducible nitric oxide synthase in degeneration of retinal capillaries in mice with streptozotocin-induced diabetes. Diabetologia 50, 1987–1996. [PubMed: 17583794]

Zheng L, Gong B, Hatala DA, Kern TS, 2007b. Retinal ischemia and reperfusion causes capillary degeneration: similarities to diabetes. Investig. Ophthalmol. Vis. Sci. 48, 361–367. [PubMed: 17197555]

Author Manuscript Author Manuscript Author Manuscript Author Manuscript

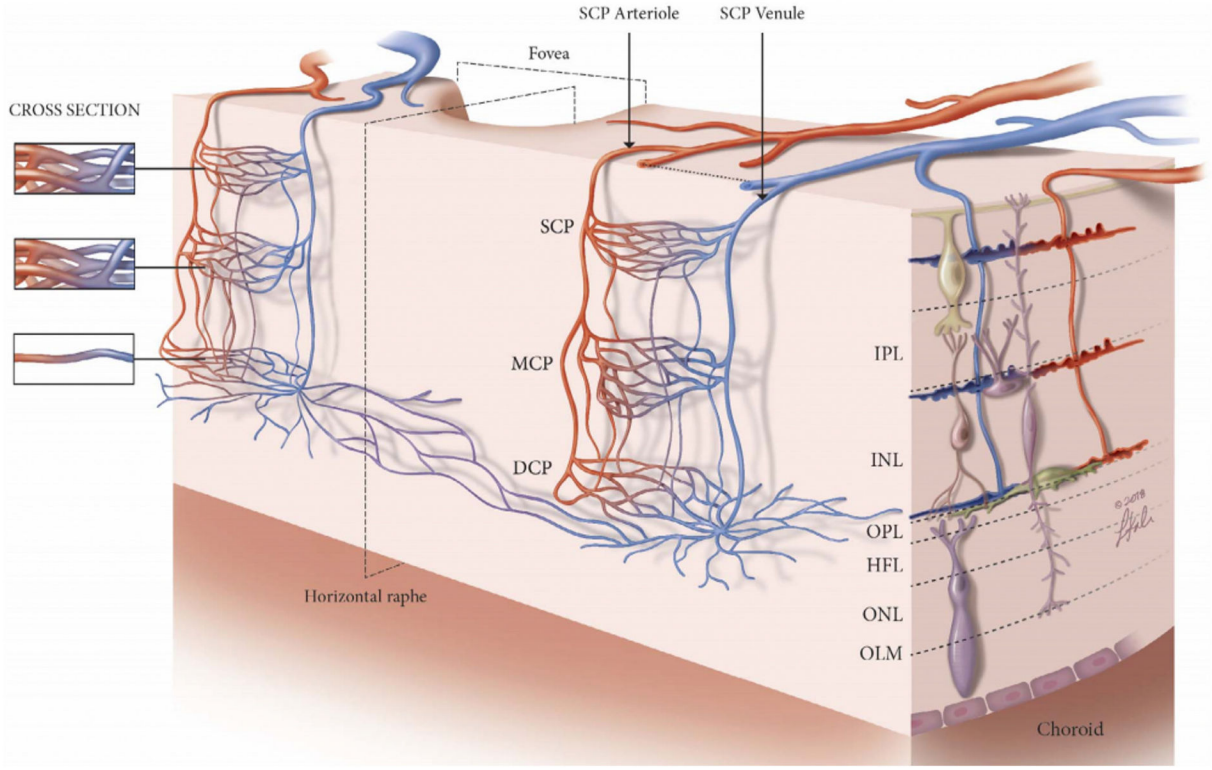

Fig. 1.

Schematic to represent the arrangement of the three retinal plexuses. The superficial capillary plexus (SCP) is located between the retinal ganglion cell layer (RGCL) and the superficial portion of the inner plexiform layer (IPL). The intermediate capillary plexus (ICP), also known as the middle capillary plexus (MCP), starts from the inner border of the IPL to the superficial portion of the inner nuclear layer (INL). The deep capillary plexus (DCP) is distributed across the outer border of the INL. DCP = deep capillary plexus; HFL = Henle's fibre layer; ICP = intermediate capillary plexus; INL = inner nuclear layer; IPL = inner plexiform layer; MCP = middle capillary plexus; OLM = outer limiting membrane; ONL = outer nuclear layer; OPL = outer plexiform layer; RGCL = retinal ganglion cell layer; SCP = superficial capillary plexuses. Figure courtesy of Nesper PL and Fawzi AA from Human Parafoveal Capillary Vascular Anatomy and Connectivity Revealed by Optical Coherence Tomography Angiography. Invest Ophthalmol Vis Sci. 2018 Aug 1; 59(10):3858–3867. https://doi.org/10.1167/iovs.18-24710.

Author Manuscript Author Manuscript Author Manuscript Author Manuscript

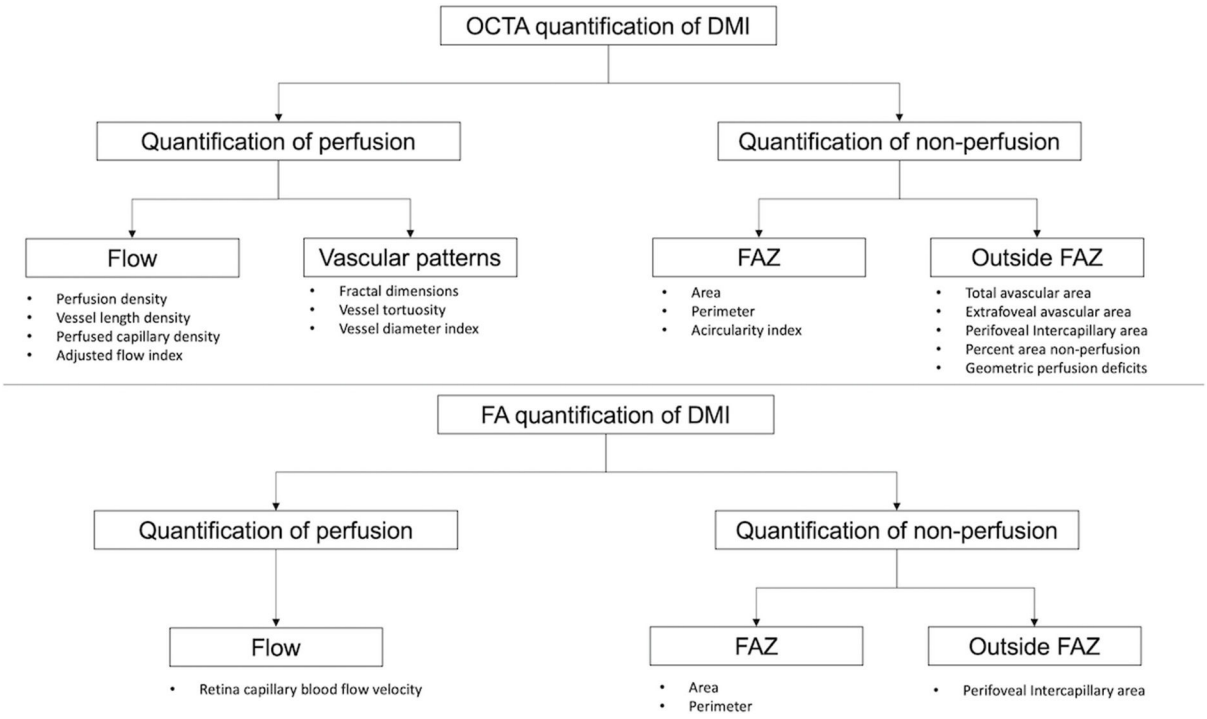

Fig. 2.

Categorisation of diabetic macular ischaemia quantification on optical coherence tomography angiography (above) and fluorescein angiography (below). DMI = diabetic macular ischaemia; FA = fluorescein angiography; FAZ = foveal avascular zone; OCTA = optical coherence tomography.

Author Manuscript Author Manuscript Author Manuscript Author Manuscript

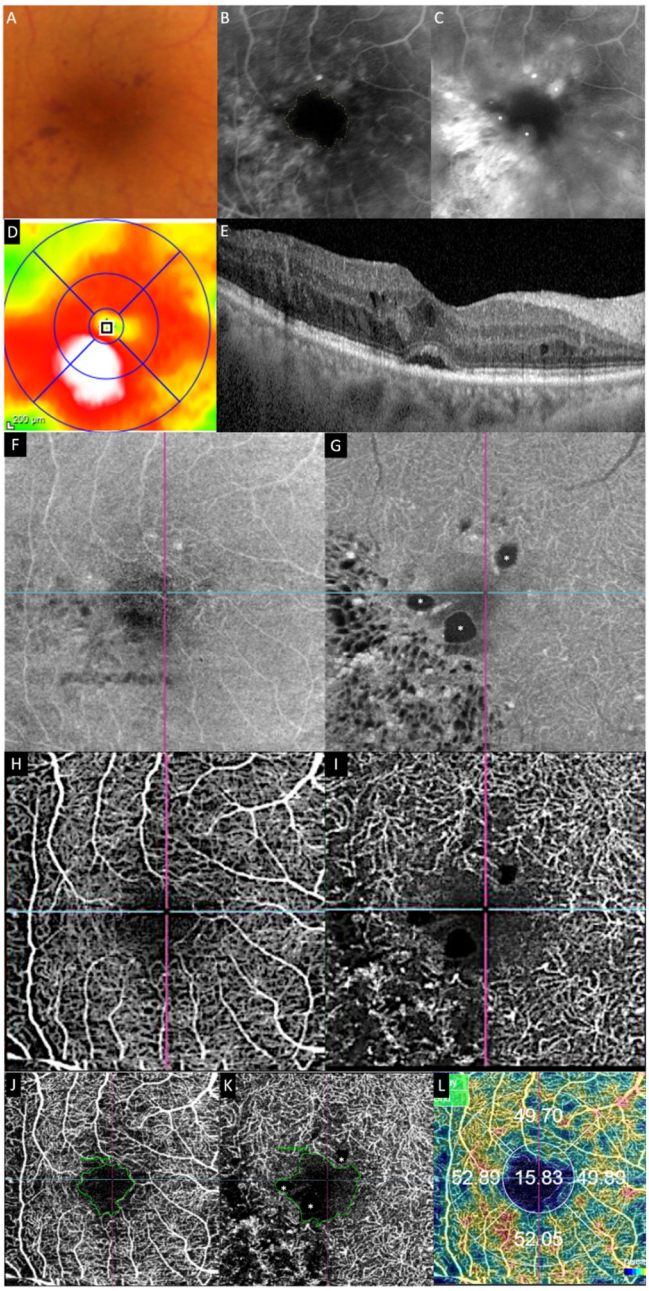

Fig. 3.

Multimodal imaging of an eye with diabetic maculopathy and diabetic macula ischaemia. (A) The colour fundus photograph illustrates the presence of dot and blot haemorrhages in the macula. (B) In the early phase of fluorescein angiography, microaneurysms can be seen. The foveal avascular zone is acircular and enlarged (dotted yellow line). (C) In the late phase of fluorescein angiography, diffuse leakage suggests the presence of macular oedema. Large cysts are detected as areas of well-circumscribed, circular areas of hyperfluorescence (*). These cysts are also represented by the * symbol in the optical coherence tomography (OCT) structural (G) and OCT angiography scans (K). (D) The Distribution of oedema can be appreciated in *en face* OCT retinal thickness map and the corresponding cross-sectional

Author Manuscript Author Manuscript Author Manuscript Author Manuscript

OCT scan (E). (E) showed the presence of intraretinal cysts and subretinal fluid, further confirming the presence of macular oedema. The central subfield thickness is 403 μm. F to L are images from Triton/Topcon platform. (F and G) are the structural enface OCT scans of the superficial capillary plexus (SCP) and the deep capillary plexus (DCP). Retinal cysts are much better appreciated on the structural scan of the DCP (G), with the three corresponding cysts on the other scans denoted by (*). H to L are images from OCT angiography (OCTA) covering a 3 × 3 mm area centred over the fovea. H and I are unannotated OCTA scans of the SCP and the DCP, respectively. (H) The FAZ outline is acircular and enlarged, with reduced perfusion in the perifoveal area. (I) In the corresponding deep plexus OCT angiography, the FAZ area appears larger than that in the superficial plexus. The capillary bed appears disrupted in the area inferotemporal to the fovea centre. J (SCP) and K (DCP) are the same OCTA images in H and L, with annotated areas of FAZ outlined manually in green and areas calculated automatically. The intraretinal cysts are marked by (*). (L) The automated perfusion density scan shows the proportion of perfused (areas with the flow) versus the total area of interest. This automated perfusion density measure is an inbuilt algorithm within the Imagenet (Topcon) software.

Author Manuscript Author Manuscript Author Manuscript Author Manuscript

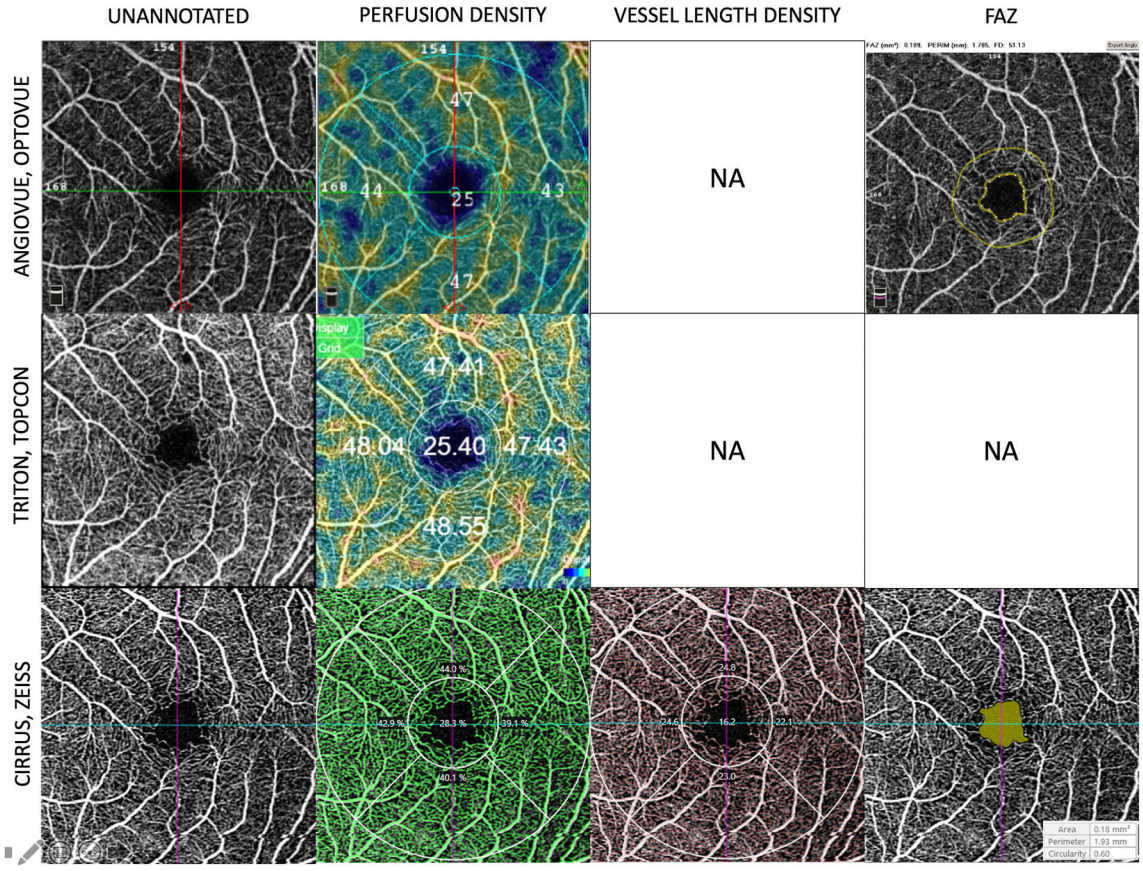

Fig. 4.

Examples of the quantification of perfusion density, vessel length density, and foveal avascular zone (FAZ) generated by the in-built algorithms available on the commercial OCTA instruments. This figure shows the automated readouts and presentation modes on the three commercially available OCTA platforms. The first column shows the unannotated OCTA images of the superficial plexus of a normal eye. The second column shows the perfusion density (expressed as a percentage of white pixels over the region of interest). The third column shows the vessel length density currently only available on the Cirrus (Zeiss platform). The last column shows the detection and quantification of the foveal avascular zone available on the Angiovue/Optovue and Cirrus/Zeiss. OCTA = optical coherence tomography angiography.

Author Manuscript Author Manuscript Author Manuscript Author Manuscript

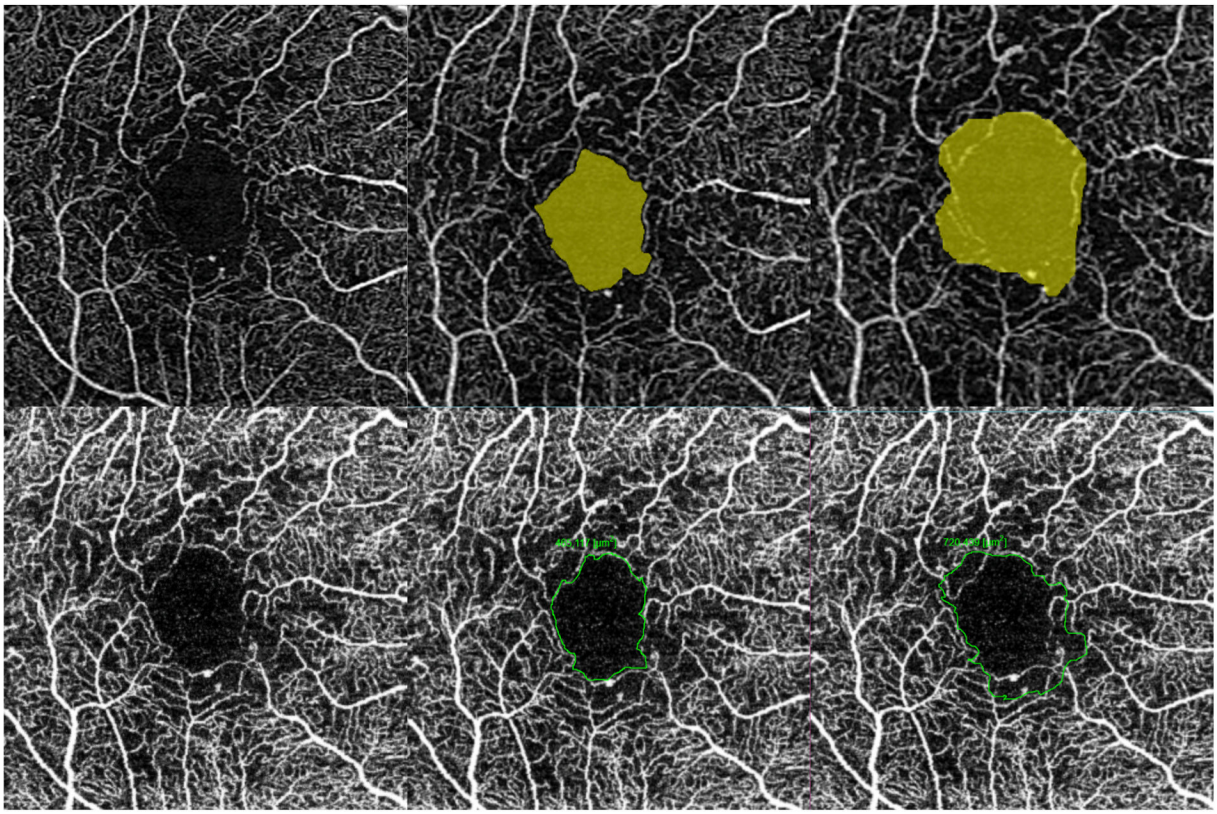

Fig. 5.

Challenges in interpreting the foveal avascular zone (FAZ) and the associated areas of capillary dropout in the perifoveal area. In this eye with DMI imaged by two commercial OCTA instruments (Top row: Cirrus, Zeiss; bottom row: Triton, Topcon), the true extent of the enlarged FAZ seen in the superficial capillary plexus (SCP) could not be reliably determined. The left-most column shows the original OCTA without delineation of the FAZ. The middle column is a conservative outline of the FAZ, but the perifoveal dropout is not reflected. The right-most column shows the FAZ outline, which considers the “moth-eaten” perifoveal areas where the capillary bed is deficient. This strategy results in a much larger FAZ readout. There is potential for significant variation in the FAZ area readout depending on the inclusion of the perifoveal nonperfusion area. This example illustrates that the FAZ area alone does not adequately describe the severity and the extent of DMI. Additional parameters to ascertain the actual ischaemia include perifoveal intercapillary area, total avascular area and extrafoveal avascular area. DMI = diabetic macular ischaemia; FAZ = foveal avascular zone; OCTA = optical coherence tomography angiography; SCP = superficial capillary plexus.

Author Manuscript Author Manuscript Author Manuscript Author Manuscript

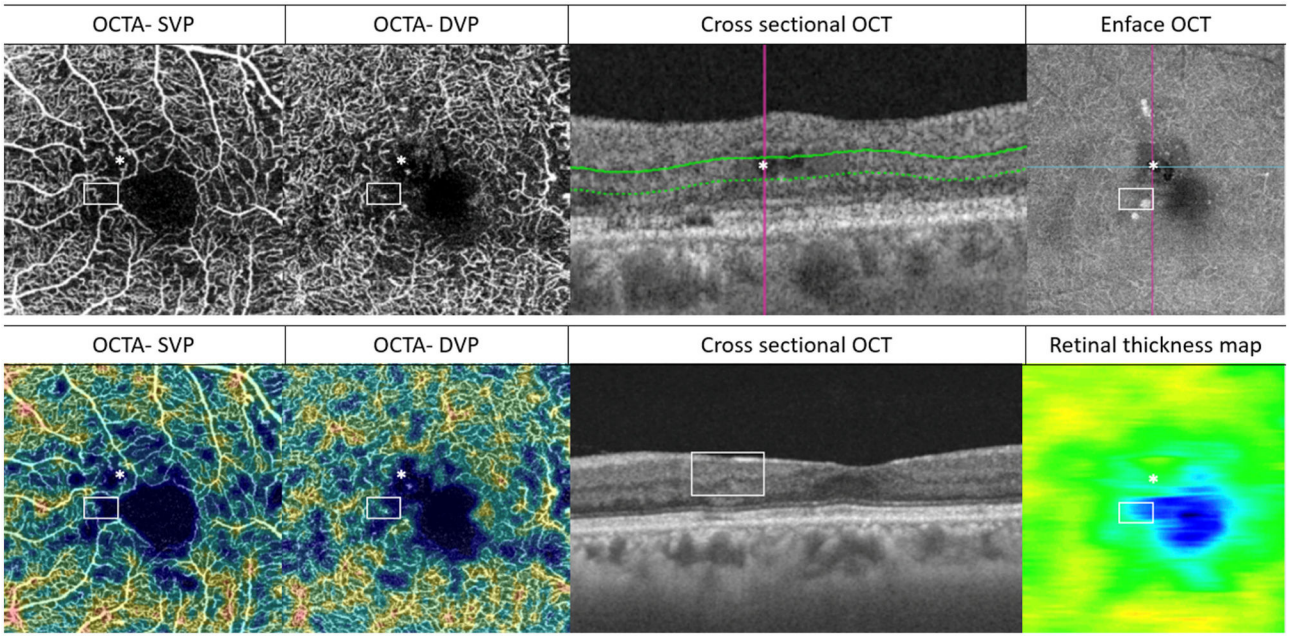

Fig. 6.

Potential artefacts and inaccurate DMI assessments in eyes with co-existing DMO (upper row) or DRIL (lower row). This figure illustrates the importance of interpreting OCTA with structural OCT (both cross-sectional and *en face*). A confluent area of perifoveal non-perfusion can be seen. Within this area, two locations (marked by a white asterisk and a white rectangle) are of specific interest. In the upper row, intraretinal cysts (*) can be identified in the structural OCT. The cyst appears as part of the confluent flow void in the superficial and deep layers on OCTA. It is challenging to determine whether this flow void represents the true capillary dropout. In the lower row, the area within the non-perfused area denoted by the rectangular white box on OCTA corresponds to an area of DRIL on cross-sectional OCT. There is corresponding retina thinning on the *en-face* structural retinal thickness map. It is important in both cases that co-existing structural changes are corrected during segmentation (with manual segmentation performed if necessary) to ensure accurate presentation of flow or non-flow areas on the *en-face* OCTA scans. The corresponding OCTA density maps are shown on the two left-most images in the bottom row. DMI = diabetic macular ischaemia; DMO = diabetic macular oedema; DRIL = disorganisation of the retinal inner layers; DVP = deep vascular plexus; OCT = optical coherence tomography; OCTA = optical coherence tomography angiography; SVP = superficial vascular plexus.

Author Manuscript Author Manuscript Author Manuscript Author Manuscript

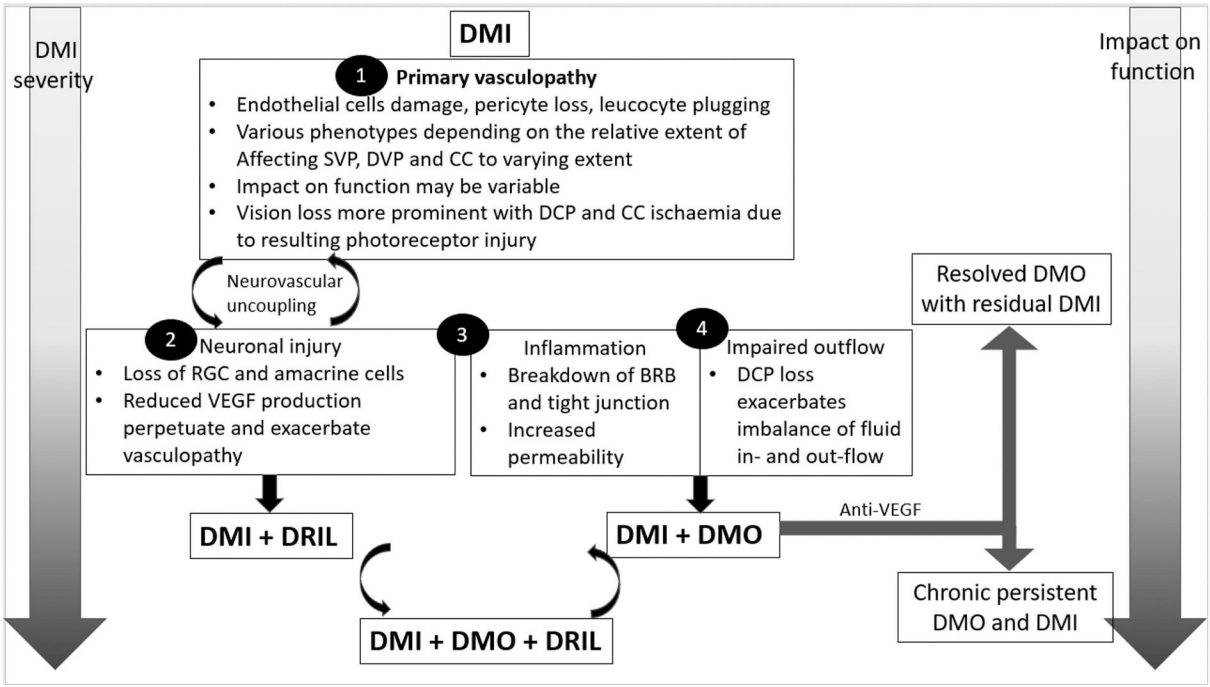

Fig. 7.

Schematic representation of the impact of DMI alone or in combination with neuronal injury, inflammation and impaired outflow on visual function. BRB = blood-retinal barrier; CC = choriocapillaris; DCP = deep capillary plexus; DMI = diabetic macular ischaemia; DMO = diabetic macular oedema; DRIL = disorganisation of retinal inner layers; DVP = deep vascular plexus; RGC = retinal ganglion cells; SVP = superficial vascular plexus; VEGF = vascular endothelial growth factor.

Author Manuscript Author Manuscript Author Manuscript Author Manuscript

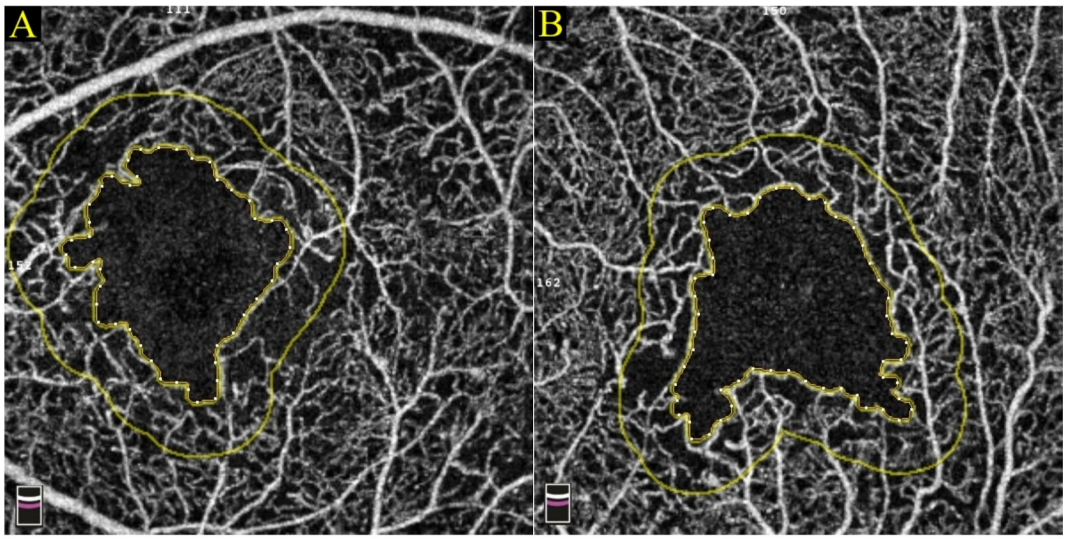

Eye	VA (letters)	FAZ (mm^2)	SCP VD (%)	DCP VD (%)	FAZ Perimeter (mm)	AI
A	**40**	**1.00**	30.5	40.1	5.10	1.44
B	**85**	**1.13**	37.0	39.2	5.97	1.58

Fig. 8.

An enlarged foveal avascular zone is not always an indicator of poor visual acuity. For example, eye A had an enormous FAZ area of 1.00 mm^2 with a poor VA of 40 letters. In contrast, eye B had a similar FAZ size but could read 85 letters on VA examination. Therefore, other vascular parameters, such as SCP VD, DCP VD, the FAZ perimeter and the FAZ-AI should also be considered when evaluating a patient's functional visual outcome. AI = acircularity index; DCP = deep capillary plexus; FAZ = foveal avascular zone; SCP = superficial capillary plexus; VA = visual acuity; VD = vessel density.

Author Manuscript Author Manuscript Author Manuscript Author Manuscript

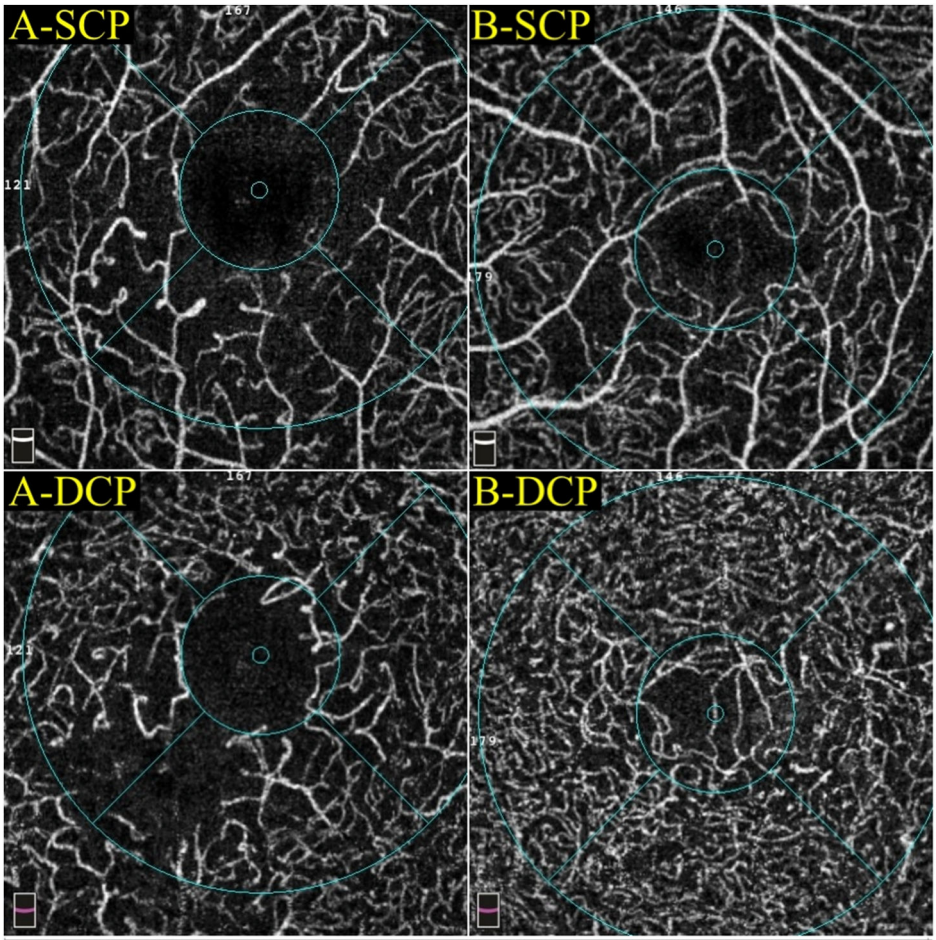

Eye	VA (letters)	FAZ (mm²)	SCP VD (%)	DCP VD (%)
A	**65**	0.70	**26.9**	**27.0**
B	**82**	0.51	**33.9**	**38.7**

Fig. 9.

Examples of eyes with generalised diabetic macular ischaemia (DMI). Generalised DMI presents with a profound reduction in both the SCP and DCP VD. Interestingly, even with severely decreased VD, the VA is not always declined. For instance, eye A and eye B both had a reduced vessel density in the superficial and deep capillary plexus. However, eye B identified much more letters than eye A did. DCP = deep capillary plexus; DMI = diabetic macular ischaemia; FAZ = foveal avascular zone; SCP = superficial capillary plexus; VA = visual acuity; VD = vessel density.

Author Manuscript Author Manuscript Author Manuscript Author Manuscript

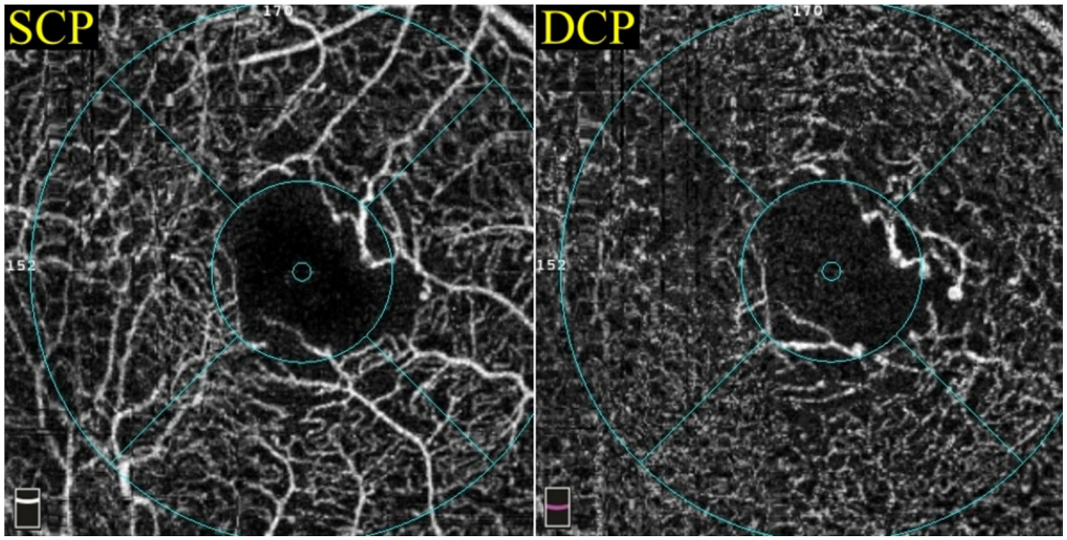

Fig. 10.

A case of predominant-DCP ischaemia. An eye with a more reduced deep vessel density may represent a more severe phenotype of diabetic macular ischaemia. In this example, the vessel density was 43% in the SCP and 37.5% in the DCP. The patient had moderate visual impairment and scored 73 letters using the ETDRS chart. DCP = deep capillary plexus; ETDRS = Early Treatment Diabetic Retinopathy Study; SCP = superficial capillary plexus.

Author Manuscript Author Manuscript Author Manuscript Author Manuscript

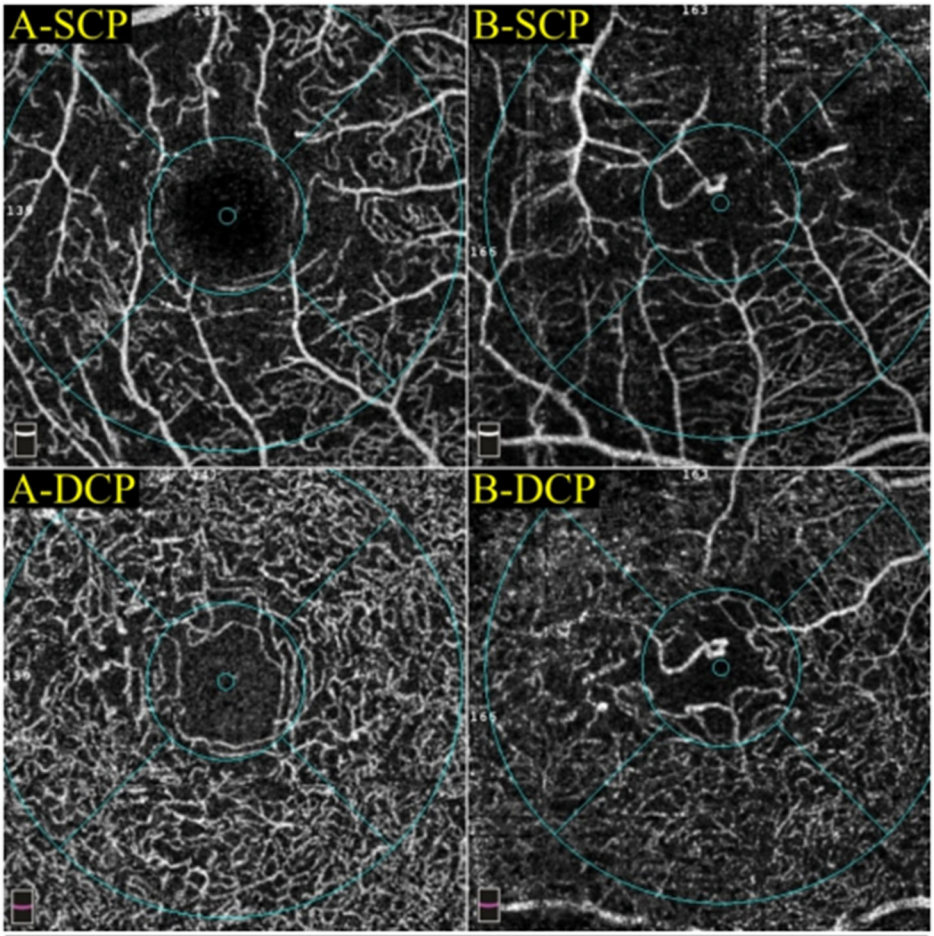

Eye	VA (letters)	FAZ (mm^2)	SCP VD (%)	DCP VD (%)
A	**75**	0.38	**34.5**	48.1
B	**65**	0.18	**31.1**	43.5

Fig. 11.

Predominant SCP-ischaemia and its relevant visual performance. Both eye A and eye B had a substantially decreased VD in the SCP whilst the DCP VD was preserved. Notably, this phenotype of DMI also had varying degrees of visual impairment but was generally less severe. DCP = deep capillary plexus; DMI = diabetic macular ischaemia; FAZ = foveal avascular zone; SCP = superficial capillary plexus; VA = visual acuity; VD = vessel density.

Author Manuscript Author Manuscript Author Manuscript Author Manuscript

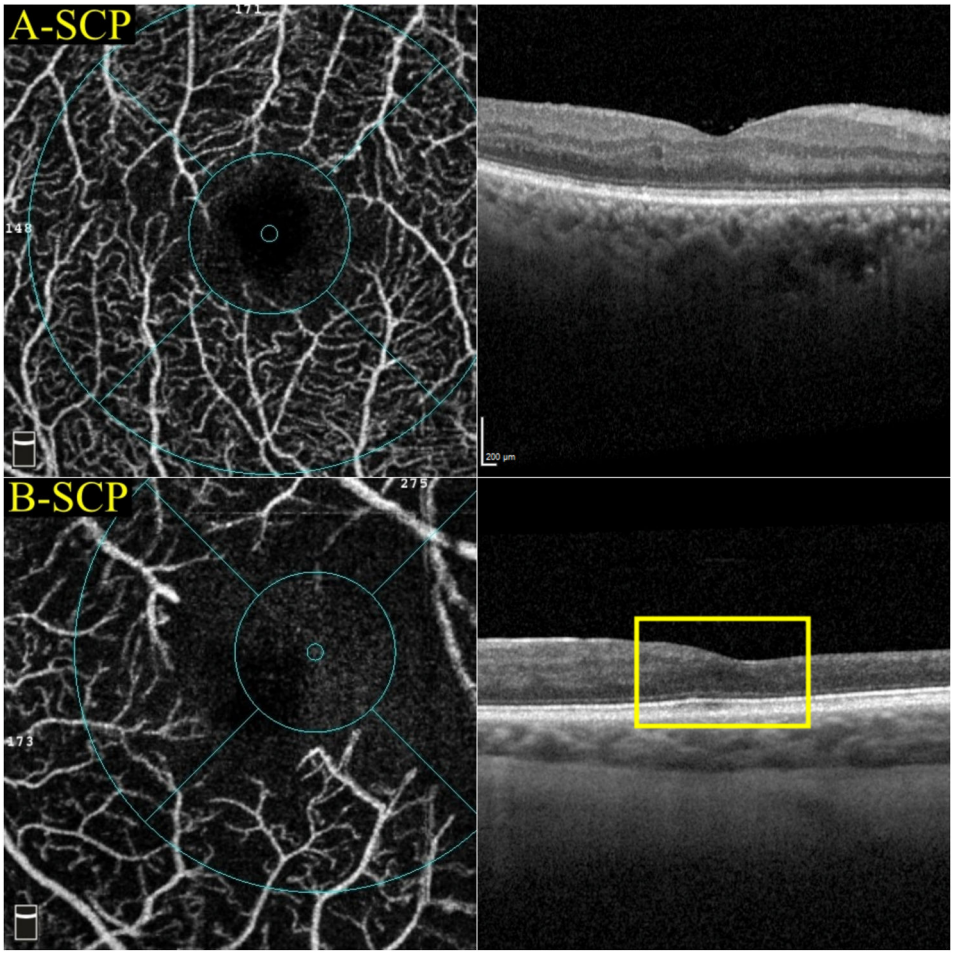

Fig. 12.

A reduced SCP VD on OCTA does not always correspond to the DRIL on OCT.

For example, both eye A and eye B had a reduced superficial VD (39% and 25.4%, respectively). However, only eye B presented with DRIL (yellow rectangle). DRIL = disorganisation of retinal inner layers; OCT = optical coherence tomography; OCTA = optical coherence tomography angiography; SCP = superficial capillary plexus; VD = vessel density.

Author Manuscript Author Manuscript Author Manuscript Author Manuscript

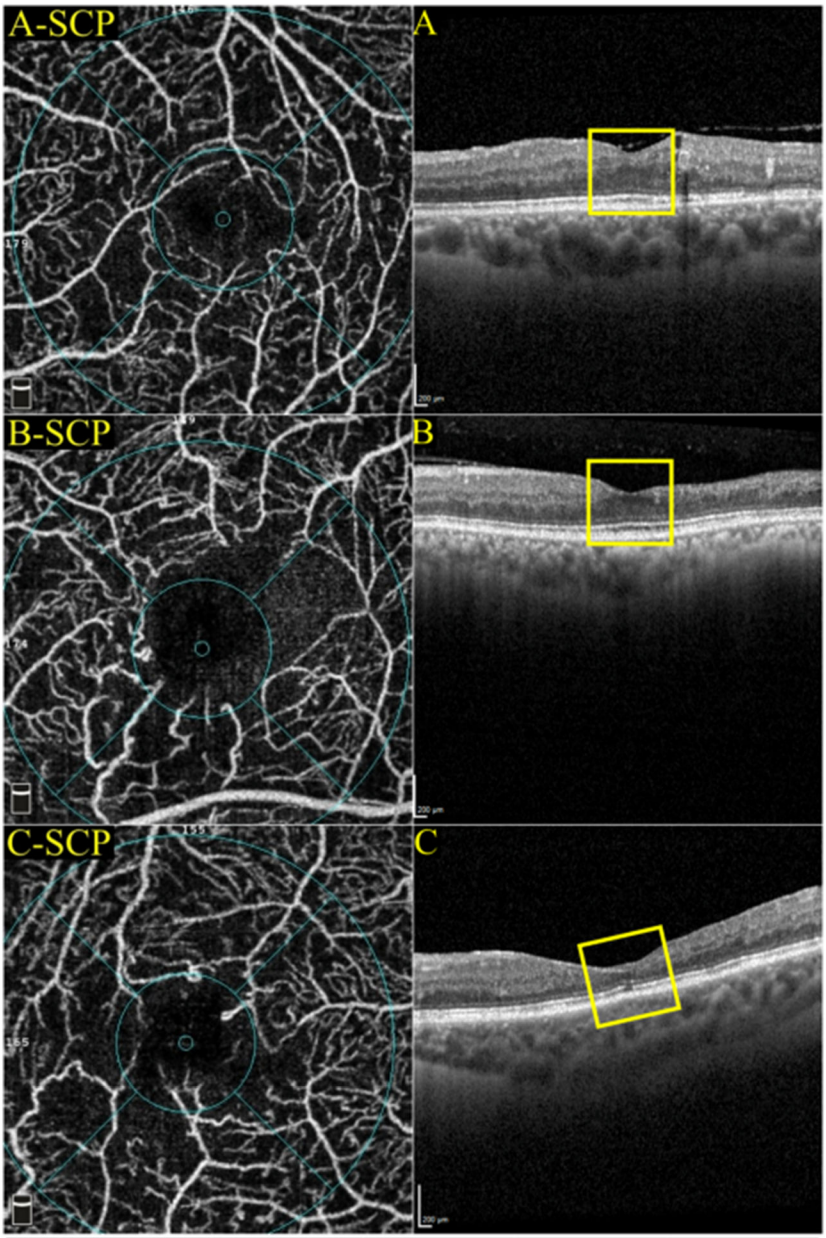

Eye	VA (letters)	FAZ (mm²)	SCP VD (%)	DCP VD (%)	DRIL
A	**82**	0.51	**33.9**	38.7	**Yes**
B	**82**	1.38	**34.6**	39.4	**Yes**
C	**84**	0.57	**35.3**	41.5	**Yes**

Fig. 13.

Patients with a reduced SCP VD and DRIL are not necessarily associated with poor visual acuity. The discrepancies reflect that there may be a higher threshold for jeopardising the visual performance. DCP = deep capillary plexus; DRIL = disorganisation of retinal inner layers; FAZ = foveal avascular zone; SCP = superficial capillary plexus; VA = visual acuity; VD = vessel density.

Author Manuscript Author Manuscript Author Manuscript Author Manuscript

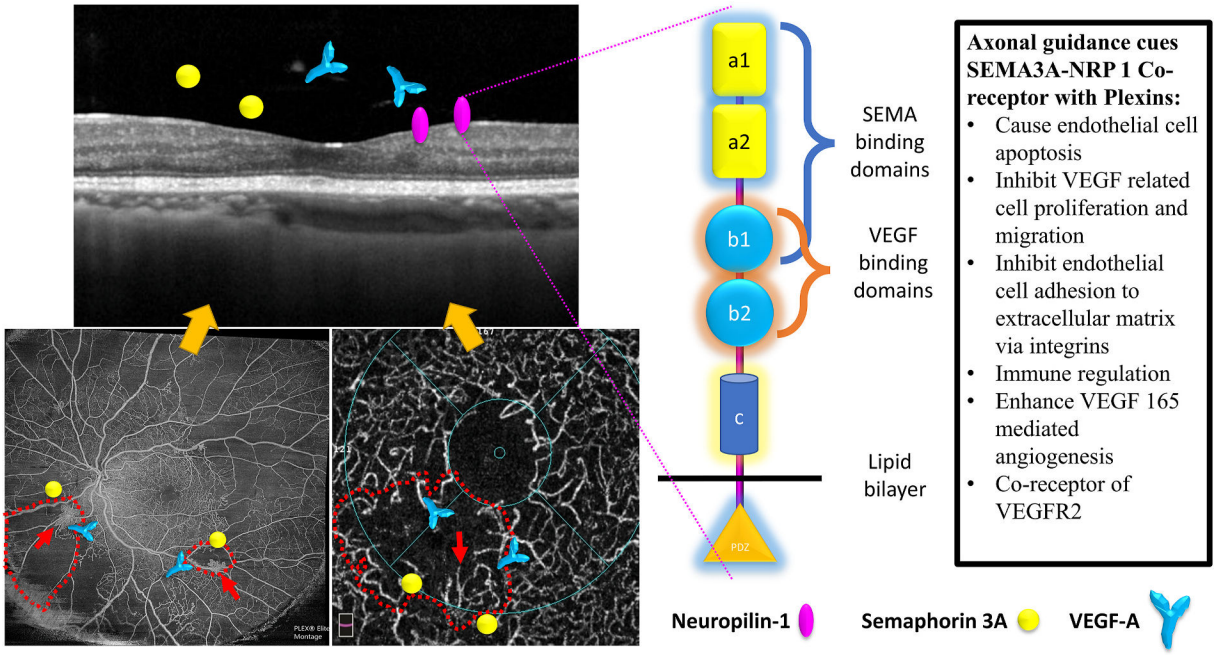

Fig. 14.

A schematic diagram of the relationship between semaphoring 3A (SEMA3A), neuropilin-1 (NRP1), and vascular endothelial growth factor A (VEGF-A). The border of the non-perfused area and perfused retina is surrounded by VEGF-A and SEMA3A molecules, both produced by the inner retina in response to hypoxia. While VEGF-A has its own receptors (VEGFR1 and VEGFR2), VEGF-A also binds to NRP1, which has both the VEGF and SEMA binding domains. These two domains have opposing effects on the non-perfused retina. VEGF-A stimulates retinal neovascularisation, and thus new vessels develop at the junction between the perfused and non-perfused areas (red arrows). SEMA3A prevents these new vessels from growing into the non-perfused areas, and hence they grow towards the vitreous. NRP = neuropilin; VEGF = vascular endothelial growth factor; VEGFR = vascular endothelial growth factor receptor; SEMA = semaphorin.

Author Manuscript

Author Manuscript

Author Manuscript

Author Manuscript

Table 1

Comparison of diabetic macular ischaemia (DMI)-related endpoints evaluated on fluorescein angiography (FA) and optical coherence tomography angiography (OCTA).

	Fluorescein angiography (mainly reflects the superficial vascular complex)	**Optical coherence tomography angiography (evaluates the superficial vascular complex and the deep vascular complex independently)**
Foveal avascular zone (FAZ)	• size • circumference • circularity • diameter • contour (qualitative)	• size • perimeter • acircularity index
Metrics of perfusion	Not available	• perfused capillary density • vessel length density • adjusted flow index • fractal dimension • vessel tortuosity • blood vascular calibre • vessel diameter index
Metrics of nonperfusion (in addition to FAZ)	Not available	• intercapillary area • total avascular area (TAA)/extrafoveal avascular area (EAA) • percent area of nonperfusion (PAN) • geometric perfusion deficits (GPD)

Author Manuscript

Author Manuscript

Author Manuscript

Author Manuscript

Table 2

Description of OCTA metrics and recommended terminology.

Description of the flow metric	Currently used nomenclature	Availability in commercial software	Recommended term
Total area of perfused vasculature per unit area in a region of interests	Vessel density, perfusion density, vessel area density	Optovue – VD Zeiss – PD Topcon – VD	Perfused pixel area density
Total vessel length per unit area in a region of interest	Vessel density, vessel length density, vessel skeleton density	Zeiss – VD	Perfused pixel length density
Total area of perfused vasculature excluding the large vessels per unit area in a region of interest	Perfused capillary density, capillary density, capillary perfusion density	–	Perfused pixel area density (excluding large vessels)
Pixel intensity as a surrogate for blood flow	Adjusted flow index, flux	–	Corrected pixel intensity
Complexity of vasculature	Fractal dimension	–	Fractal dimension

Abbreviations:VD-vessel density; PD-perfusion density.